Inaugural dissertation

for

obtaining the doctoral degree

of the

Combined Faculty of Mathematics, Engineering and Natural Sciences of the

Ruprecht - Karls - University

Heidelberg

Presented by

M.Sc. Sven Reislöhner

Born in: Nürnberg

Oral examination: 10.10.2022

Development of a xylose inducible promoter system to study ribosome biogenesis in *Chaetomium thermophilum*

Referees: Prof. Dr. Ed Hurt

Prof. Dr. Michael Brunner

SUMMARY

The thermophilic ascomycete *Chaetomium thermophilum* gains growing popularity in the field of structural biochemistry and biotechnology due to its thermostable proteome. Recently, this thermophile has been successfully utilized as platform to gain high resolution “snap-shots”, of pre-ribosomal assembly intermediates by cryogenic electron microscopy (cryo-EM). In the model organism *Saccharomyces cerevisiae,* one of the versatile tools to study ribosome biogenesis is the inducible *GAL1*-promoter. However, the genetic toolset of the emerging model organism *C. thermophilum* was limited to the random integration of expression cassettes, allowing to purify pre-ribosomal particles with constitutively expressed biogenesis factors via affinity purification.

In this PhD thesis, I focused on the establishment of an inducible promoter system to control dominant negative mutants as new tool to study ribosome biogenesis in the thermophile. Firstly, I addressed an endogenous carbon regulatable expression system that withstands the thermostable requirements. Using single carbon glucose and xylose media enabled me to characterize the transcriptome of *C. thermophilum* and to screen for the most differentially transcribed genes by mRNA Illumina sequencing. Promoter regions of xylose specifically activated genes were validated in YFP-reporter strains *in vivo* and biochemically. The most stringently xylose induced promoters originated from a xylosidase-like gene (*XYL*) and the xylitol-dehydrogenase gene (*XDH*), which were tested to study the process of ribosome biogenesis. As proof of concept, both promoters allowed us to induce the expression of a well characterized nucleolar biogenesis factor (UTP-6) using the inductive media. Expression of YFP-tagged UTP-6 under control of the *XYL*-promoter showed clear xylose induction of UTP-6 in vivo. Using the *XDH*-promoter, FTpA-tagged UTP-6 was overexpressed in xylose grown cells on affinity purified 90S pre-ribosomal particles on Coomassie stained gels. Moreover, the *XDH*-promoter allowed me to visualize an inducible dominant negative 60S-subunit export defect upon expression of the mutant pre-60S factor *rsa4* E117D in a L25-YFP reporter strain. Overall, the provided tools and transcriptomic studies described in my PhD thesis will facilitate the future work with the thermophile and future applications that benefit from its thermostable proteins.

ZUSAMMENFASSUNG

Der filamentöse Pilz *Chaetomium thermophilum* gewinnt aufgrund seiner thermostabilen Proteine zunehmend an Bedeutung als Modellorganismus im Bereich der Strukturbiochemie sowie der Biotechnologie. *C. thermophilum* wurde bereits erfolgreich eingesetzt um hochauflösende Strukturmodelle von prä-ribosomalen Proteinkomplexen mit Hilfe der Cryo-Elektronenmikroskopie (Cryo-EM) zu erhalten. In *Saccharomyces cerevisiae,* als traditionell genutzter Modellorganismus zur Studie der Ribosomenbiogenese wird der regulierbare *GAL1*-Promotor vielseitig angewandt. Solch ein regulierbarer Promoter, wie er für die Untersuchung von dominant negativen Mutanten notwendig ist, war in *C. thermophilum* bislang nicht verfügbar.

In dieser Doktorarbeit konzentrierte ich mich auf die Etablierung eines induzierbaren Promotorsystems, welches für Studien der Ribosomenbiogenese herangezogen werden kann. Dazu suchte ich nach Promotoren im Genom von *C. thermophilum*, die sich mit Hilfe von verschiedenen Zuckern regulieren lassen. Mit Hilfe eines Glukose- und Xylose- haltigen Mediums konnte ich Zucker regulierte Gene mittels Illumina-Sequenzierung identifizieren. Entsprechende Promotorregionen wurden in YFP-Reporterstämmen in vivo sowie biochemisch validiert. Die am stärksten regulierten Promotoren wurden von einem xylosidase-ähnlichen Gen (*XYL*) und dem Gen der Xylitol-Dehydrogenase (*XDH*) ausfindig gemacht und anschließend zur Induktion von Ribosomen-Biogenesefaktoren herangezogen. Als konzeptionellen Beweis habe ich mit beiden Promotoren die Induktion des gut charakterisierten nukleolären Biogenesefaktors UTP-6 zeigen können. Darüber hinaus ermöglichte mir der *XDH*-Promotor einen Exportdefekt der 60S-Untereinheit aus dem Nukleus mit Hilfe einer induzierbaren dominant negativen Mutante (*rsa4 E117D*) zu erzwingen, welchen ich mit Hilfe eines L25-YFP Reporterkonstrukts visualisierte. Die in dieser Arbeit etablierten Techniken und Transkriptomstudien stellen eine Bereicherung für *C. thermophilum* als Modellorganismus dar und ebnen den Weg für weitere Anwendungsmöglichkeiten, um von seinen thermostabilen Eigenschaften zu profitieren.

Table Of Contents

1 INTRODUCTION

1.1 *Chaetomium thermophilum* as emerging model organism providing thermostable proteins

The eukaryotic fungus *Chaetomium thermophilum* is a filamentous ascomycete that thrives at temperatures between 50 and 55 °C by hyphae extension on rotting plant material (la Touche, 1948), shown in **Figure 1**. Its hyphae are multinucleated, which is common for filamentous fungi (Glass et al., 2000). The ascomycota resemble the largest and most diverse phylum of eukaryotes in which the filamentous fungi are defined as subphylum next to the budding and fission yeasts (Shen et al., 2020). Well known representatives of the budding yeasts are the model organism *Saccharomyces cerevisiae* as well as representatives of the genus *Candida*, Filamentous fungi are skilled in dynamically changing their lifestyle, covering endophytic, pathogenic and saprophytic facets, reflecting their complex physiology (Shen et al., 2020). The research on filamentous fungi is mostly attracted by their ability to effectively degrade plant biomass by their strong secretion of carbohydrate active enzymes. Applications aim to develop sustainable strategies to produce organic high value compounds like alcohols that cater amongst others for biofuel-productions (Karnaouri et al., 2019; Sajith S et al., 2016). Unfortunately, the relevant enzymes from mesophilic fungi lack thermal stability as shortcoming in self-heating industrial reactors, thus enzymes from thermophilic fungi come into focus of research due to their natural superior stability (Karnaouri et al., 2019). Along this line, also the interest in *Chaetomium thermophilum* as source for thermostable lignocellulolytic enzymes for biotechnological applications is growing (X. Li et al., 2020). Furthermore, also the heterologous expression of lignocellulolytic genes from the thermophile significantly improved the production yield of a desired cellulase in the traditional workhorse *Trichoderma reesei* (Jiang et al., 2020). Key for the establishment of the complex filamentous fungal model organisms were also the steep technological advances that led to next generation sequencing technologies like the 454-technique followed by the Illumina sequencing technology within the first years of the 21st century (Thermes, 2014; Martinez et al., 2008; Pel et al., 2007). The initiation of *C. thermophilum* as model organism started rather recently only in 2011 when its genome was published (Amlacher et al., 2011; Bock et al., 2014).

The rational to pioneer this thermophile was to benefit from its superior protein stability in the field of structural biochemistry. In fact, this thermophile quickly proved to be powerful to gain various X-ray structures with superior resolution of individual proteins accumulating in the protein data base (Aibara et al., 2015; Baker et al., 2015). Due to the quick advances in cryogenic electron microscopy techniques (cryoEM), also intriguingly sized protein complexes like the 600 kDa INO80 complex in contact with the nucleosome allowed close insights into nucleosome remodeling (Eustermann et al., 2018). In 2016, a very early assembling ribosomal intermediate particle, known as the 90S-preribosome with a dimension of about five mega-dalton was purified from *C. thermophilum.* Its cryoEM structure allowed for unprecedented insights into the onset of ribosome biogenesis (Kornprobst et al., 2016) and paved the way for the modelling of even more refined 90S pre-ribosomal snapshots (Cheng et al., 2019). Key for the purification of such protein and complexes directly from *C. thermophilum* was the development of a transformation protocol that allows for the genomic expression of proteins as translational fusions with affinity-tags for biochemical purifications under control of the constitutively strong actin-promoter (Cheng et al., 2017; Kellner et al., 2016). For the genomic integration of the expression cassette, two thermostable selection markers were developed, namely the ergosterol-1 gene (*erg1*) conferring resistance against terbinafine and the hygromycin phosphotransferase (*hph*) gene to select for hygromycin resistant transformants (Kellner et al., 2016; Cheng et al., 2019). However, an important missing technique is a regulatable promoter to allow controlled gene-expression as it was broadly and successfully applied in the yeas *S. cerevisiae*.

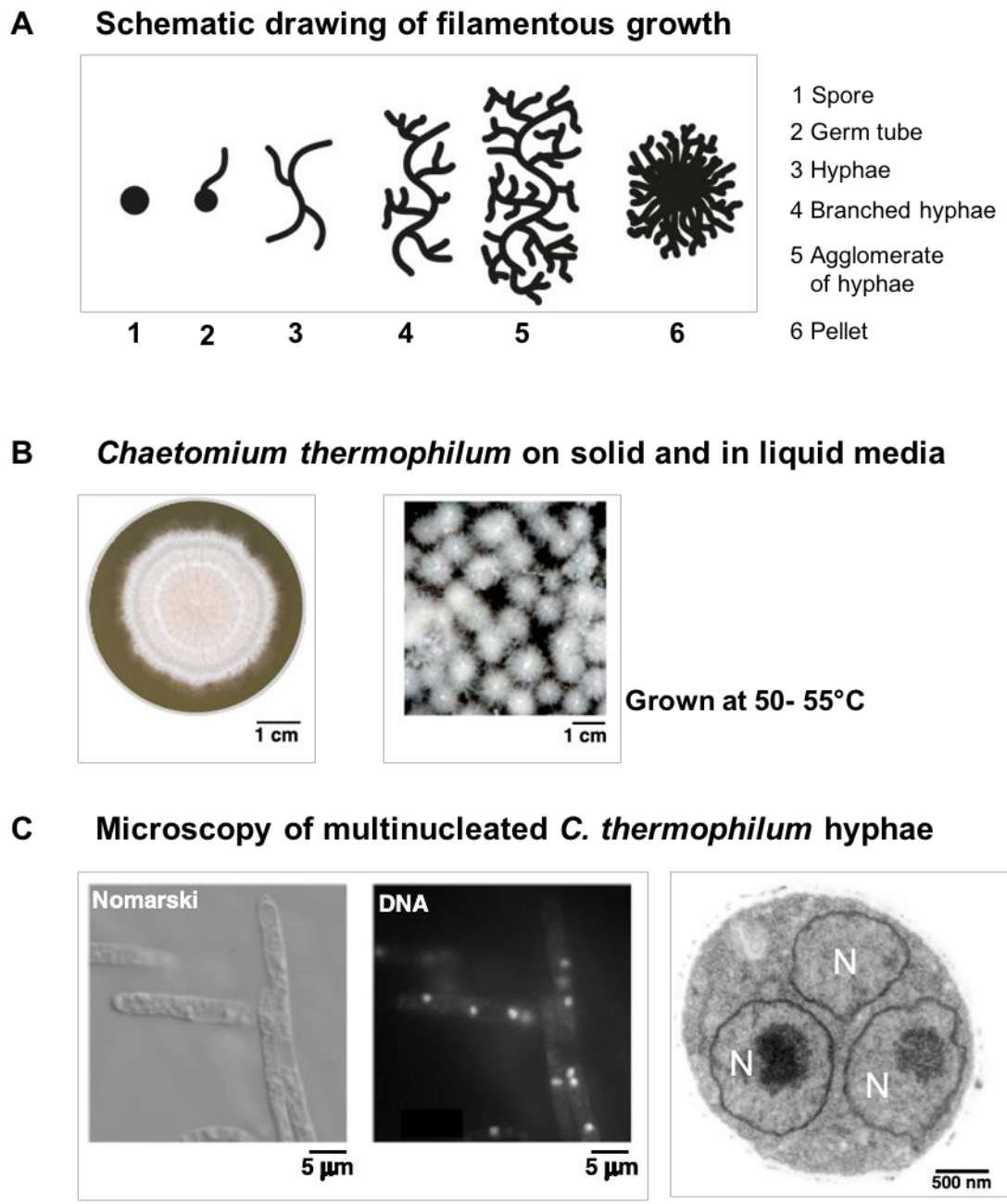

Figure 1: The characteristics of Chaetomium thermophilum. A *schematic drawing of filamentous growth. Ascomycetes like C. thermophilum form hyphae that develop out of ascospores and further branch into dense structures (pellets), adapted from* Reyes et al., 2017. ***B*** *Chaetomium thermophilum is a thermophilic eukaryote. Mycelia of this thermophile grows best around 50°C. Its growth style in laboratory conditions is shown on solid and in liquid media.* ***C*** *Chaetomium thermophilum develops multinucleated hyphae. Shown are hyphae with multiple nuclei as seen by fluorescence microscopy upon DNA-staining (left and centre) and thin section-EM (right). Nucleus (N). B and C was taken from* Amlacher et al., 2011.

1.2 Lignocellulose as complex carbon source for filamentous fungi

Lignocelluloses are robust protective structural polysaccharides of plant cell walls that consist out of cellulose, hemicellulose, and lignin as the main constituents (Malherbe & Cloete, 2002; (Sajith S et al., 2016; Heredia et al., 1995), shown in **Figure 2**. Cellulose, as the major portion is a linear polymer of α-1,4-linked D-glucose monomers that are arranged in microcrystalline structures with amorphous and crystalline regions (Malherbe & Cloete, 2002; Berlin, 2013). Hemicelluloses comprise a heterologous group of β-1,4-linked sugar chains with the most abundant one being the xylan-type (Stoklosa & Hodge, 2012). Xylans, referred to as hemicellulose hereafter consist out of a ß-1,4-linked D-xylose backbone with various decorations with alternative sidechains like D-galactose, L-arabinose, glucuronic acid, acetyl, feruloyl, and p-coumaroyl residues (de Vries & Visser, 2001; Kuhad et al., 1997). Lignin is a highly irregular and insoluble polymer consisting out of different phenylpropanoid subunits (Leonowicz et al., 1999; Tomme et al., 1995) that serves as covering and fill-material, providing a rigid shield against direct enzymatic hydrolysis (R. Sun et al., 1996). The combination of all three polymers form a complex tertiary architecture that is stabilized by a variety of covalent and non-covalent linkages which forms a strong protective barrier for plants (Leonowicz et al., 1999).

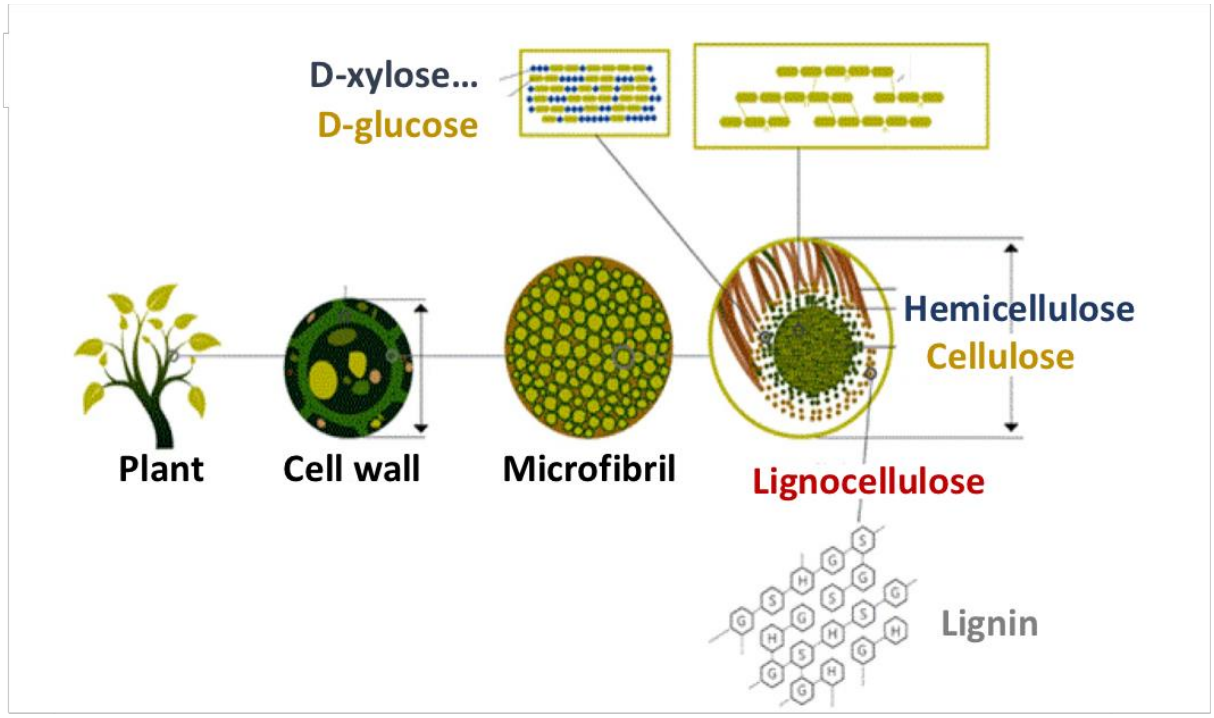

Figure 2: Origin and composition of lignocellulose as carbon source for fungi. *Plant cell walls consist largely out of lignocellulose as protective barrier. It is constituted of the three major polymers cellulose, hemicellulose and lignin that form rigid bundles (microfibrils). Cellulose is made of thousands of repetitive units of α-1,4-linkaged D-glucose molecules. Hemicellulose of the most abundant xylan-type consists out of ß-1,4-linked monomers that forms the backbone chain and is decorated by various sugars and carbohydrate side-chains. Lignin serves as matrix to wrap both sugar-polymers and protectant against enzymatic degradations. Figure adapted from* Sajith S et al., 2016.

Especially filamentous fungi are known for their superior ability to secrete an arsenal of carbohydrate-active enzymes that allows them to live from lignocellulose derived carbon sources (de Souza, 2013). The secreted cocktail of hydrolytic enzymes to degrade the lignocellulose polymer to subsequently catabolize the liberated carbohydrates are visualized in Figure 3. Cellulose degradation requires synergistic activity of glucanases, cellobiohydrolases and β-glucosidases. The endoglucanases cleave cellulose chains internally mainly from the amorphous region, releasing units to be degraded sequentially. The cellobiohydrolases cleave cellobiose units from the end of the polysaccharide chains (Aro et al., 2005). In a last depolymerization step, the β-glucosidases hydrolyze cellobiose to glucose, that enters glycolysis to generate energy (Ali et al., 2016; Béguin, 1990). Depolymerization of the hemicellulose polymer occurs by the action of the ß-1,4-endoxylanases which cleave the polymer-backbone into smaller oligosaccharides. The ß-1,4-xylosidase activity provides the sugar monomer D-xylose from the disaccharide xylobiose (Gong et al., 2018; Hasper et al., 2000). A cocktail of sidechain specific hydrolases releases attached sidechains from the xylose

units. Lignocellulolytic hydrolysates being small enough to be transported over the membrane enter the cytosol where they supply the metabolic processes.

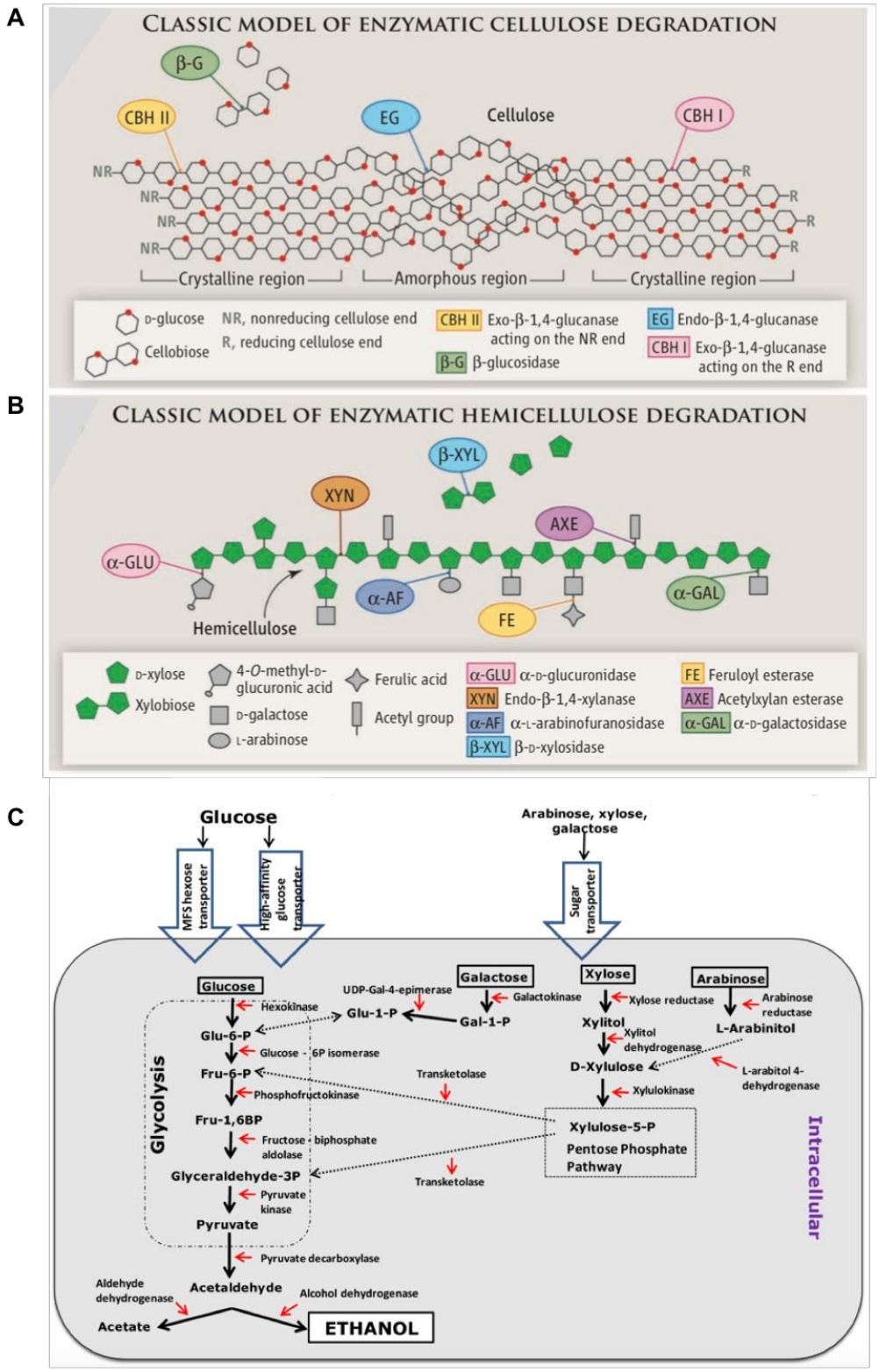

Figure 3: Schematic representation of the lignocellulolytic lifestyle of filamentous fungi*. Filamentous fungi secrete an arsenal of carbohydrate active enzymes (CaZys) to break down cellulose*

and hemicellulose polymers into metabolizable sugars. ***A*** *The required enzymes to mobilize D-glucose from cellulose.* ***B*** *The characteristic enzymes to mobilize D-xylose and other sugars from hemicellulose (adapted from* Berlin, 2013). ***C*** *Schematic representation of the metabolic processes that allow filamentous fungi to live from diverse plant cell wall derived sugars. Figure adapted from* Ali et al., 2016.

1.3 Fungal metabolism is regulated on the transcriptional level

Saccharomyces cerevisiae and filamentous fungi thrive on a variety of carbon-sources but most fungi prefer certain carbon sources more than others (Gancedo, 1993). When the primary carbon source is available, the enzymes required for the utilization of alternative carbon sources are repressed already on the transcriptional level by a conserved regulatory mechanism, termed carbon catabolite repression (CCR) (de Assis et al., 2021; Strauss et al., 1999). In *S. cerevisiae*, CCR is best understood for the galactokinase gene (*GAL1*) that is controlled by its upstream promoter. The *GAL1*-promoter activity depends mainly on the orchestration of the transcription-activator Gal4 and repressor Mig1 in a carbon dependent manner. Both factors are conducted by the sucrose nonfermenting kinase 1 (Snf1) (Conrad et al., 2014). In the presence of glucose, the repressor Mig1 is bound to the *GAL1*-promoter and the activator Gal4 is inactivated by the co-repressor Gal80 which renders the *GAL1*-promoter inactive. In the absence of glucose, the Snf1-complex is active and phosphorylates the Mig1 repressor protein. The phosphorylated Mig1 dissociates from *GAL*-promoters and is exported to the cytosol where it gets degraded by the proteasome as shown in **Figure 4**.

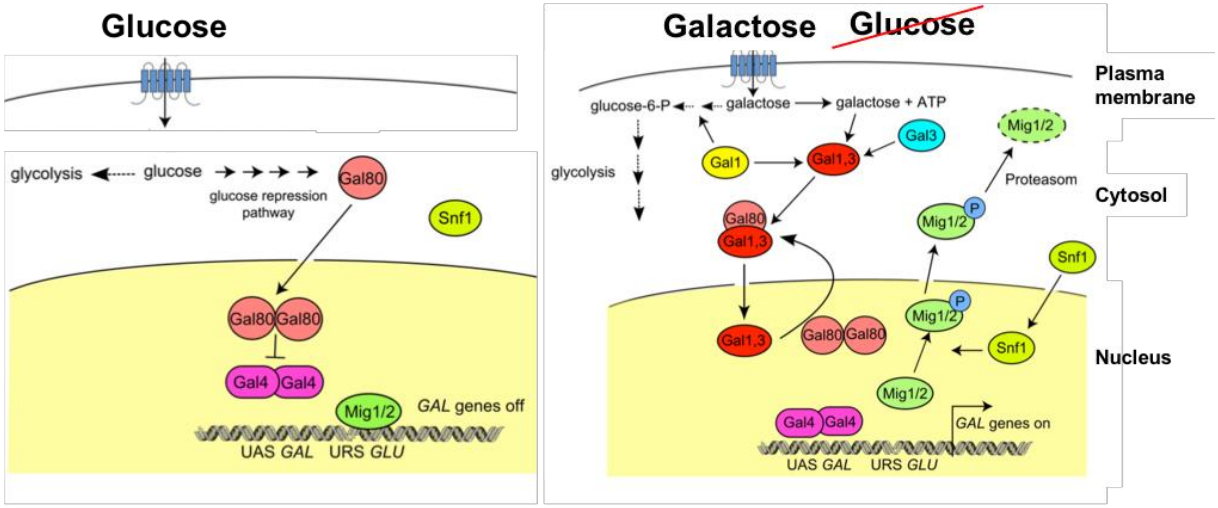

***Figure 4: Transcriptional regulation of galactose consumption in S. cerevisiae**. In the presence of glucose (preferred carbon source), the genes needed to consume alternative carbon sources like galactose are transcriptionally repressed upon binding of the repressor Mig1 to the GAL-promoter (left). In the absence of glucose and presence of galactose, the transcription repressor Mig1 is replaced by the transcription activator Gal4 that leads to GAL-genes activation. For closer details, compare text. Adapted from* Conrad et al., 2014.

When galactose is present, the regulatory protein-complex Gal-1,3 binds Gal80, thereby relieving its inhibitory action on Gal4 (Suzuki-Fujimoto et al., 1996). In turn, the Gal4 can activate the *GAL1* gene upon binding to the *GAL1*-promoter. The correct targeting of Gal4 and Mig1 to *GAL1*- promoters is channeled by conserved recognition motifs, encoded in the *GAL1*-promoter. The activator GAL4 recognizes one to four upstream-activating sequences (UAS) in the *GAL1*-promoter with its conserved N-terminal C6-zinc cluster DNA binding domain (Gancedo, 1993) and the Mig1-repressor recognizes in close proximity an upstream repressive sequence (URS) by its N-terminal C_2H_2-zinc finger domain (Griggs & Johnston, 1991).

Like yeast, also the filamentous fungi showed to apply the tight regulation mechanisms to repress genes with function in secondary catabolism during growth on preferred carbon sources (Amore et al., 2013). Homologs of the conserved carbon repressor from yeast (Mig1) were found also in the genomes of the filamentous relatives like *Aspergillus niger* (CreA), *Neurospora crassa* (Cre1) and *Trichoderma reesei* (CRE), reflecting conserved C_2H_2-zinc finger DNA binding domains (Amore et al., 2013). The CreA homologs are involved in the repression of promoters from hydrolytic acting gene products, involved in plant cell wall deconstruction in the presence of easily metabolizable carbon sources, such as glucose (Amore et al., 2013). The main

transcription activator proteins of lignocellulolytic genes are Gal4-homologs with C6-zinc finger domains, like the XYR1 (xylanase regulator 1) from *T. reesei* (Stricker et al., 2006, 2008). XYR1 activates promoters of genes with cellulolytic and hemicellulolytic acting gene products upon binding to conserved promoter regions in the absence of D-glucose and presence of hydrolysis products of cellulose and hemicellulose (Hrmova et al., 1991; Kurasawa et al., 1992; Mandels et al., 1962), as shown in **Figure 5** .

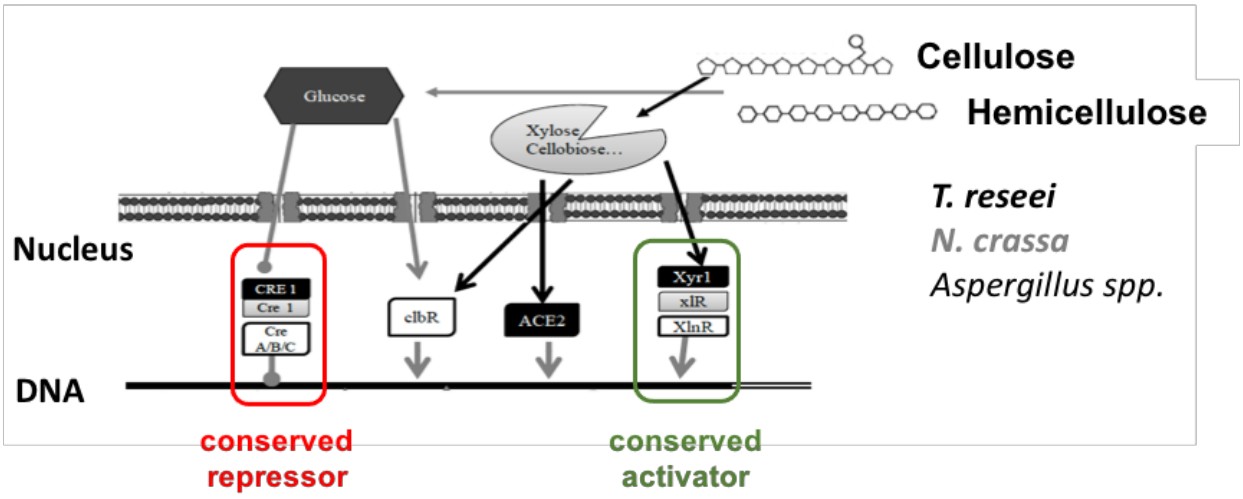

Figure 5: Transcriptional control of cellulolytic and hemicellulolytic genes in filamentous fungi*. Filamentous fungi like T. reesei, N. crassa or Aspergilli control lignocellulolytic function genes in a carbon dependent manner by carbon catabolite repression (CCR). The availability of easily metabolizable carbon sources leads to transcriptional repression of lignocellulolytic genes upon binding of CreA-homologs to CCR dependent promoters. In the absence of the preferred carbon source, alternative carbohydrate active genes are activated by XlnR-homologs. For further details, compare main text. Adapted from* Amore et al., 2013.

Even though the regulatory concept of carbon catabolite repression is conserved among the filamentous fungi, the regulatory mechanisms are as manifold as the availability of carbon sources in their complex environment. A recent study closer addressed the regulation of the CreA-repressor in the well-studied filamentous representative *A. nidulans.* There, CreA regulation comprise, similar to Mig1 in yeast, its inclusion and exclusion of the nucleus by phosphorylation dependent protein-protein interactions (Brown et al., 2013; Tanaka et al., 2018). In contrary to Mig1 in yeast, CreA becomes hyper-phosphorylated in the presence of glucose, by different protein kinases that results in CreA translocation to the nucleus where it causes promoter repression (De assis et al., 2021). In the presence of solely alternative carbon sources like hemicellulose, CreA is degraded in an ubiquitylation-dependent manner (de Assis et al., 2018) allowing initiation of gene-expression at hemicellulolytic promoters.

1.4 The strategies to control gene-expression in model organism

Gene expression systems became robust tools in the field of molecular biology that are traditionally introduced into cells on plasmids to study the physiology of organisms on a molecular level (Nora et al., 2019). In research, the expression of reporter-genes facilitates analytical and functional studies with fluorescent (Shaner et al., 2005), luminescent (Winson IY et al., 1998) or enzymatic properties (Juers et al., 2012). Expression systems exist in variable strength and can be broadly divided into constitutively active and regulatable ones, depending on the activity of the operating promoter. Especially the study of essential gene functions that are typically addressed by functional disruption of genes, requires tightly regulated promoters (Meyer et al., 2011). By now, a broad collection of regulatable promoters is described for fungi that react on various inducers, ranging from nutrients including various types of carbon and nitrogen sources to metal ions and light (Hovland et al., 1989; Hurley et al., 2012; Kluge et al., 2018; Lamb et al., 2013). Especially glucose repressed promoters that can be activated by host specific alternative carbon sources are heavily applied in filamentous fungi. These include the *cellobiohydrolase 1* (*cbh1)* promoter in *T. reesei* that is activated by a broad range of hemicellulose derived carbon sources (Chen et al., 2010; Jiang et al., 2020), the alcohol dehydrogenase promoter (*alcA)* in *A. nidulans* that is activated by ethanol (Waring et al., 1989) Felenbok et al., 2001) or the dehydroquinase promoter (*qa-2*) in *Neurospora crassa* that is activated by quinic acid (Geever et al., 1989). Whereas such native gene-expression systems typically reflect a narrow host specificity, synthetic expression systems were developed also for mesophilic filamentous fungi that allow broader host range applications as well as metabolism independent induction (Berens & Hillen, 2003; Meyer et al., 2011).

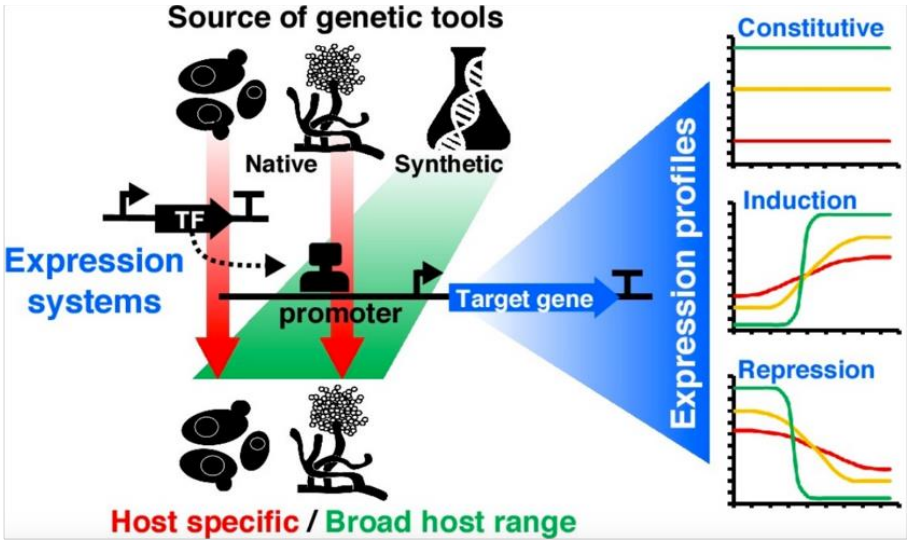

Figure 6: The Concepts of gene-expression systems in eukaryotic model systems*. Gene expression systems can be of native or synthetic nature. Depending on the promoter, constitutive or regulated gene-expression (inducible or repressible) is possible with various activities, depending on the promoter strength. Whereas native systems rely typically on host specific regulation mechanisms, synthetic systems are host independent. Adapted from* (Mojzita et al., 2019)*.*

The central concept of synthetic systems relies on the finding that the DNA binding domain (DBD) and the regulatory domains of transcription factors (TFs) stay functionally independent from each other. The most broadly applied synthetic system in eukaryotes is the tetracycline-regulatable promoter (Tet) which was also developed for selected filamentous model systems in Aspergilli and *Trichoderma reesei* (Meyer et al., 2011; Vogt et al., 2005). The central components of the “Tet-system” were exploited from a tetracycline resistance mechanism, studied extensively in *E.coli*. In the absence of tetracycline, the Tet-repressor (TetR) is bound to the operator sequence (*tetO*) of the *tet*-promoter and thus shuts off transcription of the tetracyclin resistance operon

Figure 7. To make the high affinity Tet-regulator work in eukaryotic cells, the Tet regulator was fused to the strong transcription activation domain (AD) of the herpes simplex virus protein 16 (VP16 AD) that lead to a hybrid transactivator tTA. The tTA binding is typically enforced by an array of several copies of the *tetO* sequence (tetO7) that forms together with a host specific minimal promoter (*Pmin*) the synthetic *tet*-promoter (Vogt et al., 2005). The established “Tet-OFF” system is active only in the absence of the inducer.

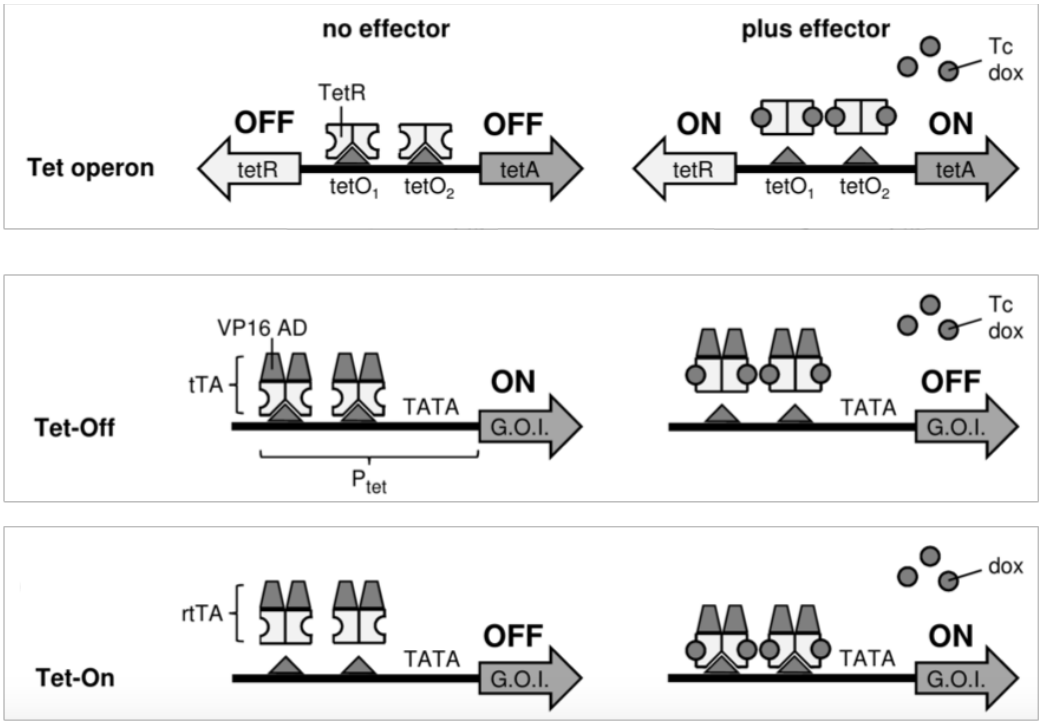

Figure 7: The synthetic "Tet"promoter-system. *The tetracycline inducible Tet-promoter system is adapted from a bacterial tetracycline resistance operon (Tet-operon) that operates with a synthetically modified transcription activator (tTA) and adapted promoter elements (tetO) that allows promoter induction in the presence of tetracycline (Tet-OFF) or its absence (Tet-ON). For further details, see text. Taken from* (Das et al., 2016).

Further mutational optimization of the tTA led later to the "Tet-ON" system. The obtained reverse tTA (rtTA) needs tetracycline as ligand to efficiently bind to the *tetO* sequence to activate the promoter and expression of a gene-product of interest, shown in (Das et al., 2016). The Tet-promoter is broadly applied next to complex filamentous fungi also in plenty of applications in the field of ribosome biogenesis in mammalian cells (Romes et al., 2016; Zorbas et al., 2015). In order to profit from such synthetic systems also in thermophilic organisms, such regulatory elements must be assembled with thermostable properties, that do not exist, yet.

1.5 The architecture of eukaryotic ribosomes

Ribosomes are highly conserved and complex nanomachines that synthesize all proteins in cells (proteome) according to the genetic information in the genome (Fox et al., 2019). The eukaryotic ribosomes consist out of the large 60S ribosomal subunit (LSU) and the small 40S ribosomal subunit (SSU), shown in Figure 8. The „S“ stands for the sedimentation coefficient Svedberg that is used to define molecular sizes by ultracentrifugation of large molecular complexes like ribosomes and its pre-cursors. As major hallmarks, the SSU harbors the characteristic structural elements head, platform, body and beak and the LSU contains the L1-stalk, the central protuberance (CP) and the P-stalk next to the peptidyl transfer center (PTC) and the polypeptide exit tunnel (Ben-Shem et al., 2011).

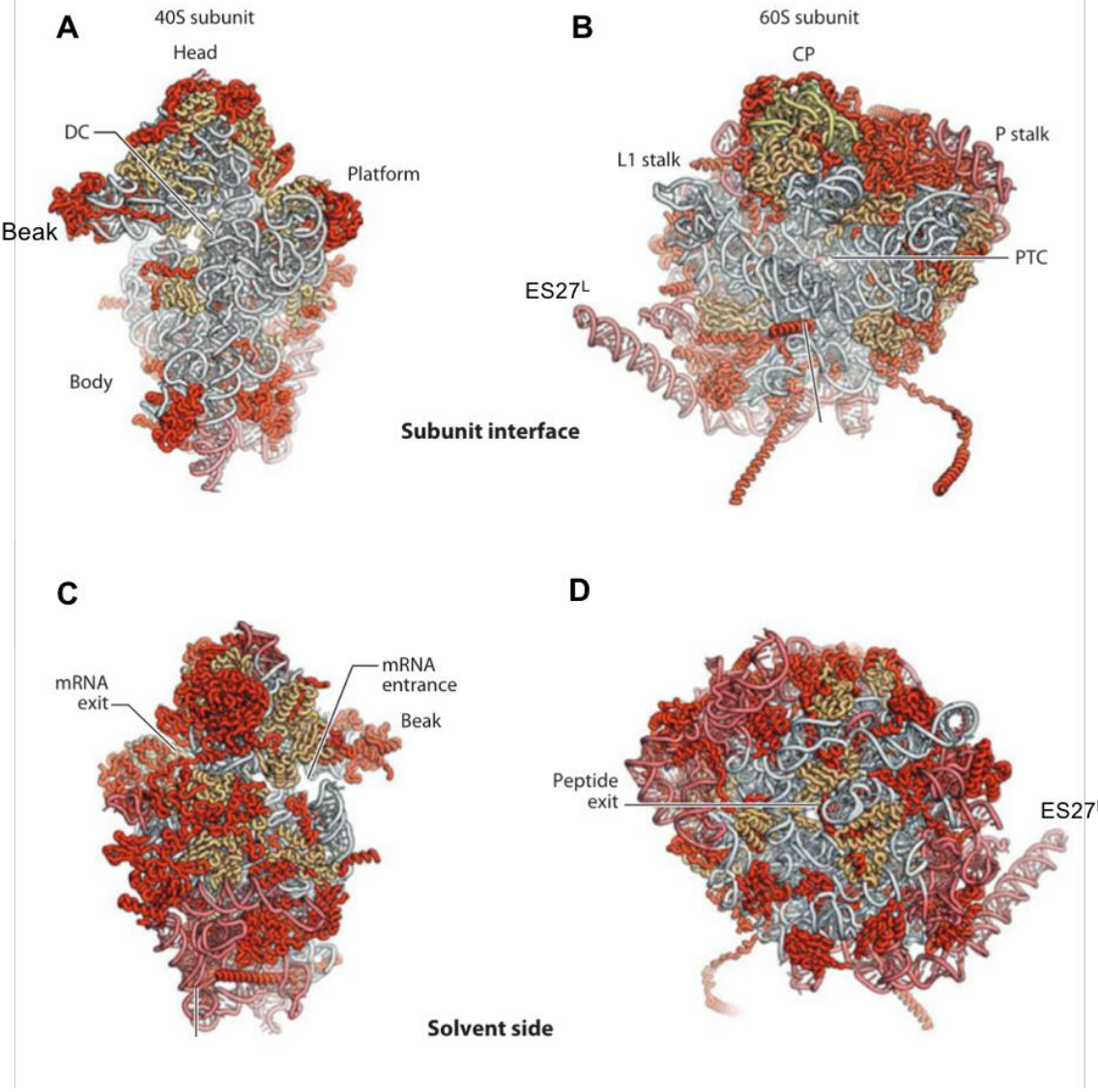

Figure 8: The architecture of the eukaryotic ribosome from S. cerevisiae. *Shown are the sub-unit interfaces of the small (A) and the large (B) sub-units as well as the solvent exposed view on the small (C) and large (D) sub-unit. Characteristic structural hallmarks of the small sub-unit comprise the head, body, platform and beak as well as the mRNA decoding center (DC), the mRNA entrance and exit sites. The large sub-unit features the L1 stalk, the central protuberance (CP), the P stalk and the peptidyl-transfer-center (PTC) as well as the peptide exit tunnel. For further explanations, see text. The ribosomal RNA core is shown in white, proteins in orange. Eukaryote-specific elements like the dynamic ES27^{L} are shown in red. Figure modified from Yusupova & Yusupov, 2014.*

During the translation process, the SSU provides the mRNA decoding center (DC) as well as the entry and exit tunnel of the mRNA template, whereas the LSU coordinates the peptidyl transferase center (PTC) to catalyze the elongation of the growing peptide chain (Bernier et al., 2018). The L1 stalk as mobile element in the LSU helps to evacuate the exit-site from tRNA. Both sub-units are physically and mechanistically coordinated by the central protuberance that forms junctions between multiple RNA

elements like the dynamic P stalk Figure 8. The 80S ribosome contains four ribosomal RNAs (rRNAs), forming a conserved core that is encapsulated by ribosomal proteins (r-proteins) (Melnikov et al., 2012). In yeast, the 40S subunit contains the 18S rRNA and 33 proteins (Ben-Shem et al., 2011; Planta and Mager, 1998) and the 60S subunit contains the three rRNAs 5S, 5.8S and 25S on which 46 L-proteins (large-sub-unit proteins) are mounted. The eukaryotic ribosomes are more complicated compared to the prokaryotic counterparts, to which eukaryote specific expansion segments (ES) like variable regions in the rDNA as well as many additional r-proteins and r-protein extensions contribute to (Armache et al., 2010). One intriguing variable rRNA region is the $ES27^{L}$ which features a unique dynamic flexibility, ranging from an orientation towards the L1 stalk and 110° away from it to the exit of the peptide tunnel that is suggested to be involved in coordinating the access of nonribosomal factors at the exit site of the peptide tunnel (Beckmann et al., 2018).

1.6 The assembly process of eukaryotic ribosomes

Ribosome biogenesis is an essential and highly energy demanding process in eukaryotes. Thus, the production of ribosomes is adapted strictly to the growth condition of the organisms to coordinate cell proliferation. In exponentially growing yeast cells, at least 2000 ribosomes are assembled each minute (Warner, 1999). For each ribosome, about 5500 nt of rRNA must be synthesized, modified, folded, and correctly assembled with 79 ribosomal proteins (r-proteins). In the assembly process of a eukaryotic ribosome, about 200 different proteinogenic biogenesis factors (BFs) and 76 different small nucleolar RNAs (snoRNAs) showed to be involved. The ribosomal RNA (rRNA) is encoded in repetitive units on Chromosome XII in the nucleolus with varying copy numbers of ribosomal DNA (rDNA) among species (Lilia Torres-Machorro et al., 2009). Interestingly, from at least 150 rDNA units in yeast, only a sub-set of the rRNA repeats is active due to transcriptional regulation mechanism (French et al., 2003). The actively transcribed rDNA units can be seen in “Chromatin miller spreads” since the growing rRNA gets co-transcriptionally decorated with r-proteins and biogenesis factors (French et al., 2003). To enable the production of translation-competent ribosomes, the concerted activity of all three RNA-polymerases (RNAPs) is needed (Turowski & Tollervey, 2015). The transcription of one rDNA unit requires the RNAP I to transcribe the polycistronic 35S rRNA, encoding for the 18S,

5.8S and 25S rRNAs and RNAP III transcribes the 5S rRNA **Figure 9**. The RNAP II is needed to synthesize all messenger-RNAs (mRNAs), encoding also for the r-proteins and assembly factors.

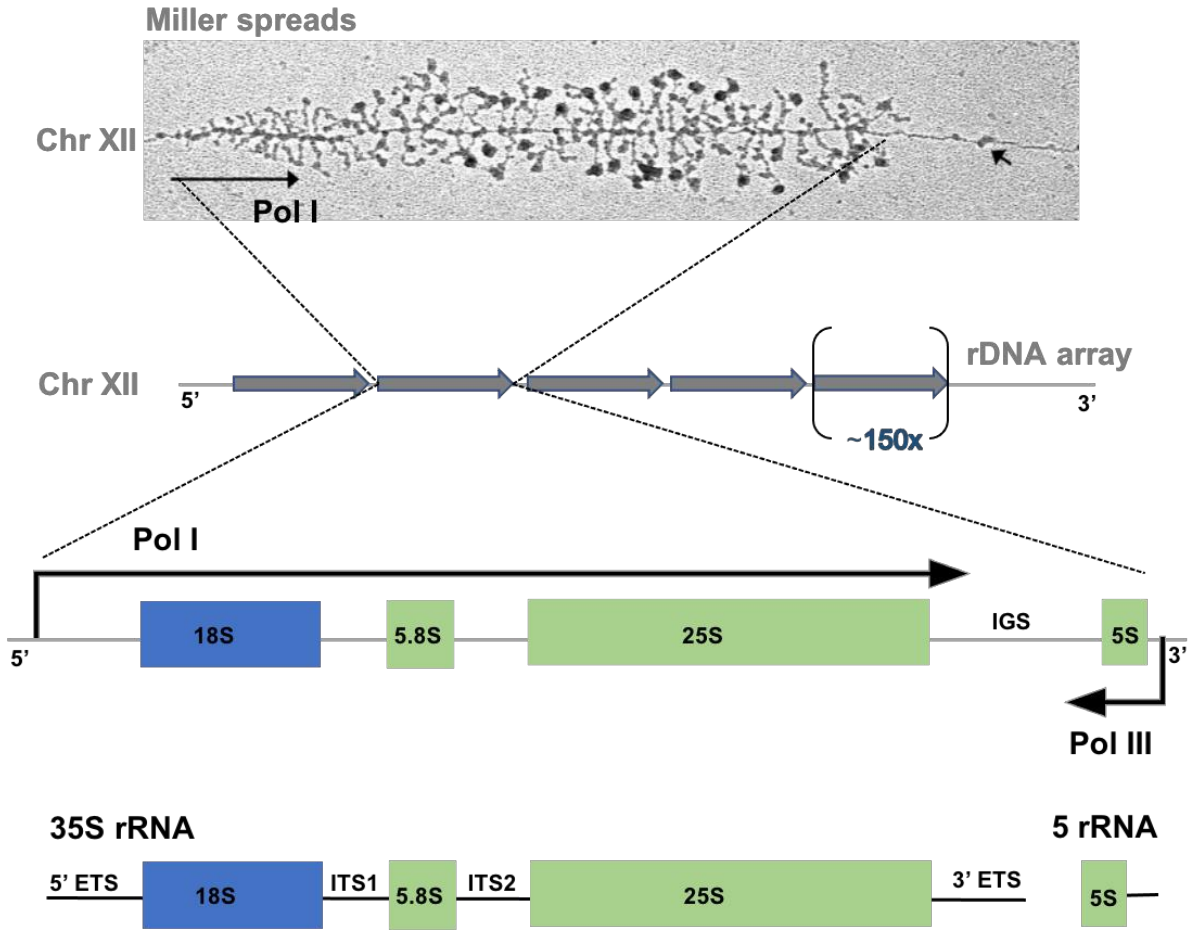

***Figure 9: The transcription of rRNA in S. cerevisiae**. Repetitive units of the ribosomal DNA (rDNA) are encoded on chromosome XII in the nucleolus. The polycistronic 35S rRNA pre-cursor is transcribed by the RNA-polymerases (Pol)) I and the 5S rRNA by Pol III. The 35S rRNA contains the 18S rRNA for the small 40S subunit (blue) and the 5.8S and 25S rRNA for the large 60S subunit (green). The rRNA genes are separated by externally transcribed sequences (ETS) and internally transcribed sequences (ITS). The separately transcribed 5S rRNA gets incorporated along the large subunit biogenesis (green). Co-transcriptional assembly of ribosomes can be seen in "Chromatin miller spreads" by co-transcriptional decoration of the rRNA with binding proteins. Miller-spreads taken from* (French et al., 2003).

The process of ribosome biogenesis has a long tradition to be studied in *S. cerevisiae*, where the induction of dominant negative and lethal biogenesis mutants led to various mechanistic insights (Barrio-Garcia et al., 2016; Baßler et al., 2010; Bernstein et al., 2006; Pertschy et al., 2007; Ulbrich et al., 2009; West et al., 2005). Together with structural analysis of pre-ribosomal intermediate particles, by cryogenic electron microscopy (cryo-EM) in the last years, a comprehensive model of ribosome

biogenesis could be built. The concepts of ribosome biogenesis of the small and large subunits are matter of the next chapters.

1.6.1 Biogenesis of the small 40S subunit

A hallmark of the small sub-unit biogenesis in yeast is the cotranscriptional assembly of the small subunit processome that is visible as terminal knobs in “chromatin miller spreads” on the nascent rRNA (French et al., 2003; Osheim et al., 2004). The growing rRNA as product of the RNAP I gets decorated in a hierarchical manner by the U3 small nucleolar RNA-associated protein modules UTP-A and UTP-B, followed by the U3 snoRNP and the Mpp10-Imp3-Imp4 modules that together build the 5’ETS particle (Dutca et al., 2011; Hunziker et al., 2016), shown in **Figure 10**.

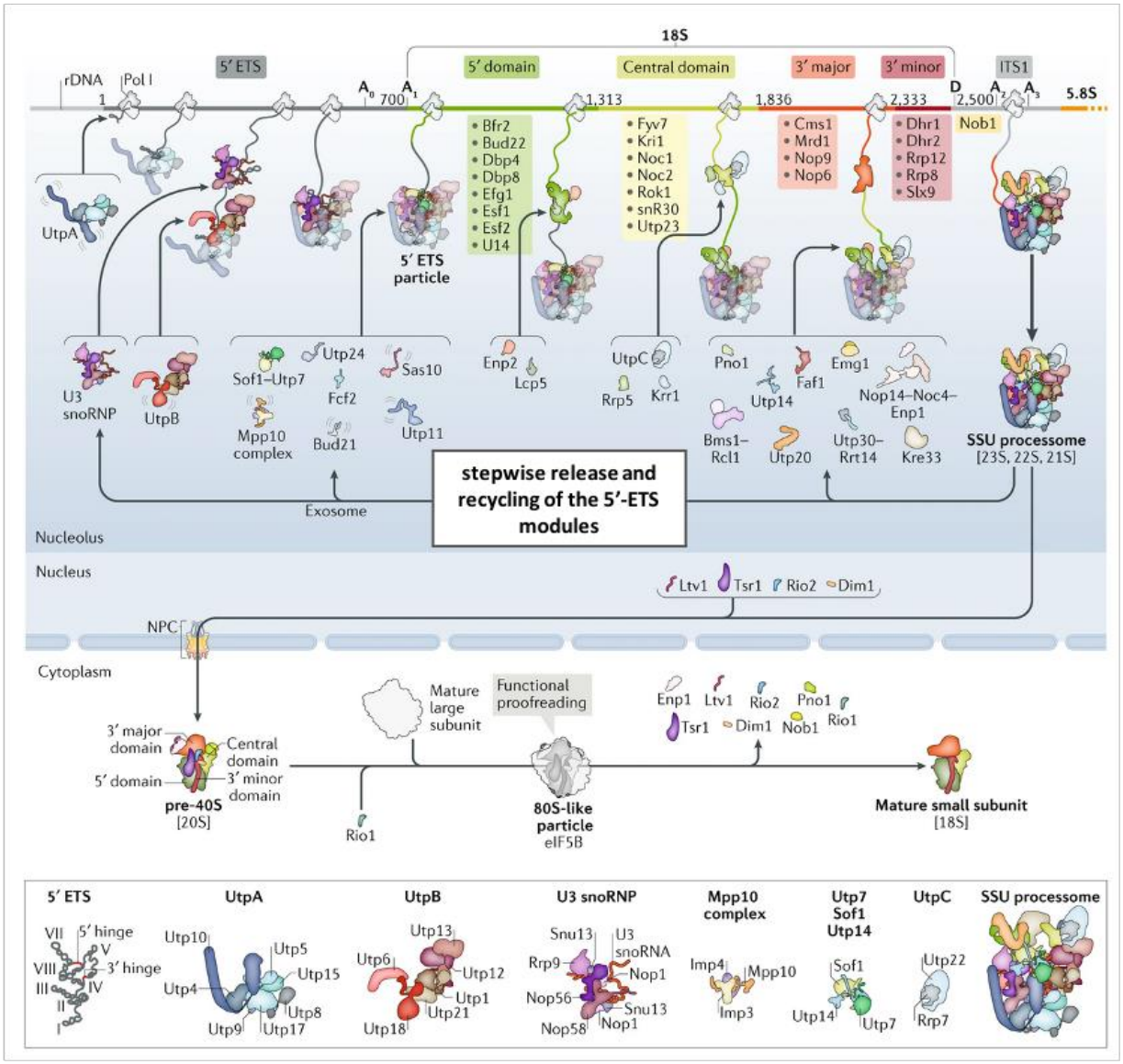

Figure 10: Biogenesis of the small ribosomal subunit (SSU). *Shown is the sequential order of co-transcriptionally binding of subcomplexes and biogenesis factors to the 5' ETS and 18S rRNA transcript that results in the SSU-processome (aka. as 90S particle). Endonucleolytic cleavage at the A_2 site in the ITS1 disconnects the processing of the small subunit processome (SSU) from the ongoing transcription of the 35S rRNA. The 5'ETS particle gets stepwise recycled in the nucleolus and the primordial 40S particle gets exported into the cytoplasm where it is subjected to a final quality control steps. For more details, see text. Taken from (Klinge & Woolford, 2019) with modified recycling of the 5' ETS modules according to* (Cheng et al., 2020).

Cotranscriptionally, further subdomains and assembly factors bind to the 5' domain, central, 3' major and 3' minor domain of the 18S rRNA, as shown in **Figure 10** (Chaker-Margot et al., 2017; Pérez-Fernández et al., 2011; L. Zhang et al., 2013). Interestingly, the folding and compaction of the 18S rRNA does not follow the order of transcription but the first transcribed 5' domain showed to be the latest one to be incorporated into the first stable pre-ribosomal particle, known as 90S intermediate (Cheng et al., 2019).

This early forming 90S pre-ribosomal particle (Grandi et al., 2002), also referred to as the small subunit processome (Dragon et al., 2002), was firstly structurally solved by cryoEM from *C. thermophilum* (Cheng et al., 2017; Kornprobst et al., 2016) allowing detailed insights into its architecture.

During the development of the 90S intermediate, two critical endo-nucleolytic cleavages in the 35S pre-rRNA take place. These cleavages occur at the A_1 site that disconnects the 5′-ETS from the 5′ end of the 18S rRNA as well as at the A_2 site in the internal transcribed spacer 1 (ITS1) that generates the 20S precursor of the 18S rRNA (Chaker-Margot et al., 2017) and the 27SA_2 precursor that further matures in an independent process towards the rRNAs of the large 60S subunit (Greber, 2016).

Following A_1 cleavage, the 5′-ETS RNA binding 90S-factors need to be released and the rRNA degraded, for which the exosome is needed. Interestingly, the exosome gets recruited to the 90S particle already before the A_1 cleavage (Lau et al., 2021) which is mediated by the endonuclease Utp24 (Bleichert et al., 2006; Wells et al., 2016). The exosome provides a ring structure, through which the substrate RNA is channeled to the associated nucleases Rrp44 and Rrp6 with endo- and 3′-5′ exonucleolytic activity (Lebreton et al., 2008; Q. Liu et al., 2006; Thoms et al., 2015), shown in **Figure 11**.

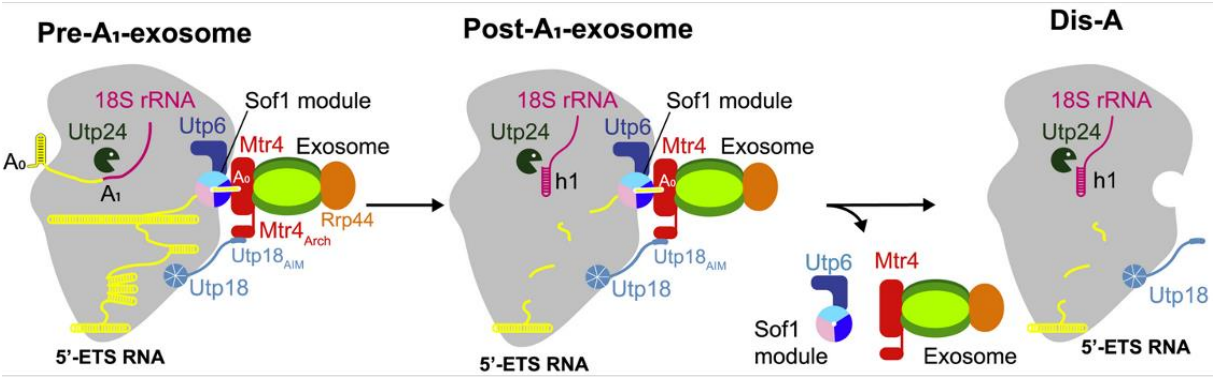

Figure 11: Model of the exosome recruitment to the 90S intermediate and the 5'-ETS degradation upon A_1 cleavage. *The exosome is recruited by Mtr4 to the 90S intermediate particle before Utp24 mediated A_1 cleavage. Mtr4 interacts with Utp18 in close proximity to the Sof1 module and UTP6 (Pre-A_1-exosome). The 3' end of the 5'-ETS-A_0 fragment is channelled into the Mtr4-exosome and degraded (post-A_1-exosome). Degradation of the 5'-ETS results in the release of the exosome together with the Sof1 module and Utp6, as it is seen in the dissociation class Dis-A. Figure taken from* Lau et al., 2021.

For the exosome recruitment, Mtr4 acts as adapter protein that allows it to bind to the 90S particle with its arch-domain that interacts with the arch interaction domain (AIM-domain) of Utp18 (Thoms et al., 2015). This interaction is suggested to be stabilized

by a platform on the 90S particle, provided by the closely located UTP-B factor UTP-6 and the Sof1 module (Utp7, Utp14, and Sof1) (Lau et al., 2021). In contrary to an earlier thought release and recycling of the 5'-ETS modules "en block", the most recent structural investigations proved a stepwise dislodging of the 5'-ETS modules from the 90S particle that leads to the pre-40S intermediate, as shown in **Figure 12**. After the A_1 cleavage, the Sof1 module is the first dislodged module, as seen in the transition from the Post-A_1 state to the first "dislodged-state" (Dis-A). Subsequently, the U3snoRNP and the UTP-A modules are released (Dis-A to Dis-B)

and finally the UTP-B and UTP-C submodules (Cheng et al., 2020). Only after the release of the UTP-B module, the helicase Dhr1 is found in its active state and bound to the remaining portion of the U3 snoRNA that binds to the 18S rRNA (Dis-C) to allow its complete release in an ATP dependent manner (Cheng et al., 2020; Roychowdhury et al., 2019; Zhu et al., 2016). The release of the U3 snoRNA plays an important role as it prevents the pre-mature formation of the central pseudoknot (CPK) by its binding to the 5'ETS and the 5' region of the 18S rRNA (Marmier-Gourrier et al., 2011; Sardana et al., 2015).

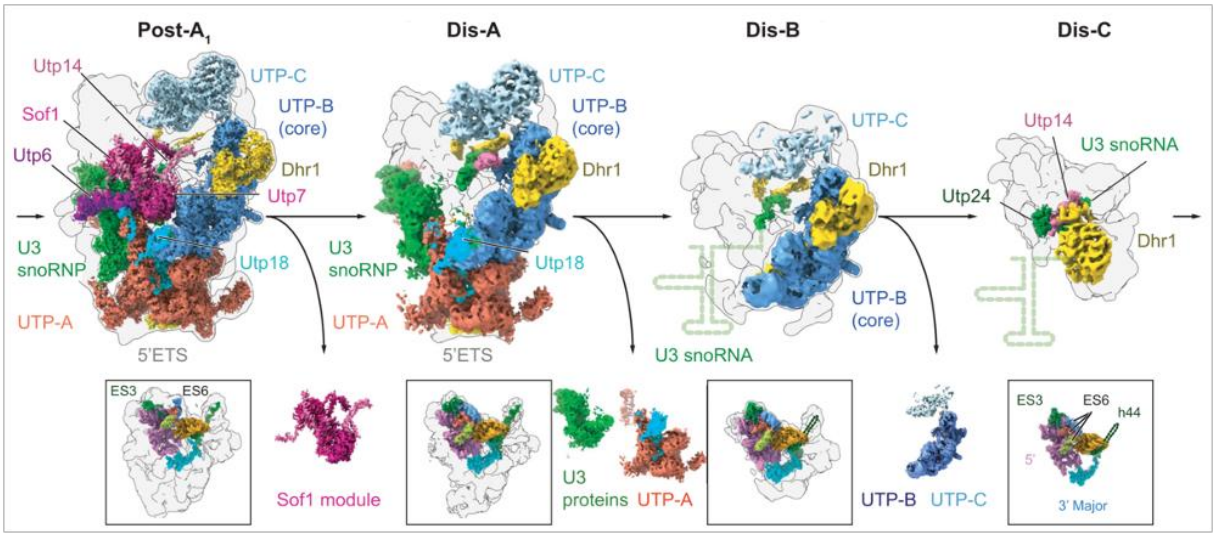

Figure 12: 90S maturation intermediates leading towards the pre-40S. *Shown is the stepwise dislodging of the 5'-ETS modules from the 90S intermediate after the A_1 cleavage (Post-A1) leading towards a pre-40S particle that is seen in the Dis-C state. For closer details, see main text. Figure taken from* Cheng et al., 2020.

In the nucleus, the pre-40S subunit associates with export factors (e.g. Ltv1 and Rio2) and export adaptors. Subsequently, the export receptor Crm1 gets recruited to the pre-40S subunit that leads to its translocation through the nuclear pore complex (NPC) into

the cytosol in a Ran-GTP dependent manner (Hurt et al., 1999). In the cytosol, the pre-40S subunit gets subsequently subjected to a final quality control step, in which an 80S-like ribosome is formed by the recruitment of a mature large 60S subunit to the pre-40S by eIF5B. The formed pre-80S ribosome is however not translation competent as the mRNA and initiator tRNAs cannot bind, yet (Strunk et al., 2012). In this translation-like test cycle, the 20S rRNA is finally processed towards the 18S rRNA upon trimming from its 3'end by the endonuclease Nob1. Concomitantly, the last biogenesis factors are released (Fatica et al., 2003; Strunk et al., 2012) which make the mRNA channel as well as the initiator tRNA binding site accessible and the small subunit is finally mature and ready to engage in translation (Strunk et al., 2011).

1.6.2 Biogenesis of the large 60S subunit

The biogenesis of the 60S subunit is a complex multistep process that is clearly different compared to the afore described 40S subunit which matures largely in the scaffolding 90S mold forming structure (Kressler et al., 2017; Woolford & Baserga, 2013). The very early stages of pre-60S formation, before and after its separation from the 90S, have been the focus of a recent study (Ismail et al., 2022). The physical link of the early 60S particle to the 90S intermediate is suggested to be provided by the UTP-C module. Indeed, the location of this physical connection toes the line with the here positioned factor Rrp5 that is described as linking factor between the small and the large subunit (Eppens et al., 1999; Hierlmeier et al., 2013; Torchet et al., 1998). Interestingly, this primordial pre-60S particle enriches a unique set of assembly factors and snoRNPs, such as the C/D box R190 and the H/ACA box snR37 (Ismail et al., 2022), which could play also a structural role, similar to the U3 snoRNA in the 90S intermediate. In principle, the assembly of the 60S subunit can be divided into the folding steps of the six domains of the 25S rRNA (I–VI) that assemble stepwise in a monolithic structure, though not according to their transcriptional order (Ben-Shem et al., 2011; Kater et al., 2017). Rather a circularization of the 5.8S sequence, the ITS2 and the domains I and II, forming the solvent interface with parts of the most 3' located domain VI is observed, while the domains III, IV and VI remain flexible. Subsequently, these flexible domains are folded to complete the formation of the peptidyl exit tunnel along the transition from the nucleolus to the nucleoplasm, as shown in Figure 13.

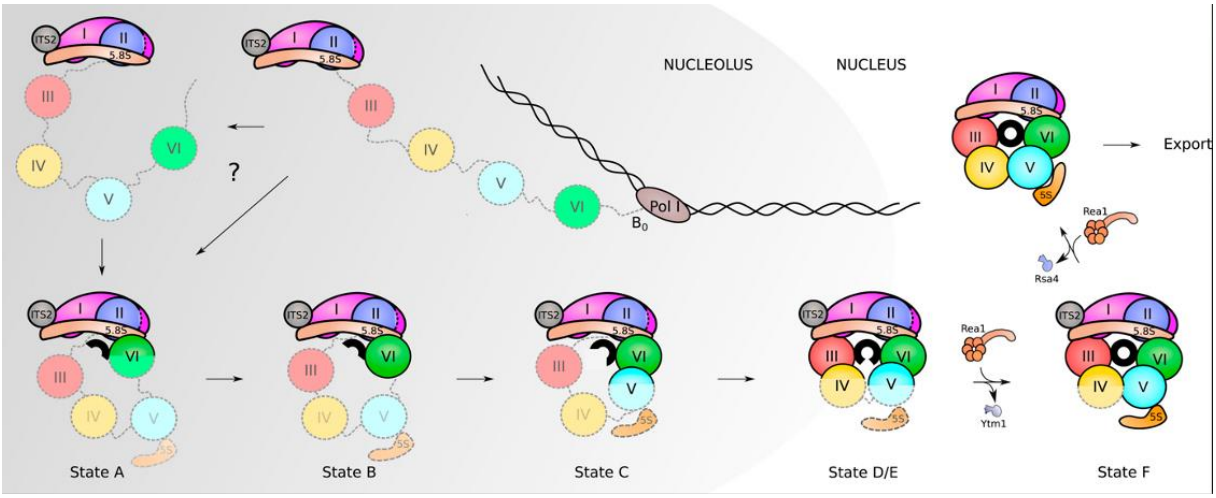

Figure 13: Schematic representation of the stepwise assembly of the large 60S subunit. *The 60S subunit assembles on the rRNA, leading to the stepwise formation of the poly peptide exit tunnel (PET) as it is illustrated by the closing black circle. Importantly, the folding of the rRNA of the large subunit does not occur co-transcriptionally. Early in the nucleolus, the portions of the 5.8S rRNA, the ITS2 region and the 25S rRNA domains I and II circularize with the domain VI of the 25S rRNA (State A). Then, the 25S domains VI-V-IV-III are incorporated to form the monolithic 60S structure, that leads to the completion of the PET in the nucleus with domain V. For more details, see main text. Figure taken from* Kater et al., 2017.

The first precursor of the large subunit, the 27SA rRNA emerges co-transcriptionally upon cleavage at the A_2 site and contains the 5.8S rRNA, the ITS2 and the 25S rRNA. Already in the nucleolus, this $27SA_2$ precursor is mostly processed by the RNase MRP (Chu et al., 1994; Lindahl et al., 1992; Schmitt & Clayton, 1993) and the exonucleases Rat1, Xrn1 and Rrp17 process the remaining ITS1 sequence, leading to the 27SB pre-rRNA with a mature 5' end of the 5.8S rRNA (Henry et al., 1994; Oeffinger et al., 2009).

The 5S rRNA is contained within the 5S RNP particle, formed by the 5S rRNA and the ribosomal proteins Rpl5 and Rpl11 that gets recruited to the maturing pre-60S subunit in the nucleolus (Kater et al., 2020; J. Zhang et al., 2007). Strikingly, the 5S RNP gets tethered to the maturing pre-60S particle in a twisted position that requires a rotation of ~180° to reach the conformation, seen in mature 60S subunits (Leidig et al., 2014). At this stage, the characteristic "foot" structure is built around the ITS2 sequence by the factors Nop7, Nop15, Nsa3 and Rlp7, that is not present in mature 60S subunits (Wu et al., 2016; Bradatsch et al., 2012). The loss of the foot structure is timely synchronized with major remodeling events on the rRNA and the interacting proteins in the area of the foot structure during the transition from the nucleolus to the nucleoplasm. These include the removal of the Erb1-Ytm1 complex by the huge dynein

related AAA+ATPase-Rea1 (Baßler et al., 2010; Thoms et al., 2016) as well as the cleavage of the ITS2 by Las1 that leads to the loss of the foot structure (Gasse et al., 2015; Thoms et al., 2016; Thomson & Tollervey, 2010). The rotation of the 5S RNP into its mature conformation requires binding of Sda1 that allows the Rix1 subcomplex (Ipi1/Rix1/Ipi3) to bind, to which the AAA+ ATPase Rea1 gets recruited (Barrio-Garcia et al., 2016). The binding of the Rix module together with the ATPase Rea1 allows the rotation of the 5S RNP upon destabilizing its interaction with Rsa4. The structural rearrangements in the 5S RNP, forming the central protuberance area, are suggested to activate the ATPase activity of Rea1 which removes Rsa4 and itself in its second mechanochemical power-stroke reaction, shown in **Figure 14** (Baßler et al., 2010; Kressler et al., 2017; Leidig et al., 2014; Ulbrich et al., 2009).

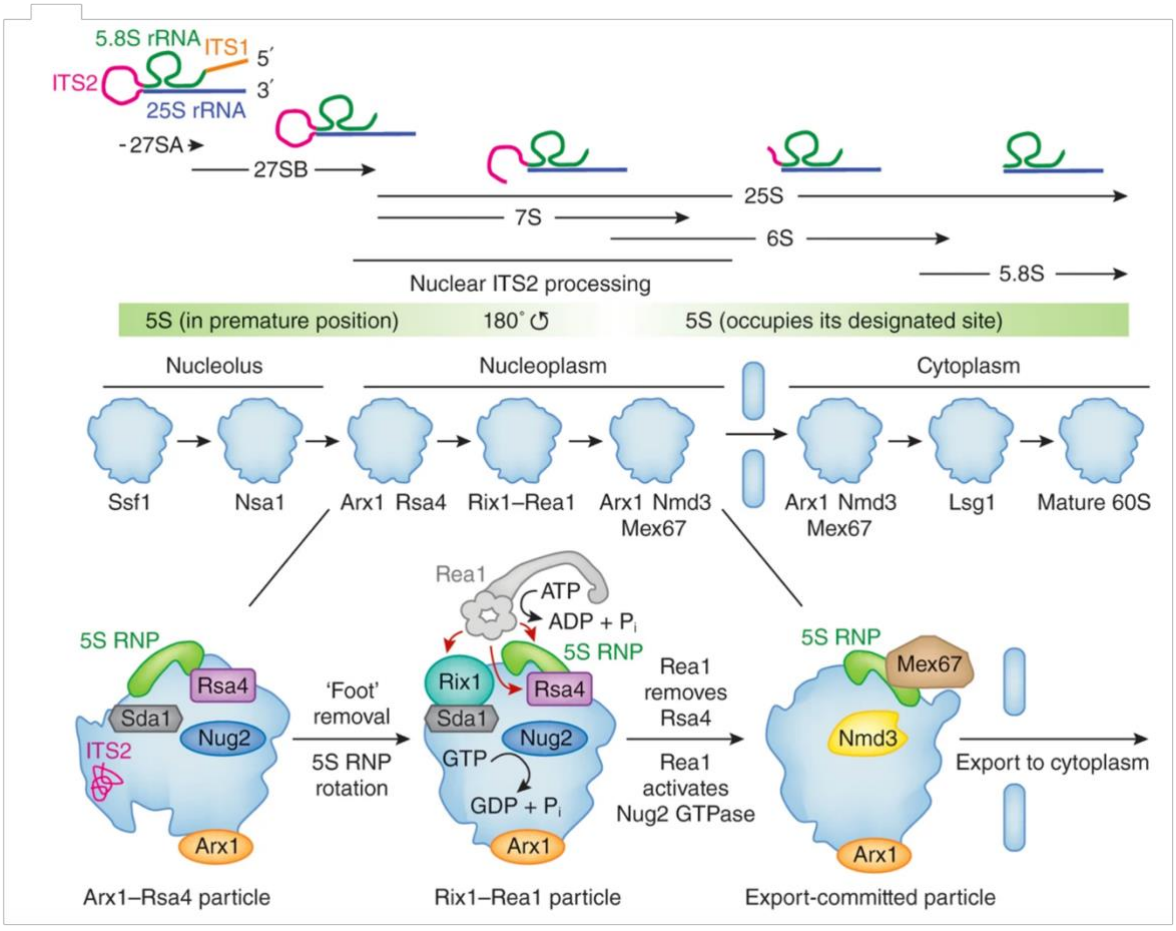

Figure 14: The biogenesis of the large 60S subunit (LSU). *Shown are the stepwise processing events of the rRNA of the LSU leading from the primary 60S specific 27SA pre-cursor containing the ITS1, 5.8S rRNA, 25S rRNA towards the mature 25S rRNA and 5.8S rRNA. Purified 60S intermediate particles are aligned according to their rRNA processing states and localization to the nucleolus, the nucleoplasm and the cytosol. Highlighted the removal of the foot structure and the rotation of the 5S RNP into its mature conformation. For closer details see text. Figure taken from (Shchepachev & Tollervey, 2016)*

The binding of the Rea1-MIDAS domain to its substrates Ytm1 and Rsa4 provides quality control before particle export into the cytosols since perturbations of these interactions result in dominant negative yeast phenotypes, when induced under control of the *GAL1*-promoter. In such mutants, 60S particles accumulate in the nucleus, as shown for the Rsa4 mutant E114D in **Figure 15** (Barrio-Garcia et al., 2016; Baßler et al., 2010; Ulbrich et al., 2009).

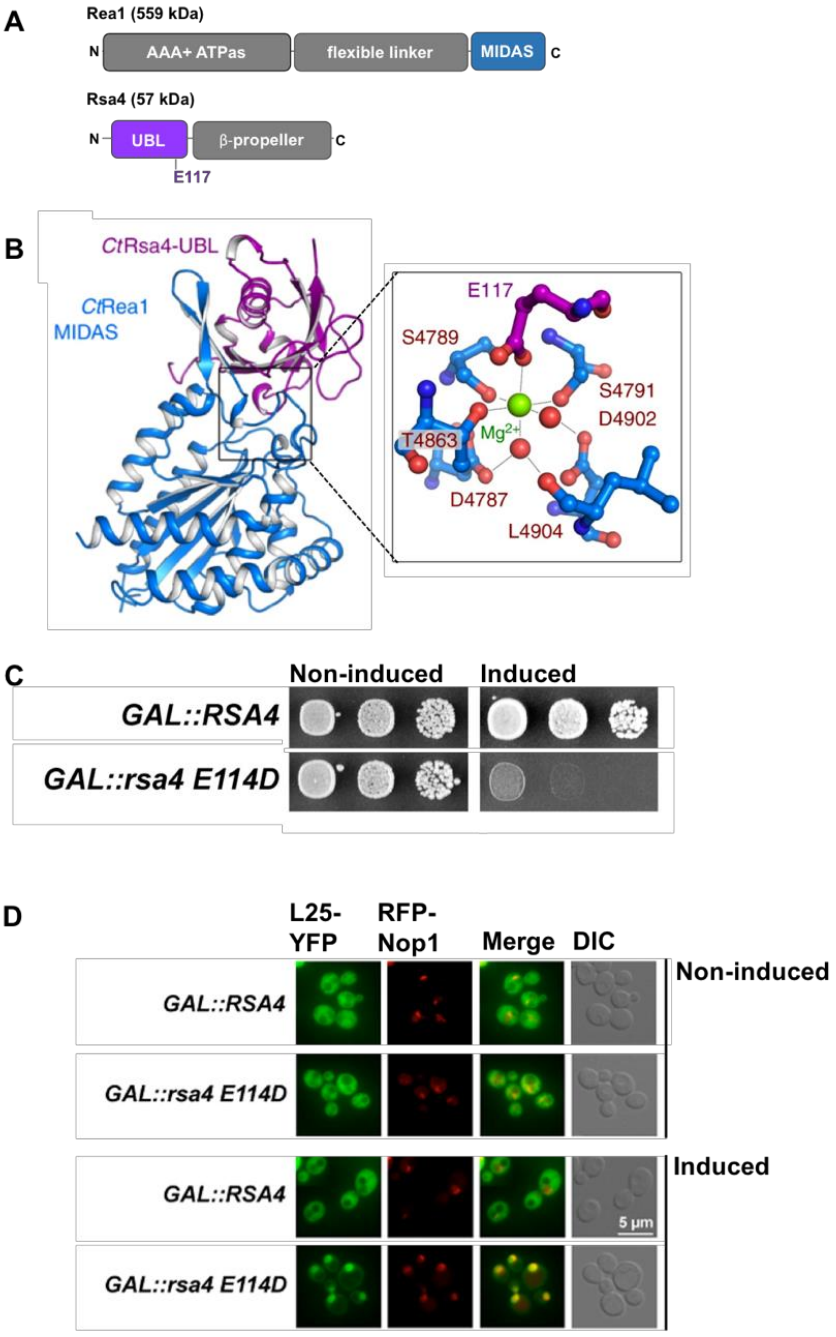

Figure 15: The essential interaction between Rea1 and Rsa4. A *Shown is a cartoon of the AAA+ ATPase Rea1 with its C-terminal MIDAS (metal ion dependent adhesion domain) that interacts with the N-terminal UBL (ubiquitin-like)-domain of Rsa4 in which the conserved E114 is essential.* ***B*** *Shows the crystal structure of the MIDAS-domain of ctRea1 (blue) in contact with the UBL domain of ctRsa4 (purple). The square shows a close-up of the interacting residues from Rea1 MIDAS that are complexing a central Mg^{2+} ion together with E114 from the UBL of Rsa4 (modified from Yasar et al., 2019).* ***C*** *Shows a dominant negative growth phenotype upon induction of the E114D mutation in the UBL of Rsa4 under control of GAL1-promoter.* ***D*** *Shows with help of a 60S subunit export reporter (L25-YFP) that induction of the E114D mutant causes 60S subunit export arrest in the nucleoplasm. RFP-Nop1 was used as nuclear marker. C and D were modified from Ulbrich et al., 2009.*

In wildtype yeast cells, the removal of Rsa4 by Rea1 in turn activates the release of the GTPase Nug2, which binding site is taken over by the export factor Nmd3 that itself

recruits the exportin Xpo1 (Crm1) with Ran-GTP (Matsuo et al., 2014). These export mediating factors together with Arx1 allow transport of the 60S pre-ribosome cargo through the nuclear pore into the cytoplasm (Gadal et al., 2001; J. H. N. Ho et al., 2000). In the cytoplasm, finally the last assembly factors Lsg1 and Nmd3 are released from the pre-60S ribosomal subunit and eventually shuttle back into the nucleus (Hedges et al., 2005;Kutay et al., 2010; Pertschy et al., 2007; Kargas et al., 2019; Ma et al., 2017). In the cytoplasm, the anti-association factor eIF6, sterically blocking ribosomal-subunit joining, is released from correctly assembled 60S subunits which are then able to form mature 80S ribosomes together with the small 40S ribosomal subunit (Weis et al., 2015).

1.7 Aims

The thermophile *Chaetomium thermophilum* was established in the lab to exploit its remarkably stable proteome to study the structures of the nuclear pore complex and the process of ribosome assembly. As prerequisite to purify proteins and associated particles with help of affinity purifications, a thermostable selection marker was developed to stably integrate expression cassettes into its genome. However, no inducible promoter was available to study dominant mutants mapping into the pathway of ribosome assembly, as it was successfully applied in the model organism *S. cerevisiae*.

The aim of this work was the development of an inducible promoter-system for *C. thermophilum* to control dominant negative ribosome biogenesis mutants. As proof of concept, we wanted to test first a known mutant from the yeast model in *C. thermophilum* under control of a regulatable promoter. In order to find regulatable promoters, we thought to explore carbon sources as inducing compounds. To identify the most strictly regulated promoters in its genome, we pursued a transcriptome deep-sequencing approach. Promoter spanning regions from the most strictly regulated transcripts could be tested with the available thermostable YFP-reporter. Subsequently, we wanted to test the promoters to study the process of ribosome biogenesis. Accordingly, I sought to study overexpression of the 90S particle purifying nucleolar assembly factor Utp-6 as bait under control of the inducible promoters. Furthermore, I aimed to demonstrate the control of the dominant negative ribosome biogenesis mutant Rsa4 E114D that arrests 60S subunit export in yeast, when expressed under control of the *GAL1*- promoter. Thus, I planned to use L25-YFP to show accumulation of the 60S subunit in the nucleoplasm when *rsa4* is induced under control of a xylose activatable promoter in *Chaetomium thermophilum*.

2 RESULTS

2.1 Identification of sugar-controlled transcription factors in *Chaetomium thermophilum*

The aim of this study was to establish an inducible promoter system for *Chaetomium thermophilum* as a genetic tool to study ribosome biogenesis. Hence, we searched for endogenously regulated promoters, which are regulated by its thermostable proteins. The rational was that the universally applied expression systems in mesophilic relatives, like the “tet-system”, was unlikely to be applicable in the thermophile due to its high growth temperature of 50°C. Encouraged by the inducing capability of different sugars on promoters to control gene-expression in other fungi, we thought to find such promoters also in *Chaetomium thermophilum*. Since I found the conserved carbon controlled transcriptional factors by a homology blastp-search in its genome, I gained confidence to find also carbon regulated promoters. Using the *trans*-repressor CREA from *Aspergillus niger* as query, I found respective homologs encoded by CTHT_0038780 and CTHT_0038840. In agreement with hits closely related mesophilic fungi, both transcription factors (TFs) in *C. thermophilum* shared the characteristic zinc-finger DNA binding domain in their N-terminal region **Figure 16**.

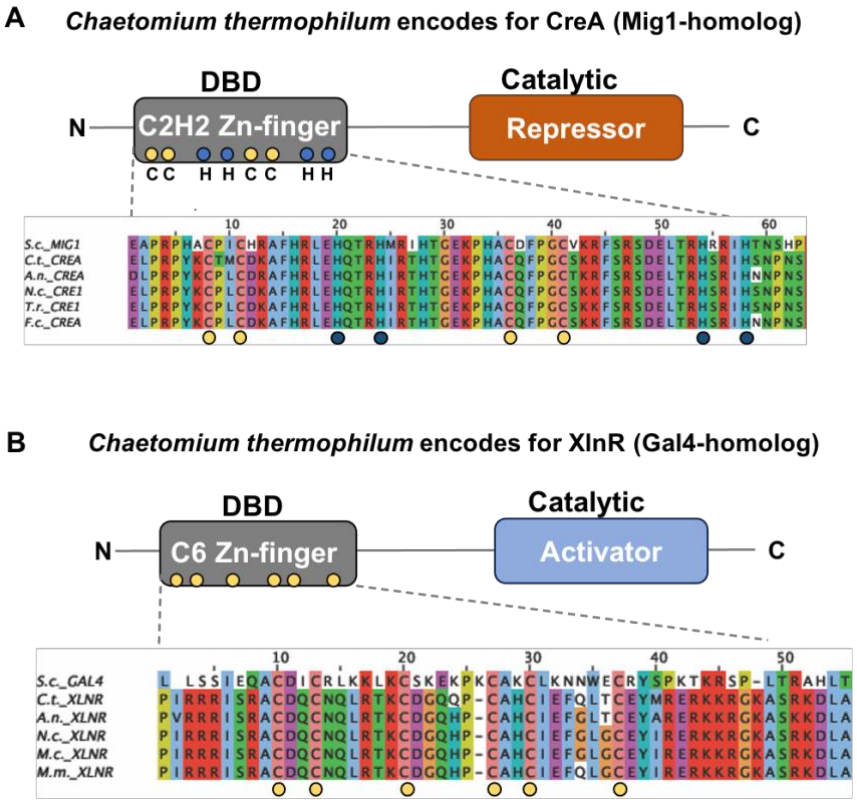

Figure 16: Identification of the conserved Gal4 and Mig1-homologs in Chaetomium thermophilum. *Shown are sequence alignments of the CCR-repressor (CREA/MIG1) and the CCR-activator (XLNR/GAL4) with respective DNA binding domains (grey boxes). The CCR-regulator sequences from Aspergillus niger were used for homology search (blastP) in the C. thermophilum genome. Obtained homologs were aligned together with representative sequences from closely related ascomycetes by Clustal-omega, the characteristic DNA-binding motif regions are shown.* ***A*** *Sequence alignment of the MIG1-like homolog from C. thermophilum encoded by CTHT_0038780. The zinc-finger DNA binding domain (C2H2) shows two conserved repeats with the consensus motif (X_2-Cys-$X_{2,4}$-Cys-X_{12}-His-$X_{3,4,5}$-His). Zn-complexing cysteines (C1-2) and histidines (H1-2) are highlighted.* ***B*** *Sequence alignment of the XLNR-like homolog from C. thermophilum, encoded by CTHT_0038840. The zinc-finger DNA binding domain (Cys6) shows the conserved Zn-complexing cysteines (C1-C6). Chaetomium thermophilum (C.t.), Saccharomyces cerevisiae (S.c.), Aspergillus niger (A.n.), Neurospora crassa (N.c.), Fusarium ambrosium (F.a.), Monosporascus cannonballus (M.c.), Trichoderma reesei (T.r.), Fusarium culmorum (F.c.).*

2.2 *C. thermophilum* can be grown on glucose and xylose containing medium

In order to use sugars as inducing compounds to activate genes in *C. thermophilum*, I first tested different sugars that allow the cultivability of the fungus. To this end, I generated a carbon depleted minimal medium by the reduction of the traditionally used complete cultivation medium (CCM) to only salts, peptone and yeast-extract, which I termed “SPY” medium. Growth analysis on plates showed that the addition of 1 % of D-glucose and D-xylose resulted in colony sizes that reached closest the CCM

propagated colony density and size within one day of incubation. Interestingly, the colony appearance changed from a defined circular appearance with regular grooves to more fluffy and ragged colony shapes in the minimal media. From here on, minimal single carbon media supplemented with D-glucose or D-xylose are termed as glucose medium and xylose medium, respectively **Figure 17**.

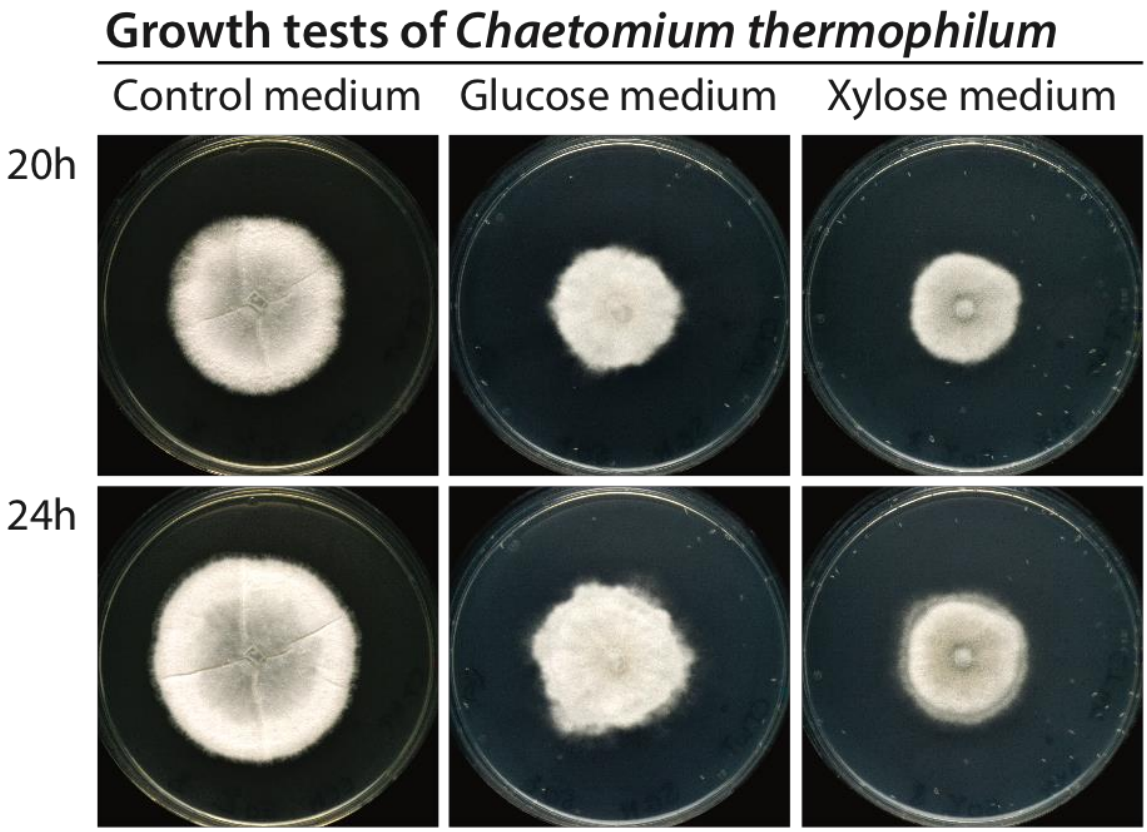

Figure 17: Growth comparison of Chaetomium thermophilum on traditional CCM and new minimal media. *A parental colony of C. thermophilum was grown for 24h on a CCM-plate at 50°C. Equally sized pieces were cut out of the outer most periphery of one colony and subsequently transferred on minimal media plates, supplemented with D-glucose (glucose medium) and D-xylose (Xylose medium) next to a CCM-plate (control medium). Plates were imaged after 20 and 24h of incubation at 50°C. The experiment was repeated at least three times.*

2.3 Investigation of transcriptional differences in cultures grown on glucose and xylose

After we established that *C. thermophilum* can be grown on glucose or xylose containing medium, I searched for sugar controllable promoters that are active only in one of these sugar conditions. The rational was that differentially transcribed genes would guide us to carbon controllable promoters. Thus, I harvested wildtype mycelia

from three independent biological replicates before and six hours after glucose and xylose induction, respectively. From these differently induced cultures, I extracted total RNA and confirmed the RNA integrity on an agarose gel for all samples. Subsequently, Dr. D. Ibberson (CellNetworks Deep Sequencing Core Facility, Heidelberg) confirmed the high quality of the extracted RNA by bioanalyzer measurements, shown in **Figure 18**.

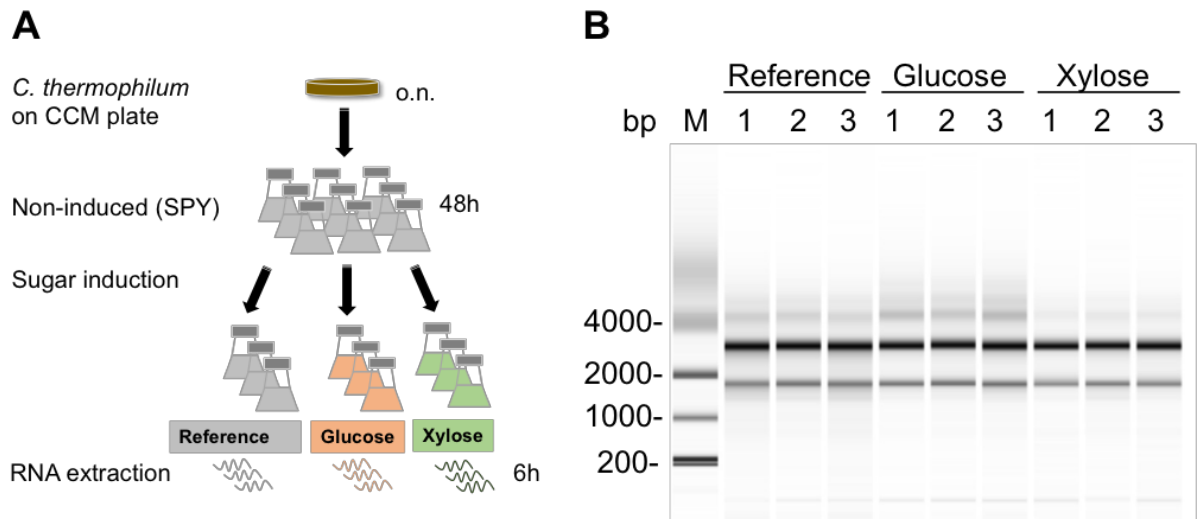

***Figure 18: RNA extraction from C. thermophilum cultures after sugar induction**. **A** C. thermophilum colonies were harvested from a rich medium grown CCM-plate, propagated 48h on carbon depleted medium (Reference) and further six hours in the presence of 1% (w/v) of D-glucose and D-xylose. Total RNA was extracted from three biological replicates for each condition. **B** Quality control of the extracted RNA. The RNA integrity was tested on a Bioanalyzer by Dr. D. Ibberson (CellNetworks Deep Sequencing Core Facility, Heidelberg). The upper band shows the intact 25S rRNA and the lower band the 18S rRNA.*

Next, the prepared mRNA was subjectable to single-end illumina sequencing and the obtained data processed by Dr. G. Shermann (Biochemistry Center Heidelberg). We obtained for the three investigated conditions similar sequencing depths with 68 and 70 million reads out of the glucose and xylose induced condition next to 75 million reads from the reference condition. From each condition, we could map about 92 % of the original sequencing reads on the genome, which underlines the high quality of the sequenced transcripts (Table 1). The approximately 60 to 70 million reads from each condition confirmed a convincing sequencing depth to further investigate differential gene expression within the approximately 7200 annotated genes of *C. thermophilum*.

Table 1: mRNA directed sequencing read output obtained from C. thermophilum cultures. Investigated were cultures grown on carbon depleted medium (Reference) and 6h after glucose or xylose induction. Genome size 28 Mbp containing 7227 annotated genes in the reference-genome.

Condition	Biological replicates	Average number of reads in million	portion of mapped reads in %	Mapped reads in million
Reference	3	75	91.5	69
Glucose	3	68	92.1	62
Xylose	3	70	91,7	64

When we started with the transcriptome analysis from the glucose grown *Chaetomium* cultures, we realized significant differences compared to the transcriptome annotation of the *Chaetomium thermophilum* reference genome (Bock et al., 2014). Around 30 % of the transcripts with their exons and introns were in our analysis novel annotated. Vice versa, 15% of the originally annotated transcripts and exons and about 25 % of the originally annotated introns were not found in our analysis. In total, we found 7044 coding transcripts, compared to the originally annotated 7165 coding transcripts in the reference genome. From the originally 7165 annotated coding transcripts, we could not confirm 749 that were potentially wrongly annotated since they showed particularly low conservation in related fungi. On the other side, we found 679 novel coding genes. Further, we encountered discrepancies for around 60 % of the previously annotated genes regarding annotated introns and exons, summarized in **Figure 19**.

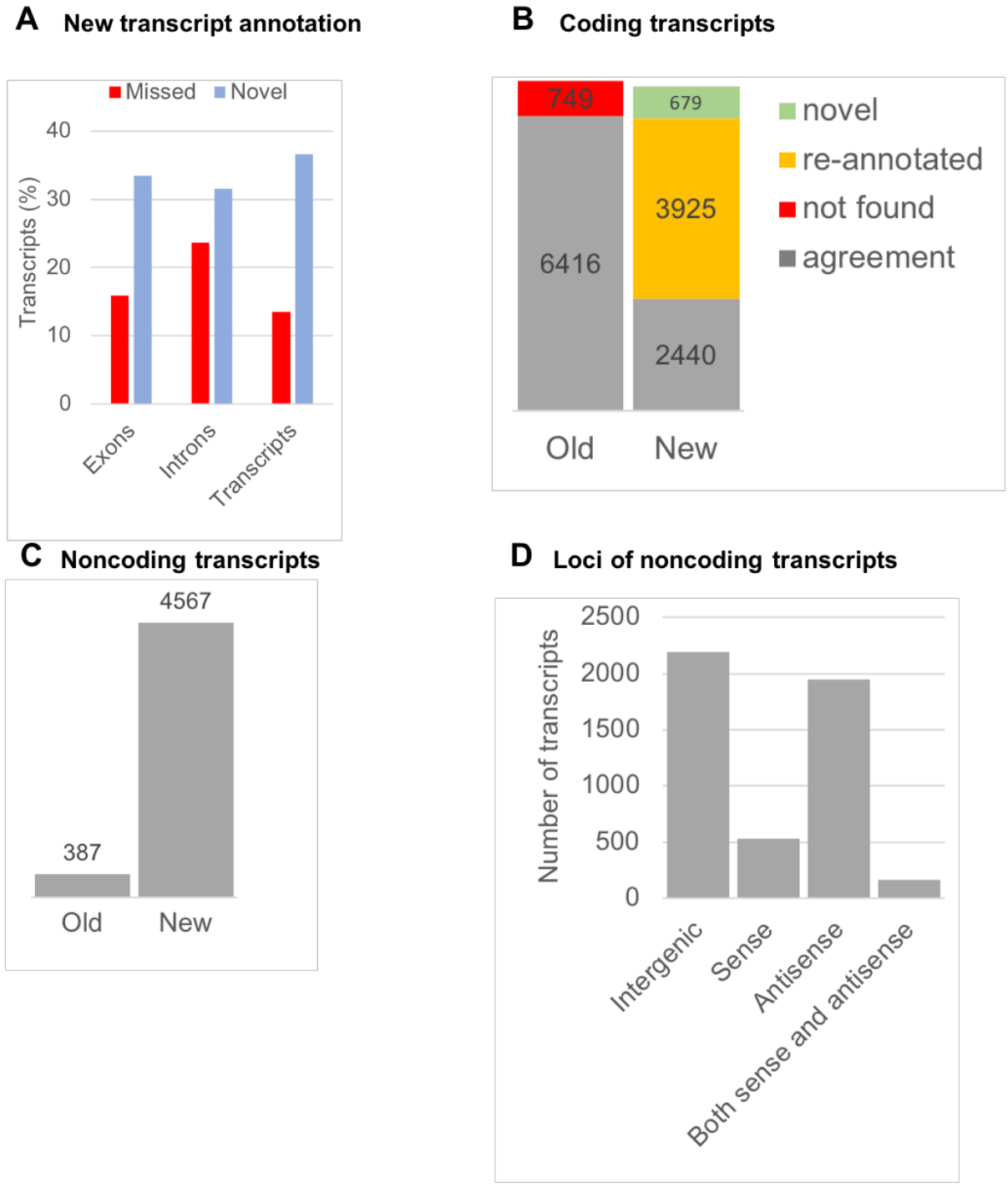

Figure 19: Annotation of the genome of C. thermophilum according to the transcriptome. *Comparison of the new annotated transcripts compared to their old annotation in the reference genome* (Bock et al., 2014). ***A*** *New transcript annotation in comparison to the reference genome. Shown are the relative numbers of exons, introns and transcripts that were not supported by the new annotation (Missed) next to newly found ones (Novel).* ***B*** *Comparison of the annotated coding transcripts. Shown are the coding transcripts of the new annotation (new) and the old annotation in absolute numbers. Coding transcripts that were found identically in both annotations (grey), not confirmed coding genes (red), newly annotated genes (green), re-annotated genes with at least one changed intron-exon junction (yellow).* ***C*** *Shown are the newly found noncoding transcripts compared to the old annotation.* ***D*** *The distribution of the noncoding transcripts are shown according to their genomic locus and orientation. Figure modified from* (Singh et al., 2021).

Moreover, we strongly expanded the set of noncoding transcripts from originally annotated 387 to 4567 transcripts, including intergenic, intronic, sense and anti-sense long noncoding RNAs (lncRNAs) and ncRNAs. Furthermore, we got evidence for alternative spliced transcripts that would result in gene-isoforms in *C. thermophilum.* To be sure that indeed alternative splice variants exist in the thermophile, the preliminary results, based on our single-end deep sequencing approach, would require a paired-end sequencing approach. Altogether, the here initiated transcriptome analysis allowed us to refine and extend the annotated genome of *C. thermophilum,* being important to correctly understand and investigate the thermophile, for closer details see Singh et al., 2021.

2.4 The most differentially transcribed genes in glucose vs. xylose grown cultures

After we analyzed the glucose induced transcriptome, we investigated also the RNA sequencing data that we obtained from the non-induced and the xylose induced condition. Our transcriptomic data showed significant correlation between the three biological replicates that we analyzed for each condition **Figure 20**. Then, we identified the fifty most differentially transcribed genes out of the 7044 identified transcripts upon glucose or xylose induction. From these fifty most differentially transcribed genes, roughly 35 % showed strong activity specifically in the presence of xylose and 65 % of genes in the presence of glucose. To confirm the transcriptome analysis, I used the initially extracted bulk RNA to verify the obtained changes in transcripts by qRT-PCR using ΔΔCT measurement. The transcript dynamics obtained by qRT-PCR analysis were in close agreement with the global deep-sequencing approach for the target genes, shown in **Figure 20**. The verified genes comprised the most stringently xylose-activated transcript, a xylosidase-like gene (CTHT_00111440) and hereafter referred to as xylosidase (XYL), that reached a 40-fold enrichment in transcripts compared to the glucose grown condition. The second most xylose activated gene, the xylitol-dehydrogenase (XDH) gene (CTHT_0073860) showed a 30-fold increase in transcripts compared to the glucose condition. Whilst the XYL-gene was specifically activated upon xylose induction, compared to the carbon depleted reference condition, the XDH-gene was the most repressed in upon glucose induction. Less stringent transcript

changes were confirmed for a putative cellulose binding protein (CBP), encoded by (CTHT_0003950) which was expected as it was also not included in the 50 most differentially transcribed genes. The most glucose activated transcript on the other side was a noncoding gene (CTHT_0011270) that showed an almost 50-fold increase compared to its xylose repressed situation. In order to shed light on the cellular function of these strongly sugar sensitively transcribed genes, we assigned gene-ontologies which were in agreement with blastP-homology searches for the protein coding transcripts.

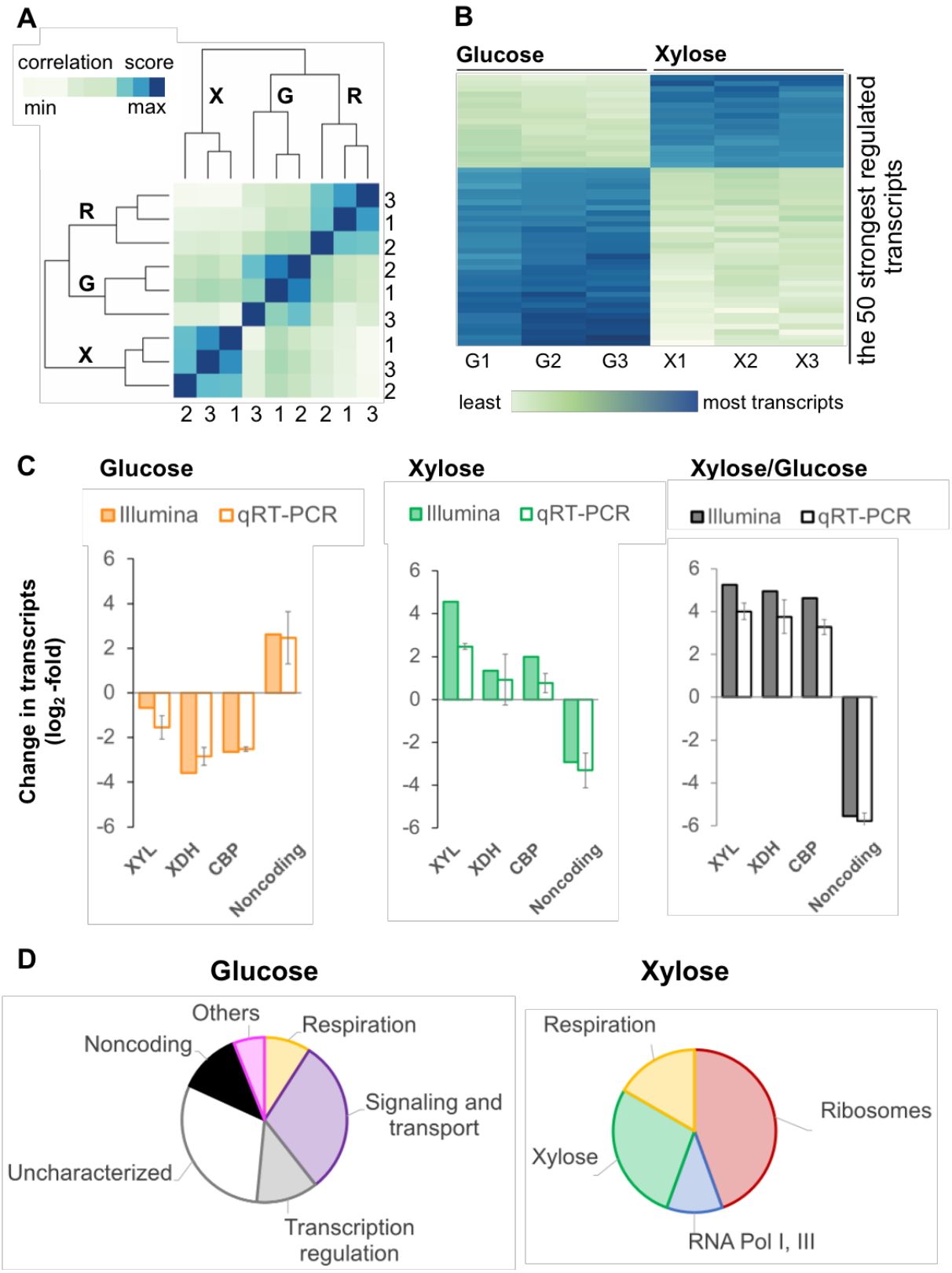

Figure 20: Identification and characterization of the most differentially transcribed genes. ***A*** *Transcriptome correlations. Shown are the overall transcriptome correlations between the reference (R), the glucose (G) and xylose (X) induced condition for the three biological replicates, respectively.* ***B*** *The 50 most differentially transcribed genes after glucose and xylose induction. The strongest glucose or xylose activated transcripts were sorted according to adjusted p-values. Each of the 50 most*

*differentially transcribed genes is shown as one line in the heatmap and coloured according to transcript quantities. The most differential expressed genes were selected based on adjusted p-values < 6.7 x 10^{-24}. **C** Validation of the transcriptome sequencing by qRT-PCR. Shown are the measured changes in transcripts (log_2-fold) for selected genes according to the mRNA-deep sequencing (Illumina) and by qRT-PCR. Changes in transcripts are shown upon glucose induction compared to the reference condition (orange), upon xylose induction (green) and between glucose and xylose induction (grey). Standard deviations shown in error bars for qRT-PCR measurements are based on two biological and three technical replicates. XYL (CTHT_0011440), XDH (CTHT_0073860), CBP (CTHT_0003950) and the strongest glucose activated gene (noncoding) (CTHT_0011270 are shown. **D** Pie charts show the function of the fifty most differentially transcribed genes in glucose and xylose according to blastP-search.*

Within the strictly glucose activated genes, about 60 % of genes could be assigned to their functions. About 20 % of genes mapped functionally into respiration as well as into noncoding genes and almost 30 % were assigned to various genes involved in cellular transport and signaling pathways next to putative transcription factor coding genes. The portfolio of the xylose specifically activated genes on the other side could all be functionally assigned and showed except for respiratory function genes strongly different functions compared to the glucose induced set of genes. Interestingly, more than 50 % of genes mapped into ribosome assembly, -export and translation elongation, next to the transcription of rRNA. Closer, the proteins of the catalytic sub-units of RNA-polymerases I and III that are both needed for the synthesis of ribosomal RNAs were found here. Moreover, the remaining 30 % of genes showed closely xylose related functions, mapping into hemicellulose degradation and xylose catabolism. Thus, the transcriptome analysis showed a xylose activation of genes with various cellular functions in addition to genes with function in xylose mobilization and its catabolism.

2.5 *YFP*-expression under control of xylose inducible promoters in reporter strains

In this study, we focused on xylose activated and glucose repressed promoters since the routinely applied cultivation conditions in the laboratory are established on glucose enriched complete cultivation (CCM) and sporulation media, as shown in materials methods in Table 4. Thus, a glucose repressed gene-expression system was more compatible with our aim to arrest ribosome biogenesis maturation steps in dominant negative or even lethal phenotypes, as they are commonly observed in yeast. The here investigated promoters belong to genes with functions in xylose mobilization and its catabolism, as shown before in **Figure 3**. Respective proteins were predicted with

extracellular localization due to the presence of a signal-peptide, like the putative cellulose binding protein (CBP) and the endo-β-xylanase (*XLN*) next to the intracellularly acting xylosidase- (XYL) and the xylitol-dehydrogenase (*XDH*). These promoter candidates were selected to search for the most adequate promoter induction strength in the presence of xylose and as little activity in the presence of glucose. Among them, the *CBP*-promoter regulated gene shares a transcription activity that is stronger than about 50 % of all genes in xylose containing medium, whereas the counted transcripts belong to the least 10 % in the genome. The *XLN*- and the *XYL*-promoter controlled genes are stronger transcribed than about 80 % and 90 % of all transcripts, respectively. In cultures that were grown in glucose containing media, the transcription activity was among the weakest 25 %. The most transcripts were found for the *XDH*-promoter controlled gene, indicative for stronger transcription in the presence of xylose, than 96 % of all genes, whilst in glucose grown cultures, the transcription activity was among the lowest 45 %, as shown in Table 2.

Table 2: The experimentally investigated glucose and xylose regulatable promoters. Promoter candidates were selected from genes with strong activity in xylose and only little activity in glucose according to the transcriptome analysis.

Promoter	Gene-ID	Description	Localization	Transcript activity (%)	
				Glucose	Xylose
CBP	CTHT_0003950	Cellulose binding protein	Extracellular	10	51
XLN	CTHT_0050050	Endo-β-xylanase	Extracellular	24	78
XYL	CTHT_0011440	Xylosidase	Cytoplasma	23	91
XDH	CTHT_0073860	Xylitol-dehydrogenase	Cytoplasma	44	96

Having identified significantly xylose induced and glucose repressed promoter candidates, I developed a reporter system to test the induction of selected promoter regions on the protein level. We defined a roughly 1.5k bp region in the 5' upstream region (5'UR) as the promoter carrying sequence. Since the protein stability depends in vivo on the identity of its N-terminal residue (Passmore et al., 1986; Varshavsky, 2011), we including also the first two translated codons of the native gene into the respective promoter-carrying region (ATG+NNN). To measure promoter inductions, we placed a YFP-reporter gene under translational control downstream of the investigated promoters. The thermotolerant YFP-reporter gene was synthesized with site directed mutations that showed to result in increased temperature stability (Aliye et al., 2015),

termed as fast-folding-thermostable *YFP* (*ffts*-*YFP*) gene that was generously provided by the Beck lab (EMBL, Heidelberg, Germany). The promoter-*YFP* fusions were flanked by an upstream- and downstream terminator to block transcriptional background activity from the genomic locus where the reporter plasmid gets randomly integrated during the transformation, as illustrated in **Figure 21 A**. The transformed plasmids carried further an ergosterol selection marker-cassette to select for positive transformants, as described by Kellner et al., 2016. As negative control, I generated a YFP-reporter strain lacking a promoter but instead contains an oligonucleotide upstream of the YFP-gene. The genotype of the control strain was validated by diagnostic PCR on extracted gDNA from the transformants. The primer pairs were selected as such that they anneal on the transformed plasmid, and result in a 180bp sized PCR product only when the YFP-cassette is present in the genome, as it is shown for the representative clone 10 in **Figure 21 B**. The representative control strain (clone 10) was used then to assure that the eventually measured YFP-expression in the reporter strains is promoter specific. To characterize the induction of the identified promoters in the presence of glucose or xylose containing media, I subjected the various reporter strains to an induction assay. The monitored induction time was oriented at the induction time of up to 8h that is typically applied using the *GAL1*-promoter to induce ribosome biogenesis mutants in *S. cerevisiae,* as shown in **Figure 21 C**. During this assay, the reporter strains were first grown in duplicates in glucose containing media to build biomass. Then one culture was transferred to xylose containing medium whilst the other one was grown in glucose containing medium as induction control. Before medium exchange and throughout the induction time, YFP-expression was monitored on the protein level in the reporter strains by immuno-blotting. Additionally after 6h and 8h after medium exchange, YFP-expressions were inspected by fluorescence microscopy.

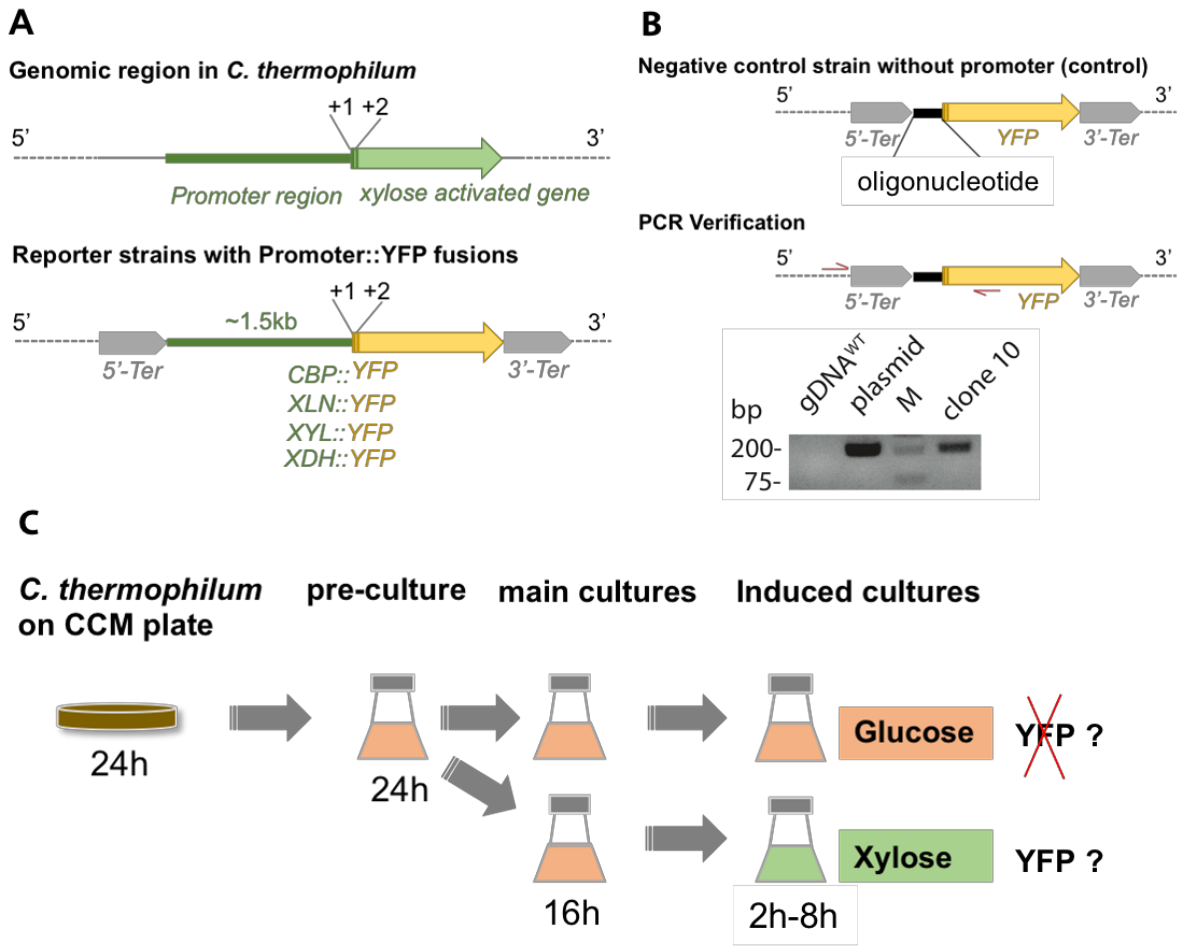

Figure 21: Development of YFP-reporter strains to investigate protein inductions under control of xylose inducible promoters. A *The genotypes of generated YFP-reporter strains to test xylose inducible promoters are shown as cartoon. Reporter-strains were generated upon plasmid transformation that carry a thermostable YFP variant (YFP) under control of selected 1,5kb spanning promoter regions from xylose activated genes (promoter) including promoters from a cellulose binding protein (CBP::YFP), a β-xylanase (XLN::YFP), a xylosidase gene (XYL::YFP) and the xylitol-dehydrogenase gene (XDH::YFP.* ***B*** *Generation of a negative control strain without promoter. In the negative control strain (control), a 20bp oligonucleotide upstream of the YFP-gene was used as adapter in front of the YFP-gene. The control strain was verified by diagnostic PCR on extracted gDNAs from the obtained transformants. A PCR products of 180 bp indicated for positive transformants with primer pairs binding upstream of the 5'-terminator and within the YFP-gene (red arrows). The plasmid born expression cassette was used as positive control and gDNA from wildtype mycelia as negative control for the PCR. The representative clone 10 was used for all further assays.* ***C*** *The experimental workflow of the induction assay. Reporter-strains were grown first on glucose containing medium as pre-cultures. The pre-culture used to grow main cultures in duplicates on glucose containing medium for 16h. To measure YFP-induction in the reporter strains, one culture was transferred to xylose medium whilst the other one was again grown in glucose containing medium for up to 8h. Immuno-blotting and fluorescence microscopy was applied to inspect YFP-expression under control of the various promoters.*

When I measured the YFP-induction in the control strain that lacked a promoter, no YFP-protein was detected by immuno-blotting, nor by fluorescence microscopy throughout the induction time up to 8h **Figure 22 A**. When I investigated YFP-induction under control of the *CBP*-promoter by immunoblotting, I could detect YFP by immuno-

blotting exclusively in cultures that were grown in xylose containing medium already after 2h of exposure to xylose but not when exposed to glucose containing medium. Since in the control strain, no YFP-protein could be detected at any point, using the same exposure time for immuno-blotting, I deduced that the xylose induced YFP was specific for the activity of the CBP-promoter. The *CBP*-promoter induced YFP in the presence of xylose was detectable from 2h after exposure to xylose onwards. However, even with extensive exposure time, the detected YFP-signal was only slightly over the detection limit of the YFP-directed anti-body. When I inspected the YFP-fluorescence by microscopy for 6h and 8h after medium exchange, the YFP-fluorescence was not visible in glucose nor xylose medium grown hyphae **Figure 22 A, B**. Thus, the reporter assay worked to detect promoter specific YFP-expression as seen for the *CBP*-promoter containing strain. However, the induction of YFP in the presence of xylose was very weak.

Surprisingly, under control of the stronger inducing promoters, the 28 kDa sized YFP-protein was detected sometimes by up to three bands by immuno-blotting, instead of an expected single 28 kDa band. Mass spectrometry on affinity purified YFP under control of the *XYL*-promoter showed that the lower two bands reflect C-terminally truncated YFP degradation species of the purified ffts-YFP, indicating for limited protein stability at 50 °C (not shown). I interpret the overall YFP-induction and thus considered all bands that were detected by the antibody, respectively.

In the *XLN*-promoter carrying reporter strain, a certain but stable YFP-induction was detected by immuno-blotting in cultures that were grown in glucose containing medium. The weaker YFP-signal corresponding to 4h of induction compared to the other time-points can be explained by slightly less loading as seen in the ponceau S staining. As soon as the strain was grown in xylose containing medium, a stronger YFP-induction could be monitored that stayed stable from 2h to 8h after medium exchange. Inspecting closer the YFP-expression after 6h and 8h in glucose containing medium by fluorescence microscopy, similar inductions were observed that were in agreement with the immuno-blotting measurement. In the xylose grown condition, fluorescence microscopy indicated for a slightly increased YFP-induction after 8h, compared to 6h. Further, cultures that were grown for 6h in xylose containing medium, did not reflect a significant induction when compared to the respective glucose grown mycelia **Figure**

22 C. Hence, immediate YFP-induction was suggested in the presence of xylose according to immuno-blotting, but confirmed by fluorescence microscopy only when cells were grown for more than 6h.

Intriguingly, a clear carbon sensitive induction of YFP was observed under control of the *XYL*-promoter. Using identical blotting settings as for the afore mentioned *XLN*-promoter containing reporter strains, no YFP-protein could be detected in glucose grown cultures by immuno-blotting. In contrast, directly 2h after the strain was grown in xylose containing medium, YFP was significantly detected by immuno-blotting. The detected YFP-protein stayed stable for up to 6h of exposure and decreased after 8h of induction. The xylose specific YFP-induction was also confirmed by fluorescence microscopy, which was observed to be rather stable comparing 6h and 8h induced cultures. I concluded that the *XYL*-promoter showed no measurable YFP-induction in glucose grown cultures, whilst exposure to xylose containing medium resulted in YFP-induction that was similar to the induction in the *XLN*-promoter carrying strain **Figure 22 D**. Thus, from the so far tested promoters, the *XYL*-promoter showed to be most stringently controlled by glucose and xylose which was in line with the expectation since the *XYL*-gene showed to be most differentially regulated in the transcriptome analysis.

When I experimentally investigated YFP-induction under control of the *XDH*-promoter by immuno-blotting, the YFP-signal had to be detected within 6-fold shorter imaging time, due to the stronger induction as compared with the *XYL*- and *XLN*-promoter. Whilst a steady YFP-signal was seen in the glucose grown cultures throughout the induction time up to 8h, a significant increase was seen in the xylose medium grown cultures already after 2h which further increase steadily up to 8h. The strong and xylose increased YFP-induction under control of the *XDH*-promoter was supported also by fluorescence microscopy. Here, the YFP-imaging time had to be reduced to 10 % compared to the other reporter strains to avoid signal saturation. Under these conditions, only weak YFP induction was observed in glucose grown mycelia, whilst in xylose medium grown cultures the YFP-fluorescence was significantly stronger and stable comparing 6h and 8h of induction. The inspected YFP-fluorescence under control of the *XDH*-promoter appeared similarly strong when compared to the induction under control of the *XYL*-promoter. Thus a roughly 10-times stronger protein-induction

under control of the *XDH*-promoter is assumed **Figure 22 E**. Indeed, an 8 to 16-fold stronger induction under control of the *XDH*-promoter, compared to the *XYL*-promoter was also deduced upon immuno-blotting on lysates from the *XYL*-reporter strain next to sequentially diluted lysates obtained from the *XDH*-reporter strain (not shown). In summary, I concluded that the *XYL*-promoter and the *XDH*-promoter were most strictly repressed by glucose and activated by xylose. Further, the *XDH*-promoter showed roughly 10-fold stronger protein induction compared to the *XYL*-promoter. Hence, using this YFP-reporter assay confirmed both promoters to be most stringently regulated, as it was suggested by the transcriptome analysis. If the promoter regions reflect the same induction dynamics, as it would be observed upon in locus integration of the YFP-gene would require further investigations.

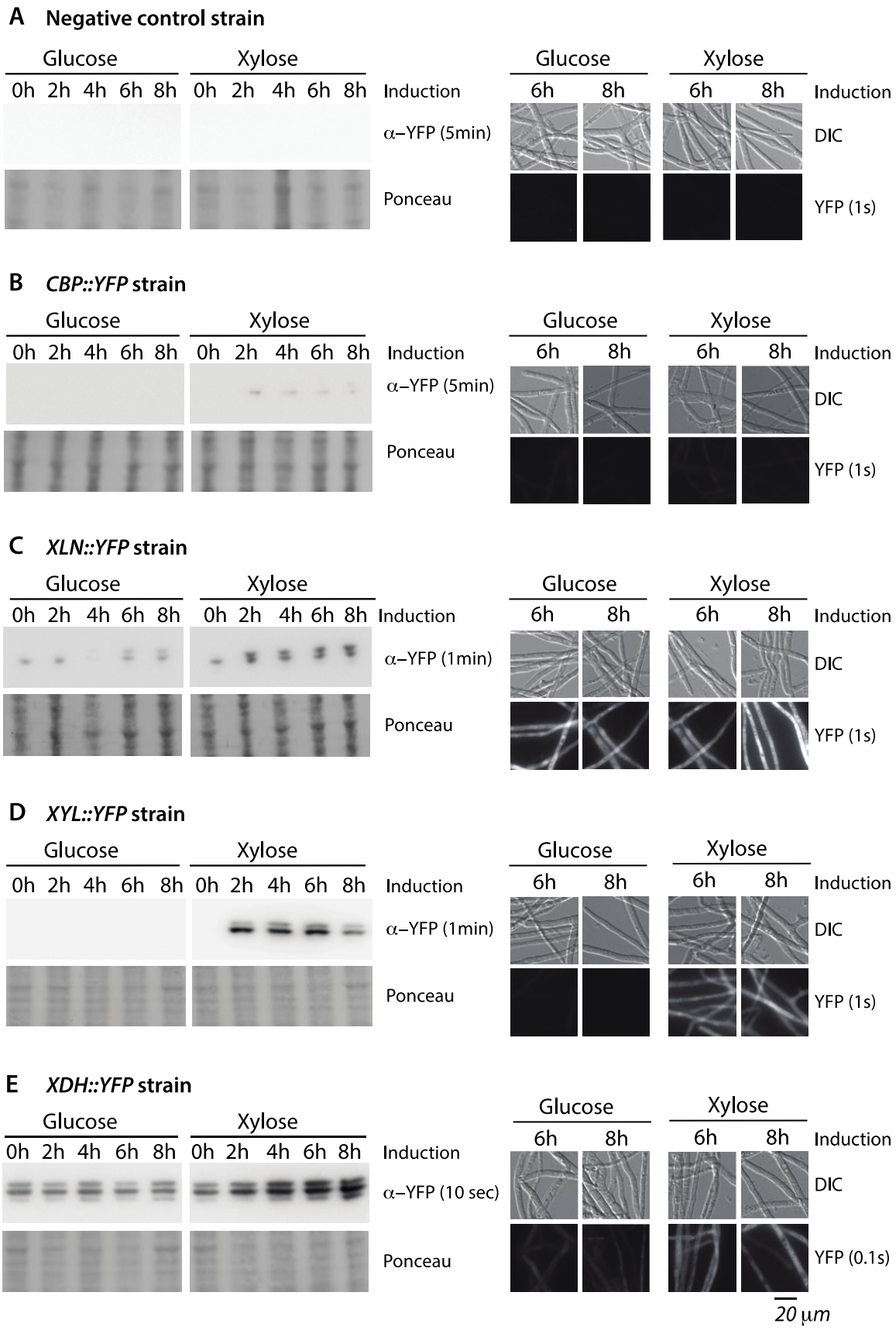
A Negative control strain
Glucose
Xylose
0h 2h 4h 6h 8h 0h 2h 4h 6h 8h
Induction
α–YFP (5min)
Ponceau
Glucose
Xylose
6h 8h 6h 8h
Induction
DIC
YFP (1s)
B CBP::YFP strain
Glucose
Xylose
0h 2h 4h 6h 8h 0h 2h 4h 6h 8h
Induction
α–YFP (5min)
Ponceau
Glucose
Xylose
6h 8h 6h 8h
Induction
DIC
YFP (1s)
C XLN::YFP strain
Glucose
Xylose
0h 2h 4h 6h 8h 0h 2h 4h 6h 8h
Induction
α–YFP (1min)
Ponceau
Glucose
Xylose
6h 8h 6h 8h
Induction
DIC
YFP (1s)
D XYL::YFP strain
Glucose
Xylose
0h 2h 4h 6h 8h 0h 2h 4h 6h 8h
Induction
α–YFP (1min)
Ponceau
Glucose
Xylose
6h 8h 6h 8h
Induction
DIC
YFP (1s)
E XDH::YFP strain
Glucose
Xylose
0h 2h 4h 6h 8h 0h 2h 4h 6h 8h
Induction
α–YFP (10 sec)
Ponceau
Glucose
Xylose
6h 8h 6h 8h
Induction
DIC
YFP (0.1s)
20 µm

Figure 22: Characterization of promoter activities in YFP-reporter strains. *The YFP-gene was placed under control of xylose inducible promoters belonging to the genes of a cellulose binding protein (CBP::YFP), an endo-β-xylanase (XLN::YFP), a xylosidase-like protein (XYL::YFP) and the xylitol-dehydrogenase (XDH::YFP). As control, a YFP reporter strain without promoter in front of the YFP-gene was inspected (control). Reporter strains were grown o.n. in non-inductive glucose medium and subsequently shifted to fresh pre-heated glucose and xylose medium. Samples were taken before medium exchange (0h) and at the indicated time-points after media exchange to either fresh glucose medium (glucose) or xylose medium (xylose).* ***A*** *YFP-measurement by immuno-blotting. Whole cell lysates were prepared and subjected to immuno-blotting against YFP. Since no anti-body for normalization purposes is available, we loaded equal protein amounts, shown by ponceau S staining. Note that lysates from glucose and xylose grown cultures were analysed on the same membrane. Exposure times had to be adjusted to the expression strength of the respective promoter, as indicated.* ***B*** *YFP-induction measurement by fluorescence microscopy. YFP-induction was inspected in vivo in the reporter strains under control of the promoters from above. Shown are DIC and YFP images. YFP-exposure times were adjusted to the induction strength of the promoter, as indicated.*

2.6 Application of xylose inducible promoters for ribosome biogenesis studies in *C. thermophilum*

After we characterized the sugar regulatable promoters, we wanted to test the *XYL*- and *XDH*-promoters to control the expression of ribosomal biogenesis factors. As proof of concept, we selected the 90S biogenesis factor Utp6 (UTP-B factor) as bait that allowed the purification of the well characterized 90S pre-ribosomes from *C. thermophilum* upon constitutive expression under control of its endogenous promoter (Kornprobst et al., 2016). Furthermore, an in vivo assay from a parallel study demonstrated the localization of the Utp6-factor to the nucleolus, when fused C-terminally to the thermostable YFP reporter and DAPI staining, as shown in **Figure 23 A** (personal communication to Dr. Nikola Kellner). I started with a *XYL*-promoter fusion to the Utp6-ORF, carrying a C-terminal FLAG-TEV-YFP linker sequence (FTY). The rational of this tagging strategy was to test xylose inducible localization of the Utp6-factor via YFP in vivo and to subsequently purify the 90S particle using the YFP- and the FLAG-tag by tandem affinity purification. When we monitored the localization of the Utp6-YFP fusion protein by fluorescence microscopy, we observed from the first timepoint of 2h up to 6h after medium shift a xylose specific localization of Utp6-YFP that was not seen in the non-inductive glucose condition **Figure 23 B**. This showed that Utp6-YFP can be induced by the *XYL*-promoter, which then localizes to the nucleolus.

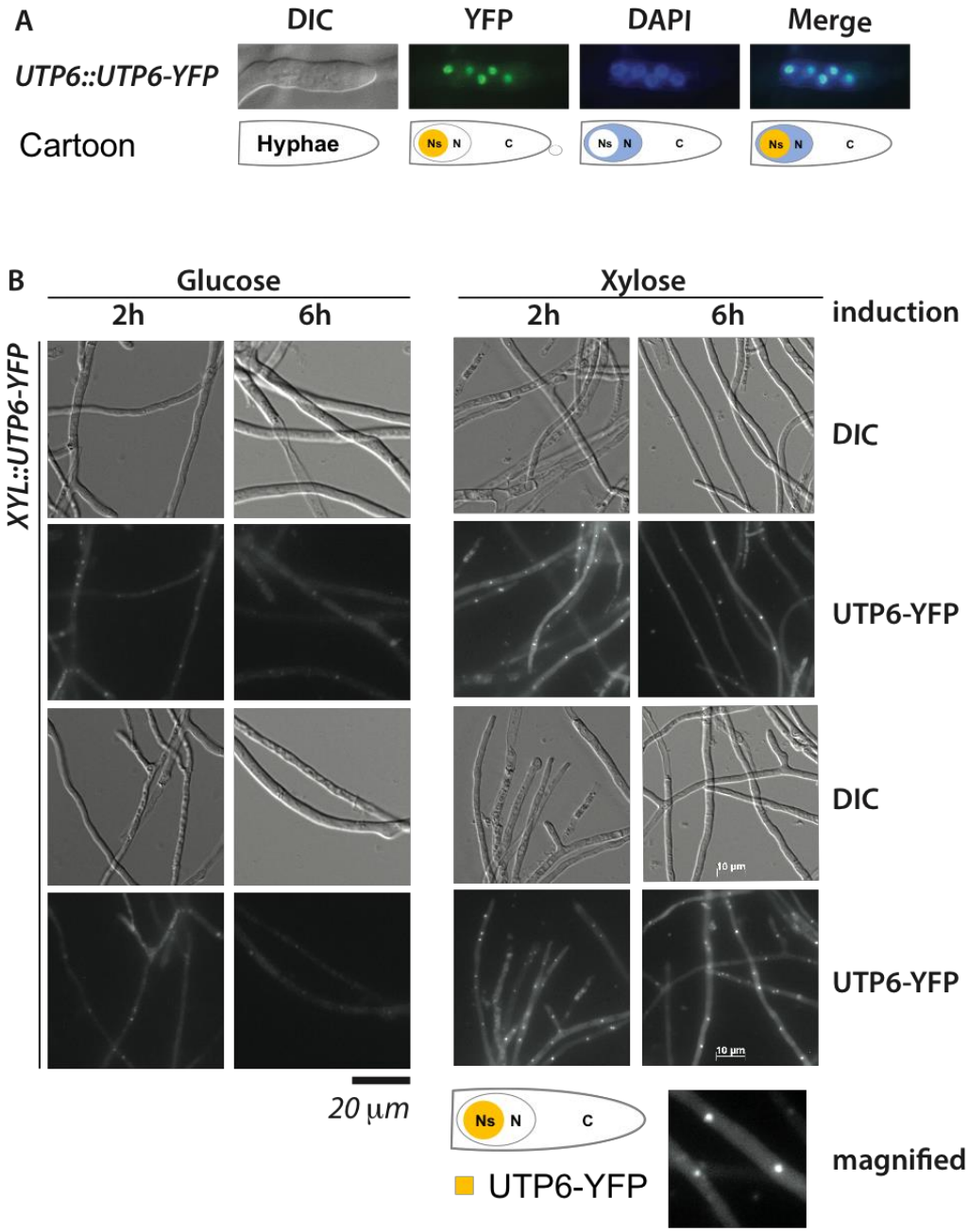

Figure 23: The XYL-promoter induces nucleolar localization of the ribosome biogenesis factor UTP6*. The expression constructs were randomly integrated into the genome of Chaetomium thermophilum together with the ergosterol selection marker.* ***A*** *Shown is the localization of the UTP6-YFP fusion protein to the nucleolus that was expressed under its endogenous promoter-spanning region and grown in CCM before hyphae were stained by DAPI and inspected by fluorescence microscopy (this data was generously provided by Dr. N. Kellner). The cartoon reflects the localization of the YFP and DAPI staining. Nucleolus (Ns), nucleoplasm (N) and cytosole (C) are indicated.* ***B*** *A UTP6-linker-YFP fusion was placed under control of the XYL-promoter that is induced by xylose and localizes to the nucleolus. The reporter strain was propagated on glucose containing medium for 16h and subsequently shifted to fresh glucose and xylose medium. Cultures inspected by fluorescence microscopy after 2h and 6h after medium exchange to fresh glucose and xylose medium. Differential interference contrast images (DIC) and fluorescence images are shown. YFP exposure time 500ms. scale bar 20 µm.*

In a next step, we tried to purify a xylose induced 90S particle and visualize them on Coomassie stained gels. For this approach, we applied the stronger xylose inducible *XDH*-promoter to express the TAP-tagged UTP6 (UTP6-FTpA). When I shifted this strain to xylose medium, I could monitor a strong bait induction by immuno-blotting after two hours, compared to the glucose condition **Figure 24 A**. In parallel, I monitored the constitutively expressed TAP-tagged Utp6-fusion which resembled protein amounts that were similar to the glucose induced Utp6 protein, when expressed under control of the *XDH*-promoter. Closer, the induction strengths varied in both strains within the monitored 2 to 6h of growths in glucose and xylose medium after the 16h in glucose grown cultures were shifted, respectively. In glucose medium, the constitutively expressed Utp6-FTpA protein got reduced within the first 2h, increased to similar levels as observed before the shift to fresh glucose medium and dropped after 8h again. Expressing Utp6-FTpA under control of the *XDH*-promoter resulted in an almost inverse induction pattern. Here, highest protein levels were observed for 2h, 6h and 8h after exposure to fresh glucose medium, compared to less protein before the shift and 4h afterwards. Also, the shift from glucose to xylose containing medium resulted in a reduced Utp6-FTpA signal, when expressed under its own promoter-region that increased slightly within 4h after the medium exchange. In the *XDH*-promoter applying strain, the highest Utp6-FTpA protein amounts were reached directly after 2h, followed by the 4h timepoint compared to the reduced levels during 6h to 8h.

Encouraged by the strong xylose induction under control of the *XDH*-promoter of the Utp6-FTpA fusion as bait for affinity purification, I purified the 90S particle out of both strains and visualized them by Coomassie stained SDS-gels **Figure 24 B**. The selected time-points for the purifications were oriented at the induction times used for the induction of the *GAL1*-promoter in yeast of 6h to 8h. Under constitutive expression conditions of Utp6-FTpA as bait, the purified 90S particle was purified in stochiometric amounts to the bait, which was highest for the 6h xylose induced condition and weakest for the 8h of induction in glucose. In contrast, when the *XDH*-promoter controlled the expression of the Utp6-FTpA fusion as bait, an over-stochiometric proportion of the bait to the purified 90S-particles was observed. Thus, additionally to the 90S-bound Utp6-FTpA, the portion of free bait proteins was observed in glucose and in xylose containing media. Closer, a weak induced bait was found before the shift that increased

after 6h of exposure to fresh glucose medium, concomitantly with increased yields in 90S particles. Whilst the shift to xylose for 6h caused a significant increase in the bait protein, the 90S particle were comparable to the glucose situation. For the 8h timepoint, the weak induced bait and 90S particle was enriched in the respective xylose induced condition. I concluded that the *XDH*-promoter is strongly induced within two hours after shift to xylose containing medium already. However, also significant induction in presence of glucose was monitored that was similar to the induction of the constitutively expressed Utp6-protein under control its native promoter region.

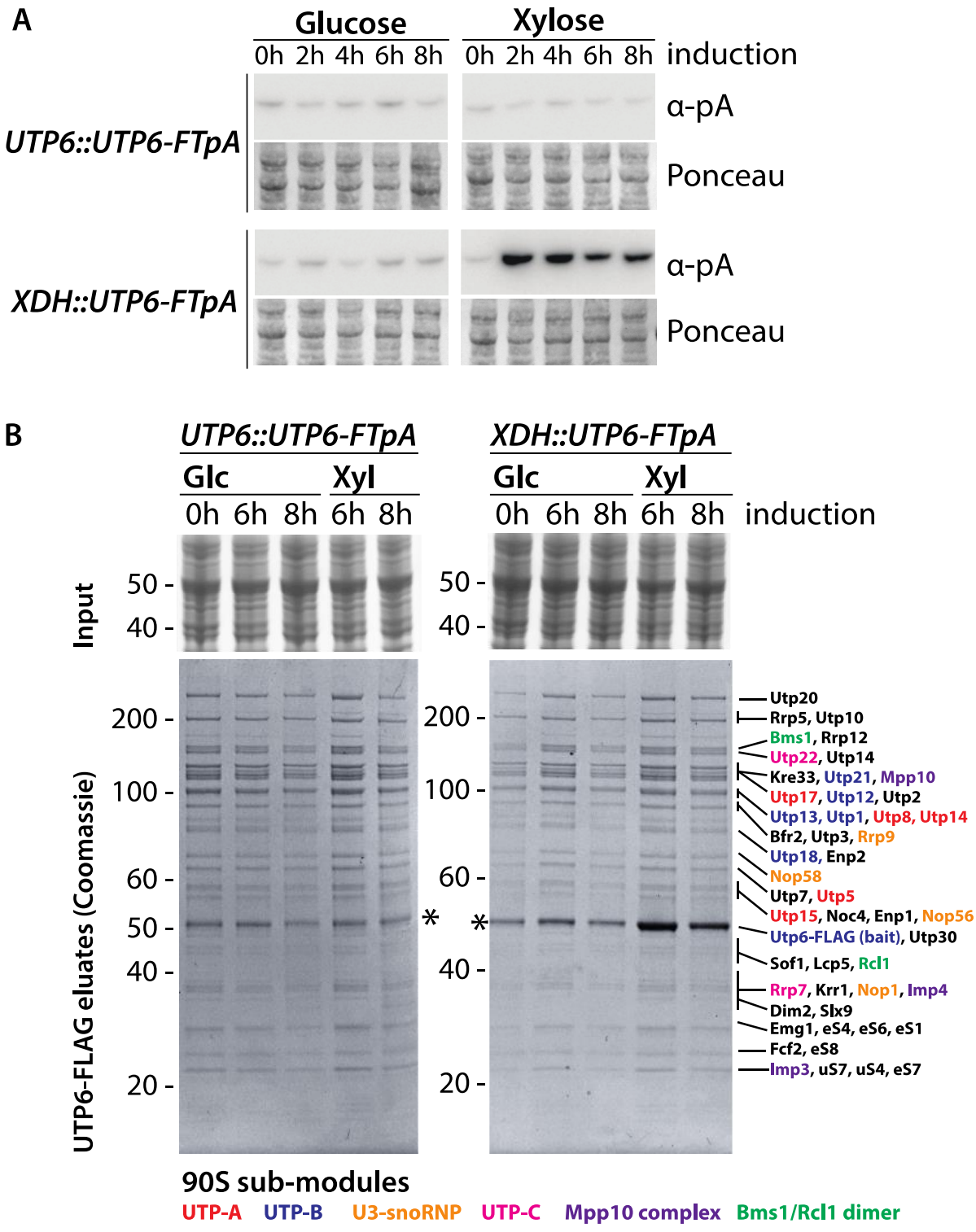

Figure 24: The XDH-promoter induces expression of the ribosomal biogenesis factor UTP6*. The TAP-tagged biogenesis factor of the 90S particle UTP6 (UTP6-FTpA) was expressed under control of its endogenous promoter according to Kornprobst et al., 2016 and under control of the xylose induced XDH-promoter in comparison. Both strains were grown for 16h in glucose medium (t=0h) and subsequently shifted to fresh, glucose and xylose media for further 8h, respectively.* ***A*** *Measurement of the UTP6-FTpA expression by immuno-blotting against the pA-affinity tag. Equal amounts of proteins were loaded as shown by Ponceau S staining.* ***B*** *Coomassie staining of affinity-purified UTP6-Flag*

eluates. UTP6-TAP eluates from equal amount culture input were analysed by SDS-PAGE and Coomassie staining. Note that the free bait protein UTP6-FLAG is enriched in the xylose condition compared to the respective glucose condition. Bands were assigned based on the purified 90S particle from Kornprobst et al., 2016. Submodules of the 90S particle are shown in the figure legend. The experiment was carried out together with B.Sc. student Max Kilian.

2.7 Exploration of xylose inducible promoters to control ribosome biogenesis mutants

Having demonstrated that the xylose activatable *XYL*- and *XDH*-promoter can be used to regulate the expression of ribosomal assembly factors using Utp6 as example, I asked next if the promoters also allow to stall the process of ribosome maturation upon xylose inducible expression of mutated ribosome biogenesis factors. The controllable maturation arrest of ribosomal intermediate particles would be helpful to structurally and functionally study maturation events in the thermophile, based on the experiences in the yeast model. In yeast, the inducible *GAL1*-promoter was successfully applied to induce dominant negative mutants which allowed to stall maturation processes in phenotypic conditions from which the accumulating intermediate particles could be purified and investigated by cryo-EM. As conceptual proof of concept, we tested if the xylose inducible promoters can recapitulate the inducible 60S subunit export arrest that was observed using the dominant negative *rsa4 E114D* mutant from yeast under control of the *GAL1*-promoter (Ulbrich et al., 2009). In L25-YFP expressing cells, accumulated localization of L25-YFP was observed in vivo in inductive conditions, indicative for export deficient 60S particles going along with a dominant negative growth phenotype.

2.7.1 Establishment of the 60S export reporter for *C. thermophilum*

In yeast the expression of the L25-YFP fusion under control of its endogenous promoter is successfully applied to monitor the localization of the 60S subunit, exploiting that this protein joins the pre-60S particle already in the nucleolus and stays present also in translationally active ribosomes. Since this fusion strain was not available yet in *C. thermophilum*, I generated the 60S export reporter strain using the *hph1* selection marker to stably expresses L25 (CTHT_0023650) fused to YFP in wildtype cells, as illustrated in **Figure 25 A**. Immunoblotting confirmed the expression of L25-YFP in the presence of glucose and xylose containing cultivation medium

Figure 25 B. To monitor L25-YFP localization in wildtype cells, I grew *C. thermohilum* first in glucose and xylose medium and inspected the YFP localization 4h and 6h after medium exchange. We observed YFP fluorescence in the nucleolus and the cytoplasm, but not in the nucleoplasm, indicative of a normal distribution of the L25-YFP fusion, shown in **C**. Further, the incorporation of L25-YFP into the 60S subunits was investigated in these cells upon sucrose gradient centrifugation with cell lysates to separate the 40S, 60S and 80S and polysomes. Polysome analysis was not done yet in *C. thermophilum*, thus I tested this assay for L25-YFP reporter strain. When I analyzed the polysome of cell lysates from mycelia that was grown in the traditional medium (CCM) aside to the minimal glucose and xylose minimal media, the profiles looked similar. The mature 80S monosomes representing peak showed to be the most prominent portion of the profile whereas the 40S peak and the polysome tail appeared in much lower intensities as in yeast. In *Chaetomium thermophilum*, the 60S subunit co-migrates largely with the 80S containing fractions. In order to separate the 60S subunits further from the 80S monosomes during sucrose gradient centrifugation, I tested various gradient compositions, however the 60S subunit unavoidably co-migrated largely with the 80S monosomes. Immuno-blotting against L25-YFP on the collected fractions along the sucrose gradient marked the distribution of the large 60S subunit starting with the shoulder of the 80S peak throughout the 80S peak and further along the polysome tail fractions, with the latter reflecting actively translating ribosomes. The strongest L25-YFP signal was obtained for the 80S peak, which became weaker along the heavier gradient fractions. In agreement with the L25-YFP localization, I concluded that L25-YFP incorporates efficiently into the 60S subunits that are efficiently exported and join the pool of translationally active ribosomes. Thus, 60S subunit exported processes can be studied now with this fusion also in the thermophile *C. thermophilum*, as shown in **Figure 25 D**. For more refined studies using the polysome separation by sucrose gradient analysis, the generation of antibodies to detect a 60S factor and a 40S factor would be desireable to clearly assign the 40S, 60S and 80S fractions, as it is possible in yeast.

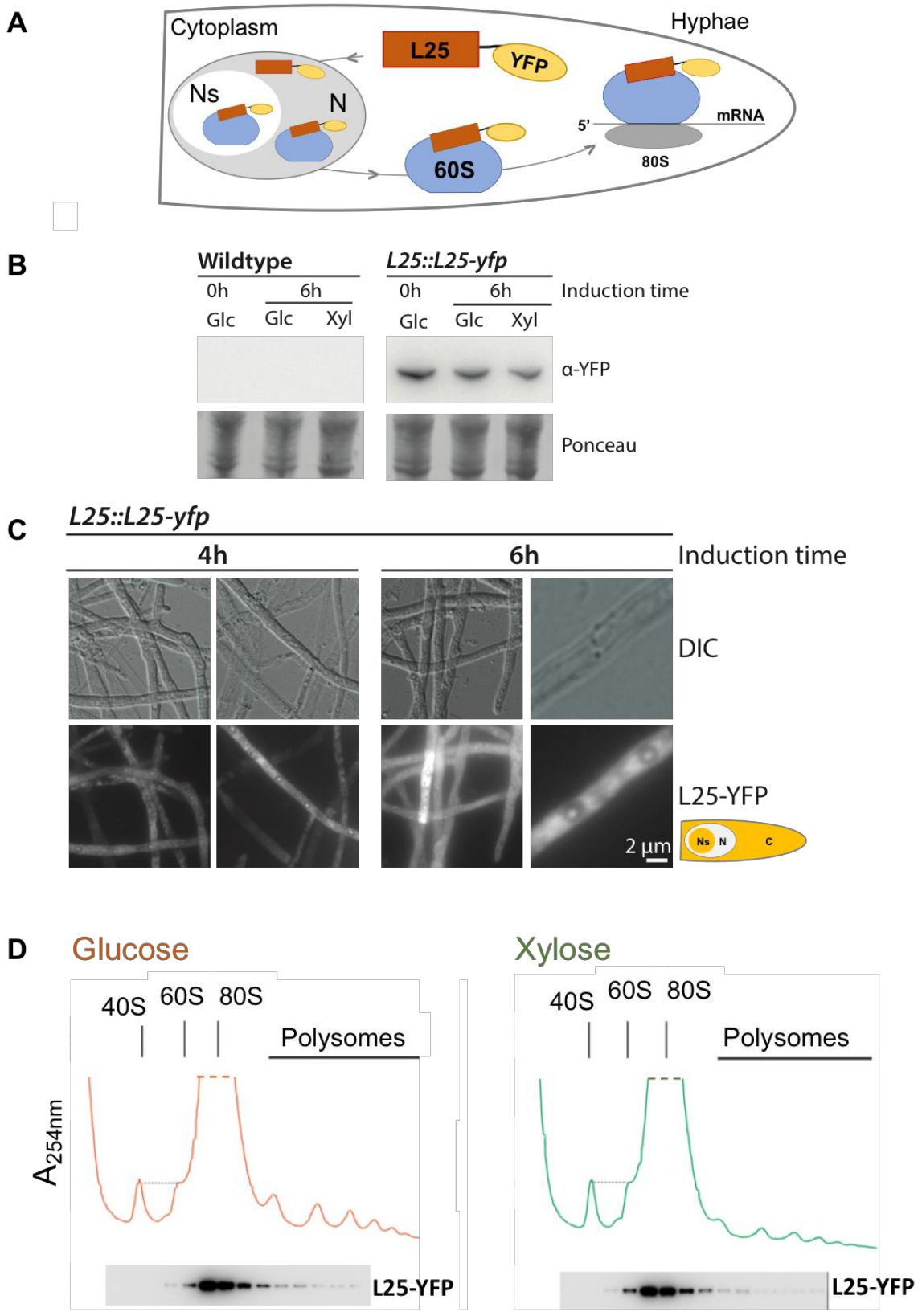

***Figure 25: Establishment of the 60S subunit export reporter L25-YFP in C. thermophilum**. **A** Schematic representation of the L25-YFP reporter that allows to localize the maturing 60S subunit in the nucleolus, the nucleoplasm and the cytoplasm where it eventually joins the pool of actively translating 80S ribosomes. The reporter strains express L25-YFP under control of its endogenous*

promoter region together with the HPH1-selection marker. The strain was grown for 16 hours in glucose medium and subsequently shifted to fresh glucose or xylose medium for up to six hours. ***B*** *Immuno-botting against L25-YFP.* ***C*** *Fluorescence microscopy of the 60S-export reporter strain. The localization of L25-YFP was inspected by fluorescence microscopy, shown here for glucose grown hyphae after 4h and 6h after medium shift to fresh glucose medium. The cartoon indicates for the L25-YFP localization to the nucleolus (NS), the nucleus (N) and the cytoplasm (C).* ***D*** *Polysome analysis of the L25-yfp reporter strain in glucose and xylose induced cultures. After 6h of growth in either glucose or xylose medium, cell lysates were separated by ultracentrifugation on a linear sucrose gradient and the UV profile recorded at 254 nm. The gradient was fractionated, precipitated by TCA and subjected to immuno-blotting against YFP. The migration of the 40S, 60S and 80S are labelled accordingly. Shown are cropped profiles to magnify the weak absorbance of the polysomes in which L25-YFP was detected next to the co-migrating 60S subunit and the 80S monosomes.*

2.7.2 The *XDH*-promoter controls export arrest of pre-60S subunits in the dominant negative mutant ct*Rsa4 E117D*

The *GAL1*-promoter in yeast allows to study ribosome biogenesis by the induction of dominant negative biogenesis mutants. As such, the export of the pre-60S subunit into the cytoplasm was stalled by the induction of the mutated assembly factor Rsa4 E114D. To test if my xylose activatable promoters in *C. thermophilum* allow to exert dominant negative mutants as potential new genetic tool, I tested as proof of concept to control the respective ctRsa4 E117D in *C. thermophilum*. Having established an assay to monitor the localization of the 60S subunit in vivo using L25-YFP, I expressed *rsa4* E117D under control of my xylose activated and glucose repressed promoters to monitor eventual accumulation of L25-YFP upon xylose induction of *rsa4* E117D, as illustrated in **Figure 26**.

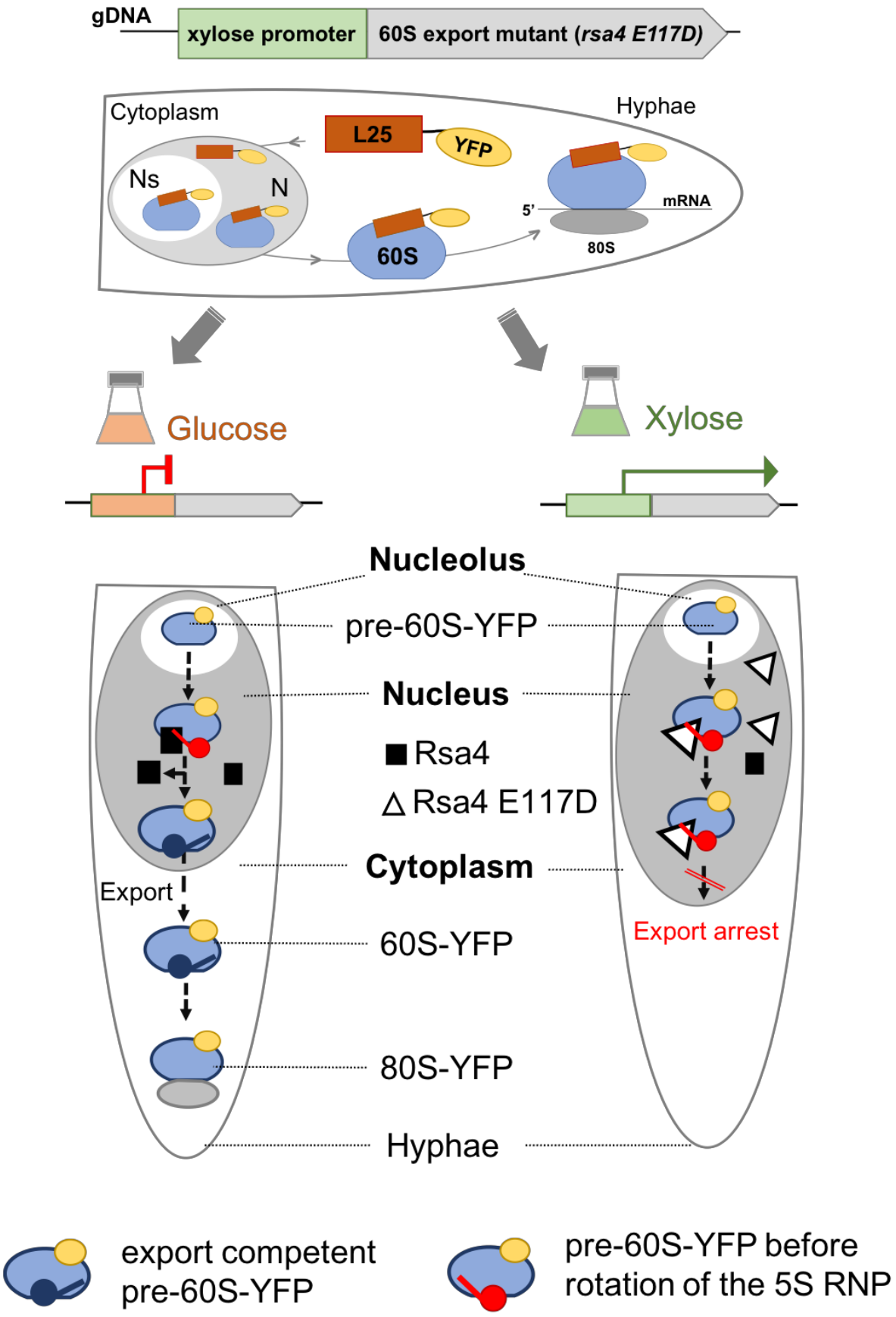
gDNA
xylose promoter
60S export mutant (rsa4 E117D)
Cytoplasm
Hyphae
L25
YFP
Ns
N
60S
5'
mRNA
80S
Glucose
Xylose
Nucleolus
pre-60S-YFP
Nucleus
Rsa4
Rsa4 E117D
Cytoplasm
Export
60S-YFP
80S-YFP
Hyphae
Export arrest
export competent pre-60S-YFP
pre-60S-YFP before rotation of the 5S RNP

Figure 26: Application of L25-YFP to monitor export arrest in 60S subunits expressing rsa4 E117D under control of the xylose activatable promoters in C. thermophilum*. The 60S export reporter strain L25-YFP gets transformed with a plasmid that randomly integrates into the genome using the erg1-selection marker. In the presence of glucose containing medium, the promoter is repressed and the controlled mutated biogenesis factor pA-Rsa4 (E117D) is not expressed. The endogenous Rsa4 (black square) gets released by the AAA+ ATPase Rea1. Uon rotation of the 5S rRNA the pre-60S subunit gains export competence and is exported into the cytoplasm where it joins the actively translating pool of ribosomes. Thus, L25-YFP should localize as it was seen in the parental L25-YFP strain. In contrary, strain exposure to xylose containing medium, activates rsa4 E117D (triangle) which competes with the endogenous Rsa4 to bind the maturing 60S-YFP particle in the nucleolus. Rsa4 E117D bound 60S-particles cannot be released, preventing rotation of the 5S rRNA, causing an arrest in pre-60S subunit export to the cytoplasm.*

I started to test the *XDH*-promoter to control a pre-60S particle export defect upon induction of the mutant factor pA-*rsa4 E117D* with the wildtype pA-Rsa4 as control. From the L25-YFP strain that was transformed with plasmids that allow to express the wildtype Rsa4, I selected three transformants for strain verification. For the mutated Rsa4 E117D strain, I tested clones with different sizes on selective CCM-plates, that I named accordingly smallest (S), medium (M) and largest (L) grown colonies after transformation. The rational was to test if positive transformants correlated with the colony sizes on selective CCM-plates since the *XDH*-promoter was observed to show a certain induction in glucose that might cause a growth defect already on the glucose rich CCM-plates.

To verify positive clones, selected transformants were confirmed by immuno-blotting after cultivation in xylose containing medium, respectivels. The Rsa4 control strain (*pA-Rsa4)* was obtained from clone 1 of the three tested colonies. Interestingly, among the *rsa4 E117D* transformed clones, the transformation success grew with the colony size that was observed on the initial selective plates. However, the expression strength of pA-Rsa4 E117D was by far strongest for the medium sized colonies 1M and 2M compared to the other ones, shown in **Figure 27**.

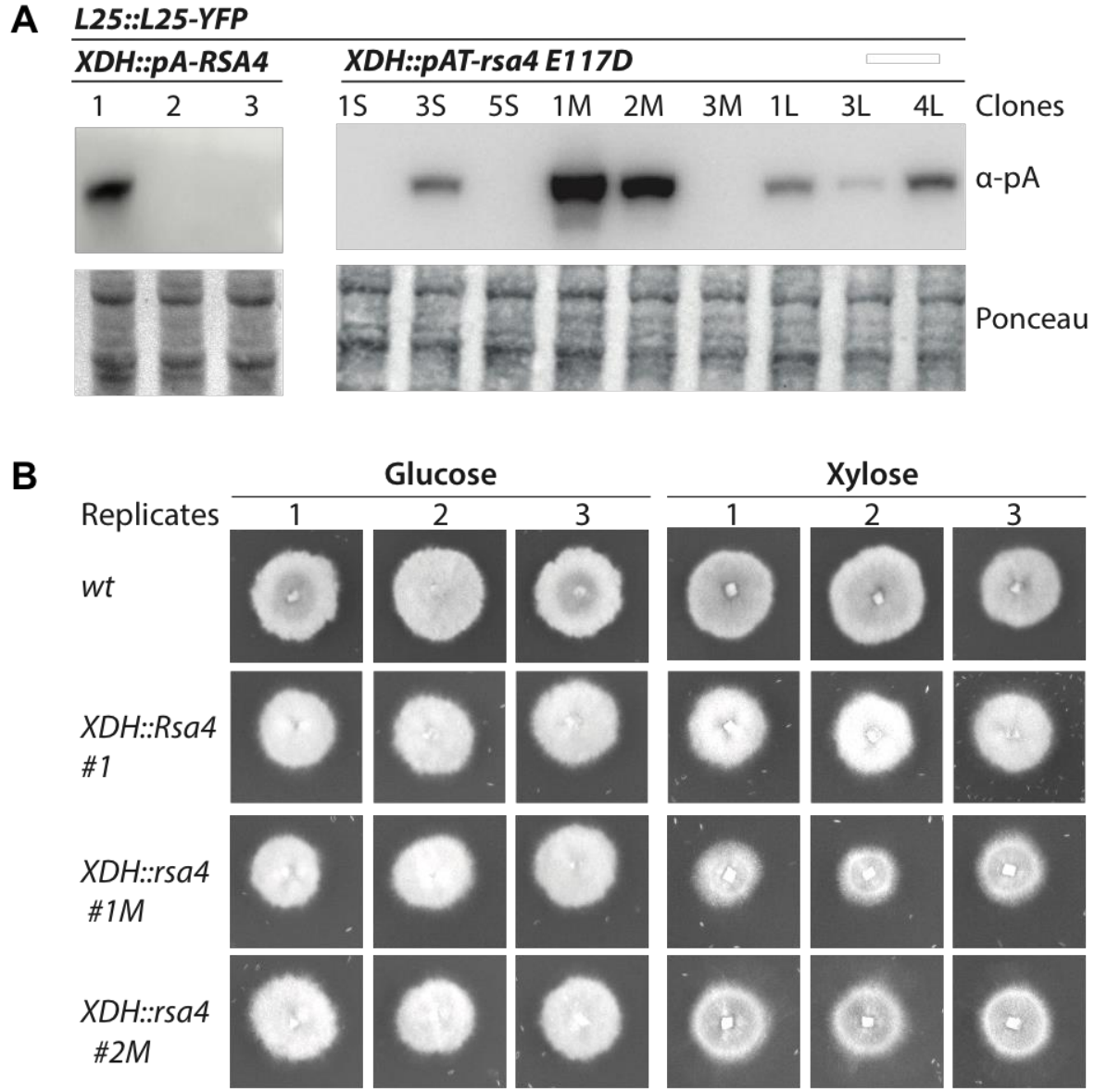

Figure 27: Characterization of clones expressing the mutant rsa4 E117D under control of the XDH-promoter in the L25-YFP reporter background*. The 60S reporter strain L25-YFP was transformed with plasmids where RSA4 (pA-RSA4) or rsa4 (pA-rsa4 E117D) is expressed under control of the xylose activatable XDH-promoter using the erg1-selection marker.* ***A*** *Clone verification by immuno-blotting. Positive transformants were identified by immuno-blotting using an anti-body against the pA-tagged Rsa4 variants. Selected colonies that were verified after transformation with the pA-rsa4 E117D construct were sorted into small (S), medium (M) and large (L) colonies according to the grown colony size on selective CCM-plates.* ***B*** *Colony growth assay on glucose and xylose containing plates. The various Rsa-strains were grown for 20h on selective CCM-plates and the wildtype on CCM plates. Equaly sized mycelia pieces were subsequently transferred from each strain on glucose or xylose containing plates for three technical replicates (1-3). Colony-sizes were imaged after 16h of growth. Importantly, whilst on glucose all strains grow similarly, on xylose containing plates colony 1M expressing rsa4 E117D under control of the XDH-promoter growth smaller.*

To characterize the growth of the obtained *pA-rsa4 E117D* and the *pA-Rsa4* expressing strains under control of the xylose activatable *XDH*-promoter, I grew the

transformants on respecitve plates next to the wildtype. On glucose containting plates, all strains grew similarly dense and large. On xylose containing plates in contrary, the *pA-rsa4 E117D* expressing mutants, shown for colony 1M and 2M showed less dense grown colonies. Additionally colony 1M showed also a smaller radial growth compared to the control strains. I concluded that expression of the mutated factor rsa4 E117D under control of the *XDH*-promoter induced a dominant negative growth defect in *C. thermophilum* upon xylose induction. Apperently, from the tested transformants, a slight phenotype was only visible for the transfromant in which the mutated *rsa4 E117D* was expressed the strongest. Worth noting, when I tested the same mutation under control of the weaker inducing *XYL*-promoter, I could not see an induced phenotype for any of the 5 positive transformants (not shown). Since the hyphae of *C. thermophilum* are multinucleated and each nucleus encodes for a wildtype copy of Rsa4, it can be assumed that the over-expression of the mutant to exert a visible growth defect is challenging and requires strong protein induction of the mutated protein in the cells as it was the case in colony 1M.

Finally I asked, if the *XDH*-promoter allows to induce a 60S subunit export defect in the hyhae of the dominant negative *rsa4* E117D mutant. First, I monitored the induction of pA-Rsa4 E117D between 2h and 6h after growth in glucose vs. xylose containing medium by immuno-blotting. After 2h of exposure to xylose, the detected mutant factor pA-Rsa4 E117D was not enriched compared to mycelia that was grown in glucose containing medium for up to 6h. Expression of pA-Rsa4 E117D was strongest after 4h of xylose induction and slightly reduced after 6h **Figure 28 A**. To avoid the risk to induce pleiotropic effects upon extensive induction of the mutant protein in the cells, I inspected the localization of L25-YFP in the mutant Rsa4 E117D and the wildtype Rsa4 expressing strains already after 4h of xylose induction. In mycelia that was grown in glucose containing medium, the *XDH*-promoter maintained a wildtype localization with homogenuous L25-YFP localization to the cytoplasm and the nucleolus. In contrary, exclusively in the mutant *rsa4 E117D* expressing strain, hyphae that were grown in xylose showed significant accumulation of L25-YFP in the nucleoplasm and strongly reduced cytosolic L25-YFP **Figure 28 B** .

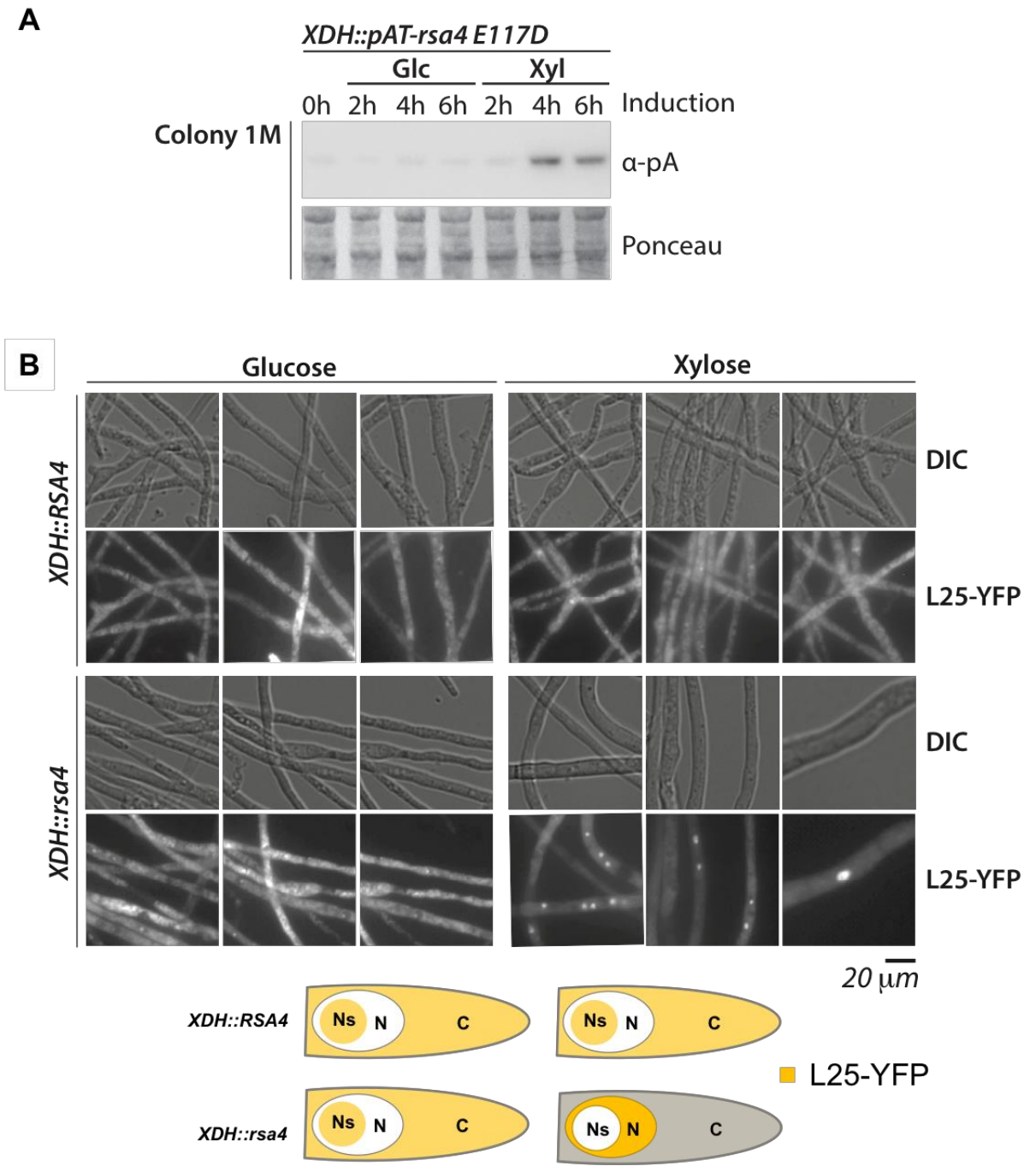

Figure 28: The XDH-promoter controls nuclear accumulation of L25-YFP upon induction of the mutant rsa4 E117D. A *Induction of pA-Rsa4 E117D under control of the XDH-promoter. The expression of Rsa4 E117D in colony 1M was monitored in glucose containing medium before medium exchange (0h) and over 6h after further cultivation in glucose or xylose containing media. Normalized amounts of cell lysates were subjected to immuno-blotting to detect the pA-tagged protein.* ***B*** *L25-YFP localization in RSA4 and rsa4 E117D expressing strains under control of the XDH-promoter. L25-YFP strains expressing pA-RSA4 (RSA4) or pA-RSA4 E117D (rsa4) under control of the XDH-promoter were grown for 16h in glucose containing medium and then shifted to fresh glucose or xylose containing medium for another 4h. Cultures were harvested, homogenized and inspected by fluorescence microscopy. Differential interference contrast images (DIC) and fluorescence images are shown.*

I concluded that the here identified *XDH*-promoter effectively arrested 60S subunit export as it was observed using the *GAL1*-promoter in *S. cerevisiae* (Ulbrich et al., 2009b). Thus, I domonstrated that the *XDH*-promoter allowed me to control a dominant negative ribosome biogenesis mutant using Rsa4 E117D as example. Future studies may show if the here identified xylose activatable promoter allow also to conduct in-vitro assays or to gain cryo-EM structures from accumulating particles, as such as it was shown to work using the *GAL1*-promoter in yeast.

3 Discussion

When I started this project, the potential of the filamentous fungus *Chaetomium thermophilum* was “en vogue” in structural research and industrial investigations due to its thermostable genome (Bock et al., 2014; Amlacher et al., 2011). At this time, the available genetic tools to work with the thermophile were restricted to the constitutive expression of gene fusions with affinity tags, allowing for affinity purifications of proteins and protein-complexes (Kellner et al., 2016b). Affinity purification of the 90S-biogenesis factor Utp6-FTpA that was expressed under control of its endogenous promoter spanning region in *C. thermophilum* shed light on the structure of the very early forming 90S pre-ribosomal particle that was solved by cryo-EM (Cheng et al., 2017; Kornprobst et al., 2016). However, no inducible promoter was available, which is necessary to study ribosome biogenesis with help of dominant negative mutants, as it showed to be a successful technique in yeast. Hence, this PhD-work was dedicated to the establishment of an inducible promoter in *C. thermophilum* to pave the way for the study of dominant negative ribosome biogenesis mutants as new genetic tool for the thermophile.

3.1 The genome of *Chaetomium thermophilum*

A correct gene-annotation is a fundamental resource in established model organism as it is crucial to study the function of genes by molecular gene editing techniques. The importance of a correct genome became evident already for the highly exploited mesophilic filamentous fungi, including the versatile used *Aspergillus niger* (Pel et al., 2007; Reilly et al., 2018; Cairns et al., 2021), and *T. reesei* as host for strong xylanase secretion (R. Liu et al., 2015; Rantasalo et al., 2019; Wong & Saddler, 1992). During the last years, it became evident that the annotation of the reference-genome from the thermophilic filamentous fungi *C. thermophilum* (Bock et al., 2014) hampers in correctness, causing problems in experimental studies of such genes. These experiences were in line with the annotation discrepancies when we mapped the transcriptome to the reference-genome in this study (Singh et al., 2021). Thus, the here provided refined genome annotation from *C. thermophilum* based on deep-sequencing of mRNAs is expected to provide a more reliable resource to correctly delineate transcription start sites of genes and corrected intron-exon boundaries. Moreover

roughly 10% of the coding genes that were annotated in the reference-genome were not supported in our analysis and on the other side replaced by closely as many novel found coding genes (Singh et al., 2021). Hence, our annotation and transcript assembly helps for the complete functional analysis of the genes and proteins in *C. thermophilum*. As an example, the complete laccase enzyme coding gene from *C. thermophilum* could now be found and annotated (Uniprot ID: Q692I0), which is a of interest regarding the growing popularity of the thermophile in the chemical industry. The additionally abundantly novel found non-coding RNAs, including the long noncoding interfering (lincRNAs) allows in the future to study their regulatory role for the expression of protein-coding genes **Figure 19**. The *GAL1/10* gene locus in yeast is a well-studied example, where the transcription of a lncRNA at the genomic *GAL1/10* locus regulates transcription of the *GAL*-genes in addition to the promoter acting *trans*-factors Gal4 and Mig1 (Yamashita et al., 2016). Furthermore, we gained evidence that the thermophile encodes for gene-isoforms as a result of alternative splicing activity which would underpin a complex genome architecture. That gene-isoforms can be found in *C. thermophilum* is worth considering from an evolutionary perspective as it is known from its related filamentous fungi like *Aspergillus flavus* (Chang et al., 2010) or *N. crassa* (Froehlich et al., 2005) in contrast to the budding yeast (Juneau et al., 2009). However, to gain higher confidence that gene-isoforms can be found in the thermophile, a more sensitive sequencing of mRNAs would be necessary, like by paired-end illumina sequencing (Rossell et al., 2014) or alternatively a ribosome profiling analysis could be applied, as described by Weatheritt et al., 2016. Intriguing would be to investigate alternative-splice events as response to the exposure of different growth conditions, like when exposed to various carbohydrates as it can be carried out with the here developed minimal single carbon media **Figure 17**. In summary, the here undertaken transcriptome analysis of the thermophile broadens our possibilities to study the genome architecture and its modes of regulation for various applications that profit from its highly stable genome and proteome.

3.2 The sugars xylose and glucose regulate the transcriptome in *C. thermophilum*

In this work, the transcriptome of *C. thermophilum* was analyzed in order to identify promoters that can be used to control gene-expression using sugars as inducers **Figure 20**. It became apparent that xylose activated precisely genes that allow the fungus to live from xylose as sole carbohydrate source, mapping into xylanolytic and metabolic function genes. Moreover, also genes with function in ribosome biogenesis, export and translation were xylose specifically activated, next to genes of proteins mapping into the transcription of rRNA by RNAP I and III **Figure 20**. This gives rise to the question if the thermophile remodels the architecture of its ribosomes as translation machinery in the presence of xylose to adapt the protein synthesis according to the environmental requirements. Indeed, a cellular heterogeneity in ribosomes to promote the translation of distinct mRNAs during nutritional stress and developmental programs is broadly described in pro- and eukaryotes (Leppek & Barna, 2019; Mercer et al., 2021; Shi et al., 2017). The recently solved high-resolution cryogenic electron microscopy structure of the mature 80S ribosome from *C. thermophilum* (Kišonaitė et al., 2022) shows, that also mature ribosomes can be successfully structurally characterized. Thus, it would be tempting to compare the composition of mature ribosomes from cells, grown on the here provided single carbon glucose with xylose medium **Figure 17**. Further, in vitro translation assays with purified ribosomes and transcripts from sugar specifically upregulated genes may help to tackle the question if specialized ribosomes indeed exist and how they deliberately recognize dedicated mRNA templates (Penzo et al., 2016).

3.3 A xylose inducible promoter system in *C. thermophilum* as new genetic tool

Here, I showed that the sugars D-glucose and D-xylose work as robust inducing compounds to control promoters in hot cultivation conditions of 50 °C, where the thermophile ideally grows (Amlacher et al., 2011). The strategy to test sugar regulated promoters was prompted by the catabolism dependent promoters in use in its mesophilic relatives (Kluge et al., 2018; Meyer et al., 2011). However, if the plasmid

born promoter-regions exert the same regulation of the controlled gene as at the endogenous genomic locus is not clear. The investigated xylose activatable promoters, spanning a sequence of 1.5kb would support a putative regulation by the *trans*-activator XlnR and the *trans*-repressor CreA that recognize promoter elements between 200 bp and 500 bp upstream of the translation start site, as shown in *A. niger* (van Peij et al., 1998) and *P. purpurogenum* (Díaz et al., 2008). However, comparison of the promoters upon YFP-induction on the protein level was in agreement with the transcriptome analysis, which confirmed that the *XYL*- and the *XDH*-promoter are most stringently regulated by glucose and xylose **Figure 22**. Intriguingly, a recently developed genetic tool for *C. thermophilum* showed that side directed transformation of DNA is doable and that in locus expressed proteins showed higher purification yields compared to the traditional technique when plasmid born expression-cassettes are randomly integrated into the genome (Kellner et al., 2022). Thus, now where strongly xylose activatable promoters were identified, in locus gene-fusions may be conducted to test for stronger xylose induction and stricter glucose repression. Along this line, also in *T. reesei* increased expression yields addressing the endogenous *cbh1*-promoter locus, compared to the gene-expression under control of a randomly introduced expression cassettes into its genome (Rahman et al., 2009). Further, the development of a thermostable Crispr/Cas9 technique for targeted gene editing would facilitate site-directed gene editing, which was recently shown for *Trichoderma reesei* (Rantasalo et al., 2018, 2019). To further optimize the here established plasmid born xylose activated gene-expression system, the optimization of the transcript stability could be addressed, for which the 5’ untranslated region (5’ UTR) and the 3’ UTR are relevant. Indeed, swapping of the 5′ UTR from the heatshock protein hsp12 strongly increased the expression level of a heterologous β-glucuronidase in the filamentous relative *Aspergillus oryzae* (Koda et al., 2006). Thus, I delineated the 5’UTR of the strongest constitutively expressed gene in *C. thermophile* (CTHT_0027570) in a 5’ RACE reaction coupled to RNA-sequencing (not shown). The identified 5’UTR sequence could be now used to replace the 5’-UTR from the xylose activatable promoters to stabilize the transcripts in inducing conditions. When a less stable transcript is desirable, like when the measurement of short induction times is desired, the destabilization of the transcript by a 3’-UTR from a transcript with a short life-time can be addressed, as it worked in *C. melanogaster* (Catalán et al., 2016; Kuersten &

Goodwin, 2003) and *C. elegans* (Lai, 2002; Wightman et al., 1993). Thus, in the here developed xylose activatable gene-expression cassette, the 3'-UTR from the constitutively strongly active GAPDH-gene could be replaced by a sugar dependently destabilized 3'-UTR. The overall plasmid architecture to generate genetically modified *C. thermophilum* strains with plasmid-born expression cassettes was strongly improved, compared to the before available plasmids. With help of the plasmid modifications in this work, the required concentrations of plasmid DNA can be conveniently reached for *C. thermophilum* transformation with help of the introduced high copy *ColE*-origin of replication. Further, the designed shuttle plasmid architecture simplifies plasmid generations by restriction cloning, as the cloning vector can now be directly used for transformation with *C. thermophilum,* as illustrated in **Figure 29**. The rapid advances in molecular biology in the field of synthetic biology (ısa Czamanski Nora et al., 2019; Nora et al., 2019) give hope for further rapid advances of the genetic toolbox to explore *C. thermophilum* as emerging model organism with a thermostable proteome.

3.4 The induction of dominant negative mutants *in C. thermophilum*

In this work, I demonstrated as proof of concept that the here identified xylose activated *XDH*-promoter allowed to control the dominant negative mutant factor Rsa4 E117D **Figure 28**. This observation was in line with the in yeast well characterized mutant, exerting the same pre-60S subunit accumulation in the nucleoplasm, when controlled under control of the *GAL1*-promoter in L25-YFP expressing cells (Ulbrich et al., 2009). Whilst the *GAL1*-promoter in yeast induced a strong dominant negative growth defect upon induction of Rsa4 E117D, using the *XDH*-promoter in C. thermophilum showed a less sever growth phenotype **Figure 27**. The inspected milder phenotype in *C. thermophilum*, compared to the stronger phenotype in yeast can be due to at least three reasons that are not mutually exclusive. Firstly, the expression of *rsa4* under control of the *XDH*-promoter might be weaker than it is the case using the *GAL1*-promoter in yeast, compared to the endogenous *RSA4* expression in *C. thermohilum* and yeast, respectively. Second, the robustness to genetic defects improved with increased cellular complexity (Stucki & Jackson, 2004). Thus, it can be speculated that

C. thermophilum is able to bypass toxic allels more efficiently than yeast cells, arguing that yeast cells are much more simply organized compared to the multicellular, multinucleated filamentous hyphae of *Chaetomium thermophilum*. Third, in yeast the *rsa4* mutant is isogenic, whereas the hyphae from *C. thermophilum* are multinucleated which makes the over-expression of the induced mutated allele more challenging. Selection for an isogenic strain in which all nuclei carry an inducible copy of the mutated *rsa4* allele would assumingly result in a more pronounced phenotype. Thus, when in the future dominant negative mutant strains are generated, it may be beneficial to subject transformants to a sporulation step since ascospores are believed to be haploid or at least tend to dominate the germinating spore population in lab conditions (Anderson et al., 2015; Neiman, 2005).

3.5 Applications of dominant negative ribosome biogenesis mutants to study early maturation events

Whereas the ribosome biogenesis steps occurring in the nucleoplasm and the cytoplasm are intensely studied already, using mainly the traditional yeast model, the earliest maturation steps are largely unknown. Pioneered by the solved structure of the early forming 90S-particle from *C. thermophilum*, structural insights into early acting biogenesis steps could be obtained (Kornprobst et al., 2016). In order to explore dominant negative mutants to arrest early assembly processes that happen even prior to the assembly of the 90S-particle in *C. thermophilum*, the early 90S particle purifying bait Efg1-FTpA can be tested. In yeast, I could purify an early 90S particle that contains the early joining factors Efg1, Bud22 next to the helicase Dbp4 as well as the snoRNA U14, which are all not present any longer on the classic Utp6-FTpA purified 90S intermediate (not shown). Since in yeast the Dbp4 helicase was suggested to release the U14 snoRNA in yeast from the assembling 90S-intermediate (Koš & Tollervey, 2005; Soltanieh et al., 2015), the *XDH*-promoter in *C. thermophilum* could be used to overexpress a catalytically inactive Dbp4 mutant to stabilize the U14 carrying Efg1-particle which can then be purified to gain structural insights from solved cryo-EM models. Regarding the early maturation events mapping into the formation of the large 60S subunit, a recent study in yeast provided a cryo-EM structure in which the 90S-particle is in physical contact to the premordial pre-60S subunit, inducing the dominant

mutant *mak5 D333A* under control of the *GAL1*-promoter in yeast (Ismail et al., 2022). In order to assign the proteins and RNAs in this premordial pre-60S particle, a higher resolution is required, which might be provided using the dominant *mak5*-mutant under control of the *XDH*-promoter in *C. thermophilum*.

3.6 genetic and biochemical tools for optimized biosynthesis of thermostable proteins

The thermophile *Chaetomium thermophilum* edges closer into focus to produce temperature stable proteins not only for structural research but also for industrial applications (Ahmed et al., 2012; Jiang et al., 2020; A. N. Li & Li, 2009; X. Li et al., 2020; Quehenberger et al., 2019). In the methylotrophic yeast *P. pastoris* (Prielhofer et al., 2015) and its filamentous relatives (Amore et al., 2013; Chroumpi et al., 2020), minimal media are routinely used to optimize growth and protein production yields. Whilst *Chaetomium thermophilum* could only be cultivated on the nutritionally complex and rich CCM in the lab, the here developed minimal media offers screening for intracellular and secreted proteins from *C. thermophilum*, grown on defined carbon sources, shown here for glucose and xylose **Figure 17**. Similar substrate dependent growth studies allowed already to catalogue the expression of industrially relevant proteins from *C. thermophilum*, as shown by (X. Li et al., 2020). Whereas its transcriptome is about to be studied, nothing is known about regulatory processes that control the steady state protein abundance, for which post-transcriptional, translational and on protein degradation mechanism are implied (Vogel & Marcotte, 2012). As a start in this direction of studies, the here performed polysome analysis allows to assign weakly and strongly translated transcripts and separate them from each other since the strongest translated mRNAs are bound by the most ribosomes and thus migrate furthest from the 80S monosomes along the sucrose gradient **Figure 21**. In the enzyme secretion factory *Aspergillus niger*, polysome profiling was successfully applied to monitor secretion stress responses to optimize cultivation conditions (Guillemette et al., 2007). The polysome profile of *C. thermophilum* can now also be used to apply ribosome profiling on the separated sucrose fractions to study properties of the transcripts that determine poor and efficiently translation (Ingolia et al., 2009). Further, the observed highly abundant 80S monosomes in the thermophile deserve closer

attention as here poorly or non-translating ribosomes like the ones that are trapped in the quality control steps before they join the actively translating ribosomes may be found and studied in these fractions in the sucrose gradient. Further, the role of upstream ATGs that result in the translation of upstream open reading frames (uORFs) in the 5′ untranslated region (5′UTR) with often regulatory effect on the translatome can be studied along the profile (Wethmar et al., 2014; Akirtava et al., 2021). Altogether, this approach helps to decipher developmental and stress dependent adaptations on the level of translation.

Conclusion

High protein stabilities of eukaryotic proteins are often highly desirable in research with focus on structural biology and various industrial applications. Thus, the thermophilic fungus *Chaetomium thermophilum* as natural producer of proteins with superior protein stabilities, compared to its mesophilic counterparts, is edging closer into focus as model organism. The here gained genomic and transcriptomic insights into the thermophile are expected to support studies that further broaden and deepen our understanding of the largely uncharacterized organism as pre-requisite for progressive applications. These may include the applications of the here developed sugar-regulatable promoter system to study cellular or extra-cellular proteins.

4 Materials and Methods

Routinely used molecular biology techniques, like the polymerase chain reaction (PCR), enzyme digestion of double-stranded DNA species, separation of DNA fragments by agarose gel electrophoresis using 1 % v/w agarose in 1xTAE buffer and DNA-ligation reactions were performed as previously described (S. N. Ho et al., 1989; Inoue et al., 1990).

PCR reactions were mixed either with the Phusion DNA polymerase or the Taq DNA polymerase (both Thermo Fisher Scientific). PCR-products were subsequently purified with the Gel Extraction kit from Sigma Aldrich according to the manufacturer's instructions to prepare DNA fragments for later DNA-ligation reactions. Promoter-regions from *Chaetomium thermophilum* genome were PCR-amplified on gDNA. Oligonucleotide stocks were purchased from Sigma Aldrich and dissolved in water to a concentration of 100 µM. Restriction enzymes from Thermo Fisher Scientific and New England Biolabs (NEB) were applied for DNA digestions according to the manufacturer instructions. The T4 DNA ligase from NEB was used for Ligation reactions. For routine procedures, plasmids were isolated from the chemical competent *E. coli* DH5α strain with the genotype *F⁻ endA1 glnV44 thi-1 recA1 relA1 gyrA96 deoR nupG purB20 φ80dlacZΔM15 Δ(lacZYA-argF)U169, hsdR17($r_K^-m_K^+$), λ⁻* with help of the Miniprep (HP) kit (Sigma Alrdrich). Cloned plasmids that carried PCR amplified products were sequenced by Eurofins MWG-Operon, Ebersberg/Germany. A complete list of plasmids used in this study is shown in Table 6. In order to prepare pRSFDuet -plasmid stocks for subsequent *C. thermophilum* transformations, I used The PureYieldTM Plasmid Midiprep System from Promega according to the providers instructions. To concentrate plasmid eluates to 5000 ng in 20 ul of water, 1/10th volume of 3M NaOAc (sodium acetate, pH 5.2) and 2 volumes of ice-cold 100 % EtOH (ethanol) were added to the sample. Subsequently, the DNA was recovered by incubated on ice for 15-30 min followed by centrifugation with 14 000 x g for 15 min at 4°C. The resulting pellet was washed with 70 % EtOH to remove the residual salt, air dried at room temperature and resuspended in nuclease-free H_2O.

4.1 Xylose inducible promoters on shuttle plasmids

In this work, a high copy shuttle plasmid system was developed to quickly introduce genes of interest under control of the D-xylose inducible *XYL*- and *XDH*- promoters in *C. thermophilum*. To optimize plasmid recovery from *E. coli* for subsequent *C. thermophilum* transformations, I used a high-copy *colE1* origin. Further, I exchanged the GAPDH-terminator of the selection marker cassette with the 3' UTR from a histone deacetylase (CTHT::0004840) to circumvent plasmid instability in *E. coli* due to duplicative terminator sequences facing each other. The combination of the ampicillin selection marker (*bla*-gene) to select transformants in *E. coli* with the *erg1* or *hph1*-markers to select for *C. thermophilum* transformants resulted in a shuttle plasmid system that allows to assemble genes, promoters and tags of interest directly in the plasmid that gets transformed with *C. thermophilum*, as shown in **Figure 29**.

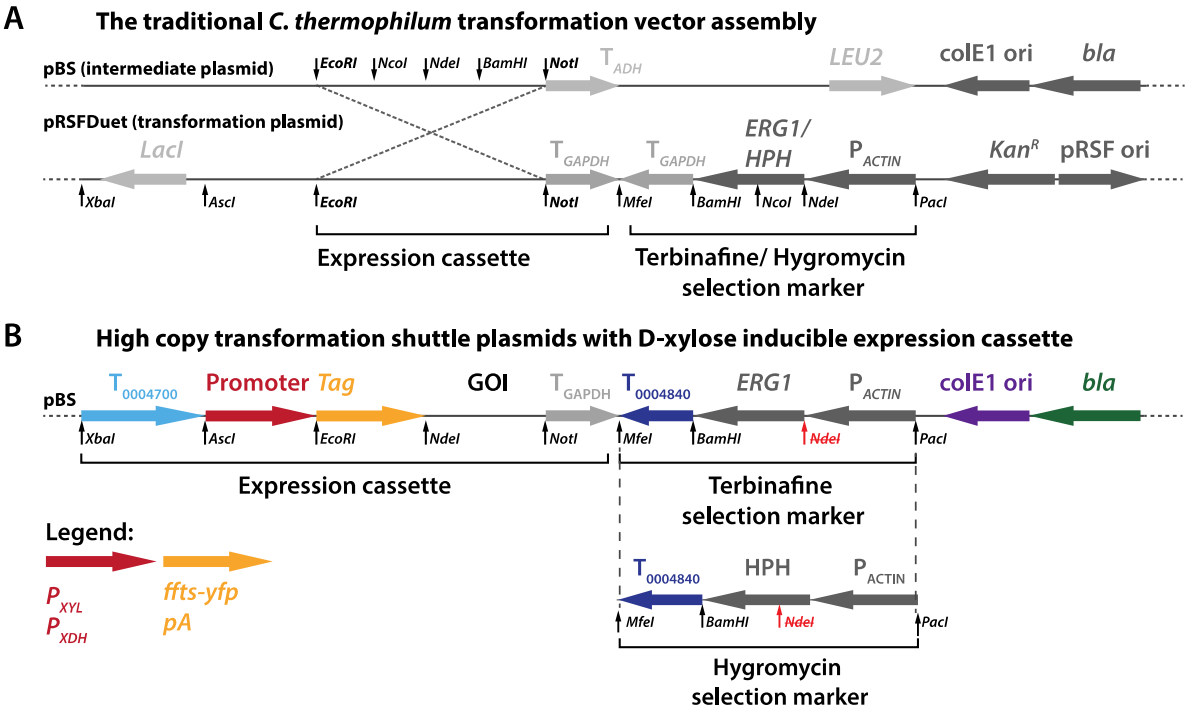

Figure 29: The genetic architecture of shuttle plasmids with xylose inducible promoters. A *Schematic representation of the traditional transformation plasmid assembly strategy according to Kellner et al., 2016. In short, a multiple cloning site in a high copy pBluescript (pBS) derivative is used to clone genes under control of the constitutively strong actin-promoter with N- or C- terminal affinity tags. In a second cloning step, the expression cassette is sub-cloned into a low copy pRSFDuet background (dotted lines) that contains the ERG1- or HPH1-marker genes to select for positive transformants by terbinafine and hygromycin, respectively.* ***B*** *Schematic representation of the herein constructed shuttle plasmids. The shuttle plasmids allows construct assemblies directly in the transformation plasmid and support high DNA recovery yields that meet the requirements for the transformation with C. thermophilum protoplasts. To this end, the shuttle plasmid was equipped with a*

high copy origin (ColE1) and selection cassettes for E. coli selection by ampicillin (bla) in mutagenized HPH and ERG1 selection cassette backbones to select for positive C. thermophilum transformants. So far, shuttle plasmid derivatives provide N-terminal yfp (ffts-yfp) and pA-affinity tags under control of the XYL- and XDH-promoter. The expression cassettes are flanked by an upstream and down-stream terminator to block potential genomic background activity. Changes to the parental transformation plasmid are highlighted in colours.

4.2 Cultivation media for *E. coli*

Table 3: LB (Lysogeny broth) medium for E. coli work.

Compound	**amount**
yeast extract	0.5 % (w/v)
tryptone	1 % (w/v)
NaCl	0.5 % (w/v)
pH 7.2	

4.3 Cultivation media used and generated to cultivate *Chaetomium thermophilum*

The complete cultivation medium (CCM) was used to recover *C. thermophilum* spores. The minimal single carbon media were developed in this work and used to characterize and apply D-xylose inducible promoters.

Table 4: Composition of the developed minimal single carbon D-glucose (SGM) and D-xylose (SXM) media compared to the parental CCM.

Classification	**complete cultivation medium (CCM)**		**minimal medium (SPY-reference)**	
	compound	amount	compound	amount
Salts	NaCl	0.5 g/L	NaCl	0.5 g/L
	MgSO4 x 7H2O	0.5 g/L	MgSO4 x 7H2O	0.5 g/L
	K2HPO4 x 3H2O	0.65 g/L	K2HPO4 x 3H2O	0.65 g/L
	Fe(III)sulfate-hydrate)	0.01 g/L	Fe(III)sulfate-hydrate)	0.01 g/L
Nitrogen source, trace elements	Peptone	1 g/L	Peptone	1 g/L
	Yeast extract	1 g/L	Yeast extract	1 g/L
	Tryptone	5 g/L	-	-
Carbon sources	Sucrose	3 g/L	D-glucose	10 g/L

	Dextrin	15 g/L	D-xylose	10 g/L
pH: 6,9-7,1				

4.4 List of genetically modified *C. thermophilum* strains used in this study

Table 5: List of strains used in this work.

strain	**genetic background**	**Selection marker**	**source**
UTP6::UTP6-FTpA	wildtype	Terbinafine	Kornprobst et al., 2016
Control (Spacer::YFP)	wildtype	Terbinafine	This work
XLN::YFP	wildtype	Terbinafine	This work
CBP::YFP	wildtype	Terbinafine	This work
XYL::YFP	wildtype	Terbinafine	This work
XDH::YFP	wildtype	Terbinafine	This work
XYL::UTP6-FLAG-TEV-YFP	wildtype	Terbinafine	This work
L25::L25-linker-yfp	wildtype	Hygromycin	This work
XYL::pAT-RSA4	L25::L25-linker-yfp	Hygromycin Terbinafine	This work
XYL::pAT-rsa4 E117D	L25::L25-linker-yfp	Hygromycin Terbinafine	This work
XDH:: pAT-ctRSA4	L25::L25-linker-yfp	Hygromycin Terbinafine	This work
XDH::pAT-rsa4 E117D	L25::L25-linker-yfp	Hygromycin Terbinafine	This work

4.5 List of assembled plasmids that were used in this work

Table 6: The following plasmids were used in this work.

name	genetic information	backbone	resistance	source
pSR41	*$Ter_{0004700::}$Spacer::YFP::Ter_{GAPDH}*	pRSF-Duet P_{actin}::ERG1::Ter_{GAPDH}	Kan, Ter	This work
pSR33	*$Ter_{0004700::}$XLN::YFP::Ter_{GAPDH}*	pRSF-Duet P_{actin}::ERG1::Ter_{GAPDH}	Kan, Ter	This work
pSR31	*$Ter_{0004700::}$CBP::YFP::Ter_{GAPDH}*	pRSF-Duet P_{actin}::ERG1::Ter_{GAPDH}	Kan, Ter	This work
pSR32	*$Ter_{0004700::}$XYL::YFP::Ter_{GAPDH}*	pRSF-Duet P_{actin}::ERG1::Ter_{GAPDH}	Kan, Ter	This work
pSR35	*$Ter_{0004700::}$XDH::YFP::Ter_{GAPDH}*	pRSF-Duet P_{actin}::ERG1::Ter_{GAPDH}	Kan, Ter	This work
pSR38	*$Ter_{0004700::}$XYL::UTP6-FLAG-TEV-YFP::Ter_{GAPDH}*	pRSF-Duet P_{actin}::ERG1::Ter_{GAPDH}	Kan, Ter	This work
pSR72	*$Ter_{0004700::}$L25::L25-linker-yfp::Ter_{GAPDH}*	pRSF-Duet P_{actin}::HPH::Ter_{GAPDH}	Kan Hyg,	This wor
pSR79	*$Ter_{0004700::}$L25::L25-linker-yfp::Ter_{GAPDH}*	pRSF-Duet P_{actin}::ERG1::Ter_{GAPDH}	Kan, Ter	This work
pSR103	*$Ter_{0004700::}$XYL::pAT-RSA4 E117D::Ter_{GAPDH}*	pBluescript $P_{actin(\Delta NdeI)}$::ERG1::$Ter_{0004840}$	Amp, Ter	This work
pSR104	*$Ter_{0004700::}$XYL::pAT-rsa4 E117D::Ter_{GAPDH}*	pBluescript; $P_{actin(\Delta NdeI)}$::ERG1::$Ter_{0004840}$	Amp, TerR	This work
pSR99	*$Ter_{0004700::}$XDH::pAT-RSA4::Ter_{GAPDH}*	pBluescript; $P_{actin(\Delta NdeI)}$::ERG1::$Ter_{0004840}$	Amp, TerR	This work
pSR100	*$Ter_{0004700::}$XDH::pAT-rsa4::Ter_{GAPDH}*	pBluescript; $P_{actin(\Delta NdeI)}$::ERG1::$Ter_{0004840}$	Amp, TerR	This work

4.6 Generation and maintenance of genetically modified *C. thermophilum* strains

Transformation of wildtype *C. thermophilum* was performed similarly as described by Kellner et al., 2016, using 5 μg of circular plasmid DNA in a volume of 20 μL and 2.5 x

107 protoplasts. To obtain protoplasts to transform DNA with, a parental strain was grown o.n. on a CCM plate. Half of the plate were scraped off by a sterile scalpel and cut into tiny pieces to inoculate 100 ml CCM in a 250 ml baffled flask with and incubated at 50°C and 100 rpm for up to 24h. The culture was poured into a sterile kitchen blender and mixed 4x 20 sec. 8 ml were homogenized mycelia mix were used to inoculate 400 ml CCM in a 1 L baffled flask and incubated at 50°C and 95 rpm for no longer than16h. Mycelium pellets were harvested over a metal sieve and washed with protoplast buffer (PP). One table-spoon full of mycelium was dropped into a 100 ml flask containing 80 ml digestion solution (PP with 10 mg BSA and 25 mg/ml lysing enzymes). The lysis mix was incubated at 30 °C and 110 rpm up to 3-4 h until protoplasts were seen in microscopy samples. Protoplasts were filtered through glass filter funnel (pore-size 1) under constant washing with PP to support protoplast clearing in 50 ml falcons. Protoplasts were carefully settled by centrifugation for 8 min at 2400 rpm at 4°C. Then, the protoplasts were washed again with 25 ml of PP and taken up in 10 ml PP. The total number of protoplasts was calculated with help of a Thoma counting chamber. 200 µl Protoplasts were pipetted carefully on ice in a mix of 2,5 µl heparin (10 mg/ml), 2 µl spermidine (50 mM) and 1 µl ATA (0,4 M) as well as 40 µl STC/PEG-solution before adding 5 to 10 µg of plasmid DNA in 10 to max. 20 µl of water. The mix was inverted gently several times until the mixture is homogenous and then incubated on ice for 20-25 min. 750 µl STC/PEG-solution was added slowly followed by inversion of the reaction cups around 20 times until the mixture is homogenous and incubate samples on a rocking shaker for 10 min. The transformation mix was plated on regeneration agar plates in 330 ul volumes per plate and incubated at 50°C for three days when selecting for terbinafine resistant clones and at 42 °C for 5 days to select for hygromycin resistant clones. Plates were incubated after the first day on with a moist tissue to avoid drying during incubation. Emerging colonies were plated on fresh selective media plates (supplemented with 0.5 µg/ml terbinafine or 75 µg/ml Hygromycin B) to check for stable resistance).

Protoplast Buffer (PP)

0.8 M Sorbitol;

0.013 M Na_2HPO_4; 0.045 M KH_2PO_4 Set pH to 6.5.

Digestion Buffer

25 mg/ml “lysing enzymes” (Sigma L1412) and 10 mg BSA solved in PP buffer.

STC

0.8 M Sorbitol; 80 mM $CaCl_2$; 10 mM Tris-HCl.

STC/PEG-solution

40% (w/v) PEG_{6000} in STC

Regeneration agar

Bottom agar

10 ml CCM-sorbitol agar, supplemented with 1 µg/ml (f.c.) terbinafine or 200 µg/ml (f.c.) hygromycin.

Top agar

10 ml CCM-sorbitol agar without antibiotic are poured shortly before plating the transformation mix.

Selection agar

CCM agar plates supplemented with 0.5 µg/ml (f.c.) terbinafine or 75 µg/ml (f.c.) Hygromycin.

4.7 Long term storage of *C. thermophilum* strains

Spores were generated from genetically modified strains for long-term storage. To this end, corn meal agar was inoculated with shredded mycelium and incubated at 37 °C for approximately seven days. Spores were scraped from the surface of the corn meal agar, resuspended in 1 M sorbitol, filtered through sterile gauze to clear agar particles, and concentrated by centrifugation by 5000 rpm for 8 min. Spore-solutions were dropped on filter paper pieces for storage at RT or dispersed in 1ml aliquots and stored at −20°C. For reactivation of strains, a spore-soaked filter paper or 50µl of a liquid spore stock were plated on a selection CCM plates, traced with hygromycin or

terbinafine depending on the selection marker used for transformation and incubated at 50°C for approximately 2 days for terbinafine resistant strains and at 42°C for hygromycin resistant strains.

4.8 Extraction of gDNA from Chaetomium thermophilum

gDNA was extracted from the wildtype *Chaetomium thermophilum* strain, as well as from the control-YFP reporter strain. Transformants were harvested from 50 ml of o.n. grown CCM cultures by sieving, dried on paper towels and formed into small flakes. Dried mycelium was lysed in 2 ml screw cap tubes with 300 µl Zirkonia beads and 500 µl Ct lysis buffer in a mini bead beater at 5000 rpm for 2x 20 sec in 4 repetitions. RNAs were degraded by 2 µl RNaseA (10 mg/ml) in a 10 min incubation period at 37°C with gentle agitation. Subsequently, 165 µl 5M NaCl were mixed with the lysates by inverting the cups several times. After centrifugation for 20 min at 13 000 rpm at RT, the supernatant was transferred into a new test tube and mixed with 800 µl Phenol/Chloroform/Isoamyl alcohol (ratio 25:24:1) by tube inversions until the solution became milky, followed by 10 min of centrifugation at 13 000 rpm at RT. The phenol/Chloroform-extraction step was carried out two to three times. The aqueous phase was transferred into a new test tube and mixed thoroughly with 2,5 volumes of pre-cooled 100 % ethanol. After centrifugation for at least 20 min, at 13 000 rpm at 4°C, the supernatant was discarded and the DNA pellet washed with 1 ml 70% ethanol by adding and centrifugation for 5 min at 13 000 rpm at RT. The gDNA pellet was air dried for approx. 10 min and resolved in 50 µl TE-buffer (pH 8.0) or H_2O at 50°C. Optionally, again 0.5 µl RNaseA were added to the TE buffer to eliminate residual RNA traces.

Ct Lysis Buffer

40 mM Tris-HCl, pH 7.5 20 mM Na-acetate
1 mM EDTA
1% (w/v) SDS

TE Buffer

10 mM Tris-HCl, pH 8.0
1 mM EDTA

4.9 Extraction of total RNA from *C. thermophilum*

Total RNA from C. thermphilum cultures was extracted using the SV total RNA extraction kit from Promega to generate Illumina-deep sequencing libraries of mRNAs. *C. thermophilum* was grown o.n. on a CCM plate, mycelia was scraped off with a scalpel and transferred into a 250 ml baffled flask containing 100ml of glucose containing medium. The cultures were incubated at 50°C at 100rpm for 18h and subsequently homogenized at 6000 rpm for 2min using a GM200 blender (Retsch, Haan, Germany). Nine 250 ml baffled flasks were filled with 100ml of SPY-medium and inoculated with 2ml of homogenized pre-culture and grown in minimal medium without sugar (SPY) for 42h. Three flasks were harvested for RNA extraction (non-induced reference condition). To three cultures, D-glucose or D-xylose was added to a final concentration of 1 % (w/v), respectively. Six hours after growth on D-glucose or D-xylose as sole carbohydrate source, all cultures were harvested by a sieve, washed with hot water and ground manually in a liquid nitrogen cooled mortar to fine powder. Approximately 100 mg of ground powder were transferred into a pre-cooled 2 ml reaction cup and immediately mixed with 600 µl of lysis buffer by thorough pipetting until the lysate became homogenous. Then, 1200 µl dilution buffer were added and the lysate mixed by pipetting. The reactions were split on two 900 µl cups and processed further according to the manufacturer instructions. The RNAs were eluted in a volume of 75 µl.

4.10 cDNA preparation and qRT-PCR analysis

C. thermophilum RNA samples were used for complementary DNA (cDNA) synthesis. Reverse transcription was performed using the Maxima First Strand cDNA Synthesis Kit for RT-qPCR (Thermo Scientific) following the manufacturer's protocol. After cDNA synthesis, cDNA samples were diluted to a final volume of 120 µL. Sequences of the target genes and the tested normalizer candidates, shown in Table 7, were obtained from the *Chaetomium thermophilum* Genome Resource (*https://c-thermophilum.bork.embl.de*). The TaqMan pRT-PCR kit was used according to the providers instruction. Respective primers and probes were designed with help of the Universal ProbeLibrary Assay Design Center (Roche). qRT-PCR was performed with a total reaction volume of 20 µl that contained 5 µl of diluted cDNA template, 0.4 µl of

forward and reverse primer, 0.2 µl of probe and 10 µl of ROX Mix. The PCR amplification procedure was set as 40 cycles of 95 °C for 2 min, 95 °C for 5 s and 60 °C for 20 s. All qRT-PCR reactions were measured in three experimental and two biological replicates. For relative quantitation of transcript dynamics, the ΔΔCT quantitation method was applied according to (Pfaffl, 2001).

Table 7: Primers and probes used for TaqMan qRT-PCR reactions.

Gene	Issue	Forward Primer (5'-3')	Reverse Primer (5'-3')	Probe
CTHT_0045510	Normalizer	atttgtacggcgaagacgat	cttgatcgtacgggcactc	15
CTHT_0011440	target	gaccacgcatcactccatc	cgcagtcgtgatggaaca	81
CTHT_0003950	target	gacaactactcgggcaccat	gatgcgcaacaggtagtcac	4
CTHT_0073860	target	gcatgggcaaggctgata	gccatagcggaaggaacc	60
CTHT_0011270	target	cctgctctcagatcgaaaaga	gcttgatctgcaagagtgga	71

4.11 The induction assay to monitor YFP-expression in promoter-YFP reporter strains

C. thermophilum var. *thermophilum* mycelium (DMSZ 1495) was propagated on CCM agarose plates as described previously (Kellner et al., 2016a). *C. thermophilum* strains used and generated in this work are listed in Table 5**.** *C. thermophilum* mycelium was grown for 20h on CCM agar plates, carefully scraped off from four plates and cut into small pieces as inoculum for liquid pre-cultures. Mycelia was propagated in 600 ml CCM traced with 100 µg/ml ampicillin in 1 L baffled flasks at 50°C and 95 rpm for 24 hours. Over-night grown cultures were shredded at 6000 rpm for 2 min in a GM200 blender (Retsch, Haan, Germany). 70 ml of homogenized mycelia were used to inoculate 2 L of glucose containing medium and xylose containing medium, shown in Table 4. In glucose medium grown pre-cultures were grown in 5 L baffled flasks at 50°C and 95 rpm for 16 hours. The mycelium was then strained through a metal sieve (ISO 3310-1, pore size 100 µm), washed thoroughly with around 50 °C hot water and shifted to 2 liters of preheated glucose or xylose containing medium for dedicated induction time.

4.12 Immunoblotting

50 ml of submerged *C. thermophilum* cultures were collected from liquid cultures, harvested with a metal sieve, dried between filter paper and quickly frozen at -20°C until lysates were prepared. Frozen mycelium was taken up in 800 µl NB-HEPES lysis buffer (20 mM HEPES, pH 7.5, 150 mM NaCl, 50 mM K(OAc), 2 mM $Mg(OAc)_2$, 1 mM dithiothreitol (DTT), 5% glycerol (v/v), 0.1% NP40 (v/v), 40 µl/ml SIGMAFAST protease inhibitor cocktail (Sigma Aldrich)), and mechanically lysed with 500 µl of zirconia beads (0.5mm diameter, Carl Roth, Karlsruhe, Germany) in a Precellys 24 homogenizer (Bertin Instruments, Montigny-le-Bretonneux, France) by 4 runs at 5.000 rpm, 2 x 20 seconds at 4°C. Obtained lysates were cleared by centrifugation at 14.000 rpm and 4°C for 25 minutes. The protein concentration was determined via A_{280} measurement with a NanoDrop 2000 spectrophotometer (Thermo Scientific, Waltham, USA) and normalized to equal total protein concentration of 10 ng/µl in SDS loading buffer (10% glycerol (v/v), 60 mM Tris-HCl pH 6.8, 2% sodium dodeyl sulfate (w/v), 10 mM DTT, 0.01% bromophenol blue (w/v)). 80 ng of total protein were loaded of each sample for SDS-PAGE (4-12% gradient Bis-Tris polyacrylamide NuPage gels from Invitrogen), run for 1h at 180V. Semidry transfer was used at 12V for 1h to transfer proteins on nitrocellulose membranes. To check for equal protein loading and transfer of samples, membranes were incubated with Ponceau S solution (Serva, Heidelberg, Germany) for protein staining since so far no suitable proteins for immunologic normalization are available in *C. thermophilum*. For anti-YFP directed immunoblotting, membranes were blocked for 1h in PBS-T with 5% (w/v) milk powder and subsequently incubated overnight at 4°C with mouse anti-GFP (1:3000, 1181446001, Roche) antibodies followed by incubated at room temperature for one hour with, washed three times for 5 min with PBS-T and subsequently incubated with HRP conjugated goat anti-mouse-IgG antibodies (1:3000, 170-6516, BioRad). For immunoblotting of pA-tagged proteins, anti-pA-HRP (1:3000, P1291, Merck) conjugated antibodies were used. Then, the membrane was washed five times with PBS-T (0.05% Tween) and developed in Immobilon Western HRP Substrate (Millipore, Burlington, USA). For imaging, an ImageQuant LAS 4000 mini biomolecular imager (GE Healthcare, Chicago, USA) was used.

4.13 Epi-fluorescence microscopy

To observe YFP expression and localization in YFP-reporter strains, 50 ml of submerged *C. thermophilum* cultures were collected at desired time points during the induction assay. Harvested mycelium was washed thoroughly in hot water and taken up in equal volume of hot water. Mycelia was immediately homogenized with a sterile hand blender for 45s and applied on top of an agarose pad (1% agarose in Tris-EDTA, pH 8) and inspected with a Zeiss Axio Imager Z1 (Zeiss, Oberkochen, Germany) with a 63x NA 1.4 Plan-Apochromat oil immersion objective lens.

4.14 Tandem affinity purification (TAP) with FLAG-TEV-pA-tag (FTpA)

Tandem-affinity purification (TAP) was applied to purify the 90S pre-ribosomal particle from different media with ctUTP6-FTpA as bait according to (Kornprobst et al., 2016). 600 µl IgG Sepharose Fast Flow beads (Cytiva, Marlborough, USA) were washed with lysis buffer and mixed with the cleared cell lysate. The mixture was incubated on a turning wheel at 4°C for 16 hours. Beads were then washed twice in 10 ml NB-HEPES lysis buffer without PI and 0.01% NP40 (v/v), loaded onto a filter column (MoBiTec, Göttingen, Germany) and eluted by 2ul of His-TEV protease cleavage for 1.5 hours at 16°C in 800 µl of fresh NB-HEPES wash buffer. The TEV-eluate was purified in a second step by incubation for 2 hours at 4°C on 80µl anti-FLAG agarose beads (Anti-Flag M2 affinity gel, Sigma-Aldrich) in spin filter columns (MoBiTec). The purified eluate was competitively eluted from anti-FLAG beads by incubation with 5x concentrated FLAG-peptides in 45 µl NB-HEPES buffer by incubation for 45 minutes, 4°C and 900 rpm in a thermoshaker. FLAG eluates were subjected to SDS-PAGE and stained o.n. by colloidal Coomassie staining (RotiBlue, Carl Roth Karlsruhe, Germany).

4.15 Polysome analysis with sucrose gradients

Polysome analysis was carried out to monitor the distribution of the L25-YFP fusion along the gradient to verify functionality of the YFP-tagged 60S subunit by the L25-YFP fusion protein. Cultures were taken at dedicated timepoints from the 50°C incubator and cooled for ten minutes in ice-bathes prior to harvesting the mycelium. The vacuum-dried mycelium was rinsed with NB-HEPES buffer with 0.025 µl/ml RiboLock and 0.2 mg/ml cycloheximide and then ground manually with a mortar and pestle submerged in liquid nitrogen. Worth noting, adding cycloheximide directly to the culture prior to harvesting did not show any effect in contrast to the typical procedure applied when working with yeast cells. Cell lysates for polysome profiling were prepared by rigorously resuspending 0.5 ml of ground frozen mycelium in an equal volume of NB-HEPES with cycloheximide. The lysate was cleared at 14.000 rpm, 4°C for 20 and another run for 5 minutes, and the RNA concentration was determined by A_{260} measurement at a NanoDrop 2000 spectrophotometer. For long term storage, the lysate was aliquoted into 200 µl fractions in PCR tubes and snap-frozen in liquid nitrogen for storage at -80°C. Sucrose density gradients were prepared from an equal volume of 15% (w/v) and 50% (w/v) sucrose in NB-HEPES buffer (20 mM HEPES, pH 7.5, 150 mM NaCl, 50 mM K(OAc), 2 mM $Mg(OAc)_2$, 1 mM dithiothreitol (DTT), 5% glycerol (v/v), 0.1% NP40 (v/v), 40 µl/ml SIGMAFAST protease inhibitor cocktail (Sigma Aldrich) in long gradient tubes using a GradientMaster (BioComp, Fredericton, Canada). 5 A_{260} ODs of lysate were then loaded onto the gradient and centrifuged for 2.5 hours at 39.000 rpm in an Optima L-90K ultracentrifuge equipped with an SW40 swinging bucket rotor (Beckman Coulter, Brea, USA). A_{254} profiles of the gradients were recorded with a FoxyJunior fraction collector with PeakTRAK software (Teledyne ISCO, Lincoln, USA), which separated the gradient into either 0.4 ml or 1.3 ml fractions. Gradient fractions were precipitated by TCA precipitation as prerequisite for subsequent immunoblotting for tagged proteins. For TCA precipitation, protein samples were precipitated twice with 10% trichloroacetic acid (TCA) on ice for 20 minutes and pelleted at 14.000 rpm at 4°C. The precipitate was then washed once with 100% acetone, pelleted again and dried at 37°C in a vacufuge plus (Eppendorf, Hamburg, Germany). The dried pellet was then taken up in 40 µl 2x SDS loading buffer supplemented with 5% 10 mM Tris-HCl pH 7.5 (v/v).

4.16 Bioinformatic analysis of proteins

The *Chaetomium thermophilum* genome browser was frequented to receive endogenous promoter regions (Bock et al., 2014). The BLAST algorithm from Altschul et al., 1990 was used to identify protein homologs from related organism in *Chaetomium thermophilum*. Protein sequences were aligned with the clustal omega multiple sequence alignment tool (The EMBL-EBI search and sequence analysis tools APIs in 2019) and visualized by Jalview (Waterhouse et al., 2009). Visualization of sequencing reads was carried out as described in (Singh et al., 2021)

Abbreviations

°C	Degree celsius
Amp	Ampicillin
ATP	Adenosin triphosphat
Bp	Base pairs
C	Cytoplasm
C-terminus	Carboxy-terminus
C. thermophilum	*Chaetomim thermophilum*
CCM	Complete cultivation medium
CCR	Carbon catabolite repression
D	Aspartic acid
DIC	Differential interference contrast
DNA	Deoxyribonucleic acid
DTT	Dithiotreitol
E	Glutamic acid
E. coli	*Escherichia coli*
E. coli	Escherichia coli
EM	Electron microscopy
ETS	External transcribed spacer
FTpA	Flag-TEV-ProteinA
***GAL*-promoter**	Galactose inducible promoter
h	Hours
IST	Internal transcribed spacer
Kan	Kanamycin
LB	Lysogeny broth
LSU	Large subunit
MDa	Mega dalton
Min	Minutes
ml	Milliliter
mRNA	Messenger RNA
MS	Mass spectrometry
N	Nucleus

N-terminus	Amino-terminus
NLS	Nuclear localization sequence
Ns	Nucleolus
Nt	Nucleotides
PCR	Polymerase chain reaction
PET	Polypeptide exit tunnel
Pol	RNA Polymerase
PTC	Peptidyl transfer center
rDNA	Ribosomal DNA
RPs	Ribosomal proteins
RNA	Ribonuclic acid
RNP	Ribonucleoprotein particle
Rpm	Rounds per minute
rRNA	Ribosomal RNA
S	Svedberg unit
S. cerevisiae	*Saccharomyces cerevisiae*
SDS-PAGE	Sodium dodecyl sulfate polyacrylamide gel electrophoresis
snoRNA	Small nucleolar RNA
snRNA	Small nuclear RNA
SSU	Small subunit
TAP	tandem-affinity purification
TCA	Trichloroaceticacid
Tet	Tetracycin
TEV	tobacco etch virus (cleavage site)
***trans*-factor**	Transcription factor
tRNA	transfer RNA
UTP	U three protein
UTR	Untranslated region
Ffts-YFP	Fast folding thermostable yellow fluorescent protein

5 References

Ahmed, S., Imdad, S. S., & Jamil, A. (2012). Comparative study for the kinetics of extracellular xylanases from Trichoderma harzianum and Chaetomium thermophilum. *Electronic Journal of Biotechnology*, *15*(3). https://doi.org/10.2225/vol15-issue3-fulltext-2

Aibara, S., Valkov, E., Lamers, M. H., Dimitrova, L., Hurt, E., & Stewart, M. (2015). Structural characterization of the principal mRNA-export factor Mex67-Mtr2 from Chaetomium thermophilum. *Acta Crystallographica Section:F Structural Biology Communications*, *71*(7), 876–888. https://doi.org/10.1107/S2053230X15008766

Akirtava, C., Charles, |, Mcmanus, J., & Mcmanus, C. J. (2021). Control of translation by eukaryotic mRNA transcript leaders—Insights from high-throughput assays and computational modeling. *Wiley Interdisciplinary Reviews: RNA*, *12*(3), e1623. https://doi.org/10.1002/WRNA.1623

Ali, S. S., Nugent, B., Mullins, E., & Doohan, F. M. (2016a). *Fungal-mediated consolidated bioprocessing: the potential of Fusarium oxysporum for the lignocellulosic ethanol industry*. https://doi.org/10.1186/s13568-016-0185-0

Ali, S. S., Nugent, B., Mullins, E., & Doohan, F. M. (2016b). Fungal-mediated consolidated bioprocessing: the potential of Fusarium oxysporum for the lignocellulosic ethanol industry. In *AMB Express* (Vol. 6, Issue 1, pp. 1–13). Springer Verlag. https://doi.org/10.1186/s13568-016-0185-0

Aliye, N., Fabbretti, A., Lupidi, G., Tsekoa, T., & Spurio, R. (2015). Engineering color variants of green fluorescent protein (GFP) for thermostability, pH-sensitivity, and improved folding kinetics. *Applied Microbiology and Biotechnology*, *99*(3), 1205–1216. https://doi.org/10.1007/s00253-014-5975-1

Amlacher, S., Sarges, P., Flemming, D., van Noort, V., Kunze, R., Devos, D. P., Arumugam, M., Bork, P., & Hurt, E. (2011). Insight into structure and assembly of the nuclear pore complex by utilizing the genome of a eukaryotic thermophile. *Cell*, *146*(2), 277–289. https://doi.org/10.1016/j.cell.2011.06.039

Amore, A., Giacobbe, S., & Faraco, V. (2013). Regulation of Cellulase and Hemicellulase Gene Expression in Fungi. *Current Genomics*, *14*(4), 230–249. https://doi.org/10.2174/1389202911314040002

Anderson, C. A., Roberts, S., Zhang, H., Kelly, C. M., Kendall, A., Lee, C., Gerstenberger, J., Koenig, A. B., Kabeche, R., & Gladfelter, A. S. (2015). Ploidy variation in multinucleate cells changes under stress. *Molecular Biology of the Cell*, *26*(6), 1129–1140. https://doi.org/10.1091/mbc.E14-09-1375

Armache, J. P., Jarasch, A., Anger, A. M., Villa, E., Becker, T., Bhushan, S., Jossinet, F., Habeck, M., Dindar, G., Franckenberg, S., Marquez, V., Mielke, T., Thomm, M., Berninghausen, O., Beatrix,

B., Söding, J., Westhof, E., Wilson, D. N., & Beckmann, R. (2010). Cryo-EM structure and rRNA model of a translating eukaryotic 80S ribosome at 5.5-Å resolution. *Proceedings of the National Academy of Sciences of the United States of America*, *107*(46), 19748–19753. https://doi.org/10.1073/pnas.1009999107

Aro, N., Pakula, T., & Penttilä, M. (2005). Transcriptional regulation of plant cell wall degradation by filamentous fungi. In *FEMS Microbiology Reviews* (Vol. 29, Issue 4, pp. 719–739). Oxford Academic. https://doi.org/10.1016/j.femsre.2004.11.006

Baker, R. W., Jeffrey, P. D., Zick, M., Phillips, B. P., Wickner, W. T., & Hughson, F. M. (2015). A direct role for the Sec1/Munc18-family protein Vps33 as a template for SNARE assembly. *Science*, *349*(6252), 1111–1114. https://doi.org/10.1126/science.aac7906

Barrio-Garcia, C., Thoms, M., Flemming, D., Kater, L., Berninghausen, O., Baßler, J., Beckmann, R., & Hurt, E. (2016). Architecture of the Rix1-Rea1 checkpoint machinery during pre-60S-ribosome remodeling. *Nature Structural & Molecular Biology*, *23*. https://doi.org/10.1038/nsmb.3132

Baßler, J., Kallas, M., Pertschy, B., Ulbrich, C., Thoms, M., & Hurt, E. (2010). The AAA-ATPase Rea1 Drives Removal of Biogenesis Factors during Multiple Stages of 60S Ribosome Assembly. *Molecular Cell*, *38*(5). https://doi.org/10.1016/j.molcel.2010.05.024

Beckmann, R., Spahn, C. M. T., Eswar, N., Helmers, J., Penczek, P. A., Sali, A., Frank, J., & Blobel, G. (2018). *Architecture of the Protein-Conducting Channel Associated with the Translating 80S Ribosome* (pp. 274–285). https://doi.org/10.1142/9789813234864_0026

Béguin, P. (1990). Molecular biology of cellulose degradation. In *Annual Review of Microbiology* (Vol. 44, pp. 219–248). Annual Reviews Inc. https://doi.org/10.1146/annurev.mi.44.100190.001251

Ben-Shem, A., de Loubresse, N. G., Melnikov, S., Jenner, L., Yusupova, G., & Yusupov, M. (2011). The structure of the eukaryotic ribosome at 3.0 Å resolution. *Science*, *334*(6062), 1524–1529. https://doi.org/10.1126/science.1212642

Berens, C., & Hillen, W. (2003). Gene regulation by tetracyclines. Constraints of resistance regulation in bacteria shape TetR for application in eukaryotes. *European Journal of Biochemistry*, *270*(15), 3109–3121. https://doi.org/10.1046/j.1432-1033.2003.03694.x

Berlin, A. (2013). No barriers to cellulose breakdown. In *Science* (Vol. 342, Issue 6165, pp. 1454–1456). Science. https://doi.org/10.1126/science.1247697

Bernier, C. R., Petrov, A. S., Kovacs, N. A., Penev, P. I., & Williams, L. D. (2018). Translation: The universal structural core of life. *Molecular Biology and Evolution*, *35*(8), 2065–2076. https://doi.org/10.1093/molbev/msy101

Bernstein, K. A., Granneman, S., Lee, A. v., Manickam, S., & Baserga, S. J. (2006). Comprehensive Mutational Analysis of Yeast DEXD/H Box RNA Helicases Involved in Large Ribosomal Subunit Biogenesis. *Molecular and Cellular Biology*, *26*(4), 1195–1208. https://doi.org/10.1128/MCB.26.4.1195-1208.2006/ASSET/F8BC324C-2A6D-4907-9E41-331C4B31F4B8/ASSETS/GRAPHIC/ZMB0040657170008.JPEG

Bleichert, F., Granneman, S., Osheim, Y. N., Beyer, A. L., & Baserga, S. J. (2006). The PINc domain protein Utp24, a putative nuclease, is required for the early cleavage in 18S rRNA maturation. *Proceedings of the National Academy of Sciences of the United States of America*, *103*(25), 9464–9469. https://doi.org/10.1073/pnas.0603673103

Bock, T., Chen, W. H., Ori, A., Malik, N., Silva-Martin, N., Huerta-Cepas, J., Powell, S. T., Kastritis, P. L., Smyshlyaev, G., Vonkova, I., Kirkpatrick, J., Doerks, T., Nesme, L., Baßler, J., Kos, M., Hurt, E., Carlomagno, T., Gavin, A. C., Barabas, O., … Bork, P. (2014). An integrated approach for genome annotation of the eukaryotic thermophile Chaetomium thermophilum. *Nucleic Acids Research*, *42*(22), 13525–13533. https://doi.org/10.1093/NAR/GKU1147

Bradatsch, B., Leidig, C., Granneman, S., Gnädig, M., Tollervey, D., Böttcher, B., Beckmann, R., & Hurt, E. (2012). Structure of the pre-60S ribosomal subunit with nuclear export factor Arx1 bound at the exit tunnel. *Nature Structural and Molecular Biology*, *19*(12), 1234–1241. https://doi.org/10.1038/nsmb.2438

Brown, N. A., de Gouvea, P. F., Krohn, N. G., Savoldi, M., & Goldman, G. H. (2013). Functional characterisation of the non-essential protein kinases and phosphatases regulating Aspergillus nidulans hydrolytic enzyme production. *Biotechnology for Biofuels*, *6*(1), 1–17. https://doi.org/10.1186/1754-6834-6-91/FIGURES/9

Cairns, T. C., Barthel, L., & Meyer, V. (2021). Something old, something new: challenges and developments in Aspergillus niger biotechnology. *Essays in Biochemistry*, *65*(2), 213–224. https://doi.org/10.1042/EBC20200139

Catalán, A., Glaser-Schmitt, A., Argyridou, E., Duchen, P., & Parsch, J. (2016). An Indel Polymorphism in the MtnA 3' Untranslated Region Is Associated with Gene Expression Variation and Local Adaptation in Drosophila melanogaster. *PLOS Genetics*, *12*(4), e1005987. https://doi.org/10.1371/journal.pgen.1005987

Chaker-Margot, M., Barandun, J., Hunziker, M., & Klinge, S. (2017). Architecture of the yeast small subunit processome. *Science*, *355*(6321). https://doi.org/10.1126/science.aal1880

Chang, K. Y., Ryan Georgianna, D., Heber, S., Payne, G. A., & Muddiman, D. C. (2010). Detection of alternative splice variants at the proteome level in aspergillus flavus. *Journal of Proteome Research*, *9*(3), 1209–1217. https://doi.org/10.1021/pr900602d

Chen, X., Jiang, Z. H., Chen, S., & Qin, W. (2010). Microbial and bioconversion production of D-xylitol and its detection and application. In *International Journal of Biological Sciences* (Vol. 6, Issue 7, pp. 834–844). Ivyspring International Publisher. https://doi.org/10.7150/ijbs.6.834

Cheng, J., Baßler, J., Fischer, P., Lau, B., Kellner, N., Kunze, R., Griesel, S., Kallas, M., Berninghausen, O., Strauss, D., Beckmann, R., & Hurt, E. (2019). Thermophile 90S Pre-ribosome Structures Reveal the Reverse Order of Co-transcriptional 18S rRNA Subdomain Integration. *Molecular Cell*, *75*(6), 1256-1269.e7. https://doi.org/10.1016/J.MOLCEL.2019.06.032

Cheng, J., Kellner, N., Berninghausen, O., Hurt, E., & Beckmann, R. (2017). 3.2-Å-resolution structure of the 90S preribosome before A1 pre-rRNA cleavage. *Nature Structural and Molecular Biology*. https://doi.org/10.1038/nsmb.3476

Cheng, J., Lau, B., la Venuta, G., Ameismeier, M., Berninghausen, O., Hurt, E., & Beckmann, R. (2020). 90S pre-ribosome transformation into the primordial 40S subunit. *Science*, *369*(6509). https://doi.org/10.1126/SCIENCE.ABB4119

Chroumpi, T., Mäkelä, M. R., & de Vries, R. P. (2020). Engineering of primary carbon metabolism in filamentous fungi. *Biotechnology Advances*, *43*, 107551. https://doi.org/10.1016/J.BIOTECHADV.2020.107551

Chu, S., Archer, R. H., Zengel, J. M., & Lindahl, L. (1994). The RNA of RNase MRP is required for normal processing of ribosomal RNA. *Proceedings of the National Academy of Sciences of the United States of America*, *91*(2), 659–663. https://doi.org/10.1073/pnas.91.2.659

Conrad, M., Schothorst, J., Kankipati, H. N., van Zeebroeck, G., Rubio-Texeira, M., & Thevelein, J. M. (2014). Nutrient sensing and signaling in the yeast Saccharomyces cerevisiae. In *FEMS Microbiology Reviews* (Vol. 38, Issue 2, pp. 254–299). Oxford Academic. https://doi.org/10.1111/1574-6976.12065

Das, A. T., Tenenbaum, L., & Berkhout, B. (2016). Tet-On Systems For Doxycycline-inducible Gene Expression. *Current Gene Therapy*, *16*(3), 156–167. http://www.ncbi.nlm.nih.gov/pubmed/27216914

de Assis, L. J., Silva, L. P., Bayram, O., Dowling, P., Kniemeyer, O., Krüger, T., Brakhage, A. A., Chen, Y., Dong, L., Tan, K., Wong, K. H., Ries, L. N. A., & Goldman, G. H. (2021). Carbon Catabolite Repression in Filamentous Fungi Is Regulated by Phosphorylation of the Transcription Factor CreA. *MBio*, *12*(1). https://doi.org/10.1128/mbio.03146-20

de Assis, L. J., Ulas, M., Ries, L. N. A., el Ramli, N. A. M., Sarikaya-Bayram, O., Braus, G. H., Bayram, O., & Goldman, G. H. (2018). Regulation of Aspergillus nidulans CreA-mediated catabolite repression by the F-Box proteins Fbx23 and Fbx47. *MBio*, *9*(3). https://doi.org/10.1128/MBIO.00840-18/SUPPL_FILE/MBO003183942ST2.DOCX

de Souza, W. R. (2013). Microbial Degradation of Lignocellulosic Biomass. In *Sustainable Degradation of Lignocellulosic Biomass - Techniques, Applications and Commercialization*. InTech. https://doi.org/10.5772/54325

Díaz, J., Chávez, R., Larrondo, L. F., Eyzaguirre, J., & Bull, P. (2008). Functional analysis of the endoxylanase B (xynB) promoter from Penicillium purpurogenum. *Current Genetics*, *54*(3), 133–141. https://doi.org/10.1007/S00294-008-0205-Y

Dragon, F., Compagnone-Post, P. A., Mitchell, B. M., Porwancher, K. A., Wehner, K. A., Wormsley, S., Settlage, R. E., Shabanowitz, J., Osheim, Y., Beyer, A. L., Hunt, D. F., & Baserga, S. J. (2002). A large nucleolar U3 ribonucleoprotein required for 18S ribosomal RNA biogenesis. *Nature 2002 417:6892*, *417*(6892), 967–970. https://doi.org/10.1038/nature00769

Dutca, L. M., Gallagher, J. E. G., & Baserga, S. J. (2011). The initial U3 snoRNA:pre-rRNA base pairing interaction required for pre-18S rRNA folding revealed by in vivo chemical probing. *Nucleic Acids Research*, *39*(12), 5164–5180. https://doi.org/10.1093/NAR/GKR044

Eppens, N. A., Rensen, S., Granneman, S., Raué, H. A., & Venema, J. (1999). The roles of Rrp5p in the synthesis of yeast 18S and 5.8S rRNA can be functionally and physically separated. *RNA*, *5*(6), 779–793. https://doi.org/10.1017/S1355838299990313

Eustermann, S., Schall, K., Kostrewa, Di., Lakomek, K., Strauss, M., Moldt, M., & Hopfner, K. P. (2018). Structural basis for ATP-dependent chromatin remodelling by the INO80 complex. *Nature*, *556*(7701), 386–390. https://doi.org/10.1038/s41586-018-0029-y

Fatica, A., Oeffinger, M., Dlakić, M., & Tollervey, D. (2003). Nob1p Is Required for Cleavage of the 3′ End of 18S rRNA. *Molecular and Cellular Biology*, *23*(5), 1798–1807. https://doi.org/10.1128/mcb.23.5.1798-1807.2003

Felenbok, B., Flipphi, M., & Nikolaev, I. (2001). Ethanol catabolism in Aspergillus nidulans: a model system for studying gene regulation. *Progress in Nucleic Acid Research and Molecular Biology*, *69*, 149–204. https://doi.org/10.1016/S0079-6603(01)69047-0

Fox, J. M., Rashford, R. L., & Lindahl, L. (2019). Co-Assembly of 40S and 60S Ribosomal Proteins in Early Steps of Eukaryotic Ribosome Assembly. *International Journal of Molecular Sciences*, *20*(11), 2806. https://doi.org/10.3390/ijms20112806

French, S. L., Osheim, Y. N., Cioci, F., Nomura, M., & Beyer, A. L. (2003). In Exponentially Growing Saccharomyces cerevisiae Cells, rRNA Synthesis Is Determined by the Summed RNA Polymerase I Loading Rate Rather than by the Number of Active Genes . *Molecular and Cellular Biology*, *23*(5), 1558–1568. https://doi.org/10.1128/mcb.23.5.1558-1568.2003

Froehlich, A. C., Noh, B., Vierstra, R. D., Loros, J., & Dunlap, J. C. (2005). Genetic and molecular analysis of phytochromes from the filamentous fungus Neurospora crassa. *Eukaryotic Cell*, *4*(12), 2140–2152. https://doi.org/10.1128/EC.4.12.2140-2152.2005

Gadal, O., Strauß, D., Kessl, J., Trumpower, B., Tollervey, D., & Hurt, E. (2001). Nuclear Export of 60S Ribosomal Subunits Depends on Xpo1p and Requires a Nuclear Export Sequence-Containing Factor, Nmd3p, That Associates with the Large Subunit Protein Rpl10p. *Molecular and Cellular Biology*, *21*(10), 3405–3415. https://doi.org/10.1128/mcb.21.10.3405-3415.2001

Gancedo, J. M. (1993). Carbon catabolite repression in yeast. In *EJB Reviews* (pp. 105–121). Springer Berlin Heidelberg. https://doi.org/10.1007/978-3-642-78046-2_9

Gasse, L., Flemming, D., & Hurt, E. (2015). Coordinated Ribosomal ITS2 RNA Processing by the Las1 Complex Integrating Endonuclease, Polynucleotide Kinase, and Exonuclease Activities. *Molecular Cell*, *60*(5), 808–815. https://doi.org/10.1016/J.MOLCEL.2015.10.021

Geever, R. F., Huiet, L., Baum, J. A., Tyler, B. M., Patel, V. B., Rutledge, B. J., Case, M. E., & Giles, N. H. (1989). DNA sequence, organization and regulation of the qa gene cluster of Neurospora crassa. *Journal of Molecular Biology*, *207*(1), 15–34. https://doi.org/10.1016/0022-2836(89)90438-5

Glass, N. L., Jacobson, D. J., & Shiu, P. K. T. (2000). The genetics of hyphal fusion and vegetative incompatibility in filamentous ascomycete fungi. *Annual Review of Genetics*, *34*(1), 165–186. https://doi.org/10.1146/annurev.genet.34.1.165

Gong, W., Dai, L., Zhang, H., Zhang, L., & Wang, L. (2018). A highly efficient xylan-utilization system in Aspergillus niger An76: A functional-proteomics study. *Frontiers in Microbiology*, *9*, 430. https://doi.org/10.3389/fmicb.2018.00430

Grandi, P., Rybin, V., Baßler, J., Petfalski, E., Strauß, D., Marzioch, M., Schäfer, T., Kuster, B., Tschochner, H., Tollervey, D., Gavin, A. C., & Hurt, E. (2002). 90S Pre-Ribosomes Include the 35S Pre-rRNA, the U3 snoRNP, and 40S Subunit Processing Factors but Predominantly Lack 60S Synthesis Factors. *Molecular Cell*, *10*(1), 105–115. https://doi.org/10.1016/S1097-2765(02)00579-8

Greber, B. J. (2016). Mechanistic insight into eukaryotic 60S ribosomal subunit biogenesis by cryo-electron microscopy. In *RNA* (Vol. 22, Issue 11). https://doi.org/10.1261/rna.057927.116

Griggs, D. W., & Johnston, M. (1991). Regulated expression of the GAL4 activator gene in yeast provides a sensitive genetic switch for glucose repression. *Proceedings of the National Academy of Sciences*, *88*(19), 8597–8601. https://doi.org/10.1073/PNAS.88.19.8597

Guillemette, T., van Peij, N. N. M. E., Goosen, T., Lanthaler, K., Robson, G. D., van den Hondel, C. A. M. J. J., Stam, H., & Archer, D. B. (2007). Genomic analysis of the secretion stress response in the enzyme-producing cell factory Aspergillus niger. *BMC Genomics*, *8*(1), 1–17. https://doi.org/10.1186/1471-2164-8-158

Hasper, A. A., Visser, J., & De Graaff, L. H. (2000). The Aspergillus niger transcriptional activator XlnR, which is involved in the degradation of the polysaccharides xylan and cellulose, also regulates D-xylose reductase gene expression. *Molecular Microbiology*, *36*(1), 193–200. https://doi.org/10.1046/j.1365-2958.2000.01843.x

Hedges, J., West, M., & Johnson, A. W. (2005). Release of the export adapter, Nmd3p, from the 60S ribosomal subunit requires Rpl10p and the cytoplasmic GTPase Lsg1p. *EMBO Journal*, *24*(3). https://doi.org/10.1038/sj.emboj.7600547

Henry, Y., Wood, H., Morrissey, J. P., Petfalski, E., Kearsey, S., & Tollervey, D. (1994). The 5' end of yeast 5.8S rRNA is generated by exonucleases from an upstream cleavage site. *EMBO Journal*, *13*(10). https://doi.org/10.1002/j.1460-2075.1994.tb06530.x

Heredia, A., Jiménez, A., & Guillén, R. (1995). Composition of plant cell walls. In *Zeitschrift für Lebensmittel-Untersuchung und -Forschung* (Vol. 200, Issue 1, pp. 24–31). Springer-Verlag. https://doi.org/10.1007/BF01192903

Hierlmeier, T., Merl, J., Sauert, M., Perez-Fernandez, J., Schultz, P., Bruckmann, A., Hamperl, S., Ohmayer, U., Rachel, R., Jacob, A., Hergert, K., Deutzmann, R., Griesenbeck, J., Hurt, E., Milkereit, P., Baßler, J., & Tschochner, H. (2013). Rrp5p, Noc1p and Noc2p form a protein module which is part of early large ribosomal subunit precursors in S. cerevisiae. *Nucleic Acids Research*, *41*(2), 1191–1210. https://doi.org/10.1093/nar/gks1056

Ho, J. H. N., Kallstrom, G., & Johnson, A. W. (2000). Nmd3p Is a Crm1p-Dependent Adapter Protein for Nuclear Export of the Large Ribosomal Subunit. *Journal of Cell Biology*, *151*(5), 1057–1066. https://doi.org/10.1083/JCB.151.5.1057

Ho, S. N., Hunt, H. D., Horton, R. M., Pullen, J. K., & Pease, L. R. (1989). Site-directed mutagenesis by overlap extension using the polymerase chain reaction. *Gene*, *77*(1), 51–59. https://doi.org/10.1016/0378-1119(89)90358-2

Hovland, P., Flick, J., Johnston, M., & Sclafani, R. A. (1989). Galactose as a gratuitous inducer of GAL gene expression in yeasts growing on glucose. *Gene*, *83*(1), 57–64. https://doi.org/10.1016/0378-1119(89)90403-4

Hrmova, M., Petrakova, E., & Biely, P. (1991). Induction of cellulose- and xylan-degrading enzyme systems in Aspergillus terreus by homo- and heterodisaccharides composed of glucose and

xylose. *Journal of General Microbiology*, *137*(3), 541–547. https://doi.org/10.1099/00221287-137-3-541/CITE/REFWORKS

Hunziker, M., Barandun, J., Petfalski, E., Tan, D., Delan-Forino, C., Molloy, K. R., Kim, K. H., Dunn-Davies, H., Shi, Y., Chaker-Margot, M., Chait, B. T., Walz, T., Tollervey, D., & Klinge, S. (2016). UtpA and UtpB chaperone nascent pre-ribosomal RNA and U3 snoRNA to initiate eukaryotic ribosome assembly. *Nature Communications*, *7*, 12090. https://doi.org/10.1038/ncomms12090

Hurley, J. M., Chen, C. H., Loros, J. J., & Dunlap, J. C. (2012). Light-inducible system for tunable protein expression in neurospora crassa. *G3: Genes, Genomes, Genetics*, *2*(10), 1207–1212. https://doi.org/10.1534/g3.112.003939

Hurt, E., Hannus, S., Schmelzl, B., Lau, D., Tollervey, D., & Simos, G. (1999). A novel in vivo assay reveals inhibition of ribosomal nuclear export in Ran-cycle and nucleoporin mutants. *Journal of Cell Biology*, *144*(3). https://doi.org/10.1083/jcb.144.3.389

Ingolia, N. T., Ghaemmaghami, S., Newman, J. R. S., & Weissman, J. S. (2009). Genome-wide analysis in vivo of translation with nucleotide resolution using ribosome profiling. *Science*, *324*(5924). https://doi.org/10.1126/science.1168978

Inoue, H., Nojima, H., & Okayama, H. (1990). High efficiency transformation of Escherichia coli with plasmids. *Gene*, *96*(1), 23–28. https://doi.org/10.1016/0378-1119(90)90336-P

Ismail, S., Flemming, D., Thoms, M., Gomes-Filho, J. V., Randau, L., Beckmann, R., & Hurt, E. (2022). Emergence of the primordial pre-60S from the 90S pre-ribosome. *Cell Reports*, *39*(1), 110640. https://doi.org/10.1016/j.celrep.2022.110640

ısa Czamanski Nora, L., Westmann, A., Martins-Santana, L., de atima Alves, L. F., Maria Oliveira Monteiro, L., ıa-Eugenia Guazzaroni, M., & Silva-Rocha, R. (2019). The art of vector engineering: towards the construction of next-generation genetic tools. *Microbial Biotechnology*, 125–147. https://doi.org/10.1111/1751-7915.13318

Jiang, X., Du, J., He, R., Zhang, Z., Qi, F., Huang, J., & Qin, L. (2020). Improved Production of Majority Cellulases in Trichoderma reesei by Integration of cbh1 Gene From Chaetomium thermophilum. *Frontiers in Microbiology*, *11*, 1633. https://doi.org/10.3389/fmicb.2020.01633

Juers, D. H., Matthews, B. W., & Huber, R. E. (2012). *LacZ* β-galactosidase: Structure and function of an enzyme of historical and molecular biological importance. *Protein Science*, *21*(12), 1792–1807. https://doi.org/10.1002/pro.2165

Juneau, K., Nislow, C., & Davis, R. W. (2009). Alternative Splicing of PTC7 in Saccharomyces cerevisiae Determines Protein Localization. *Genetics*, *183*(1), 185–194. https://doi.org/10.1534/GENETICS.109.105155

Kargas, V., Castro-Hartmann, P., Escudero-Urquijo, N., Dent, K., Hilcenko, C., Sailer, C., Zisser, G., Marques-Carvalho, M. J., Pellegrino, S., Wawiórka, L., Freund, S. M., Wagstaff, J. L., Andreeva, A., Faille, A., Chen, E., Stengel, F., Bergler, H., & Warren, A. J. (2019). Mechanism of completion of peptidyltransferase centre assembly in eukaryotes. *ELife*, *8*. https://doi.org/10.7554/ELIFE.44904

Karnaouri, A., Antonopoulou, I., Zerva, A., Dimarogona, M., Topakas, E., Rova, U., & Christakopoulos, P. (2019). Thermophilic enzyme systems for efficient conversion of lignocellulose to valuable products: Structural insights and future perspectives for esterases and oxidative catalysts. In *Bioresource Technology* (Vol. 279, pp. 362–372). Elsevier Ltd. https://doi.org/10.1016/j.biortech.2019.01.062

Kater, L., Mitterer, V., Thoms, M., Cheng, J., Berninghausen, O., Beckmann, R., & Hurt, E. (2020). Construction of the Central Protuberance and L1 Stalk during 60S Subunit Biogenesis. *Molecular Cell*, *79*(4), 615-628.e5. https://doi.org/10.1016/J.MOLCEL.2020.06.032

Kater, L., Thoms, M., Barrio-Garcia, C., Cheng, J., Ismail, S., Ahmed, Y. L., Bange, G., Kressler, D., Berninghausen, O., Sinning, I., Hurt, E., & Beckmann, R. (2017). Visualizing the Assembly Pathway of Nucleolar Pre-60S Ribosomes. *Cell*, *171*(7), 1599-1610.e14. https://doi.org/10.1016/J.CELL.2017.11.039

Kellner, N., Griesel, S., & Hurt, E. (2022). A Homologous Recombination System to Generate Epitope-Tagged Target Genes in Chaetomium thermophilum: A Genetic Approach to Investigate Native Thermostable Proteins. *International Journal of Molecular Sciences*, *23*(6), 3198. https://doi.org/10.3390/ijms23063198

Kellner, N., Schwarz, J., Sturm, M., Fernandez-Martinez, J., Griesel, S., Zhang, W., Chait, B. T., Rout, M. P., Kück, U., & Hurt, E. (2016a). Developing genetic tools to exploit Chaetomium thermophilum for biochemical analyses of eukaryotic macromolecular assemblies. *Scientific Reports*, *6*, 20937. https://doi.org/10.1038/srep20937

Kellner, N., Schwarz, J., Sturm, M., Fernandez-Martinez, J., Griesel, S., Zhang, W., Chait, B. T., Rout, M. P., Kück, U., & Hurt, E. (2016b). Developing genetic tools to exploit Chaetomium thermophilum for biochemical analyses of eukaryotic macromolecular assemblies. *Scientific Reports*, *6*(1), 1–10. https://doi.org/10.1038/srep20937

Kellner, N., Schwarz, J., Sturm, M., Fernandez-Martinez, J., Griesel, S., Zhang, W., Chait, B. T., Rout, M. P., Kück, U., & Hurt, E. (2016c). Developing genetic tools to exploit Chaetomium thermophilum for biochemical analyses of eukaryotic macromolecular assemblies. *Scientific Reports*, *6*(1), 20937. https://doi.org/10.1038/srep20937

Kišonaitė, M., Wild, K., Lapouge, K., Ruppert, T., & Sinning, I. (2022). High-resolution structures of a thermophilic eukaryotic 80S ribosome reveal atomistic details of translocation. *Nature Communications*, *13*(1), 476. https://doi.org/10.1038/s41467-022-27967-9

Klinge, S., & Woolford, J. L. (2019). Ribosome assembly coming into focus. In *Nature Reviews Molecular Cell Biology* (Vol. 20, Issue 2). https://doi.org/10.1038/s41580-018-0078-y

Kluge, J., Terfehr, D., & Kück, U. (2018). Inducible promoters and functional genomic approaches for the genetic engineering of filamentous fungi. *Applied Microbiology and Biotechnology*, *102*(15), 6357–6372. https://doi.org/10.1007/s00253-018-9115-1

Koda, A., Bogaki, T., Minetoki, T., & Hirotsune, M. (2006). 5′ untranslated region of the Hsp12 gene contributes to efficient translation in Aspergillus oryzae. *Applied Microbiology and Biotechnology*, *70*(3), 333–336. https://doi.org/10.1007/s00253-005-0083-x

Kornprobst, M., Turk, M., Kellner, N., Cheng, J., Flemming, D., Koš-Braun, I., Koš, M., Thoms, M., Berninghausen, O., Beckmann, R., & Hurt, E. (2016). Architecture of the 90S Pre-ribosome: A Structural View on the Birth of the Eukaryotic Ribosome. *Cell*, *166*(2), 380–393. https://doi.org/10.1016/j.cell.2016.06.014

Koš, M., & Tollervey, D. (2005). The putative RNA helicase Dbp4p is required for release of the U14 snoRNA from preribosomes in Saccharomyces cerevisiae. *Molecular Cell*, *20*(1), 53–64. https://doi.org/10.1016/j.molcel.2005.08.022

Kressler, D., Hurt, E., & Baßler, J. (2017). A Puzzle of Life: Crafting Ribosomal Subunits. In *Trends in Biochemical Sciences* (Vol. 42, Issue 8, pp. 640–654). Elsevier Ltd. https://doi.org/10.1016/j.tibs.2017.05.005

Kuersten, S., & Goodwin, E. B. (2003). The power of the 3′ UTR: Translational control and development. In *Nature Reviews Genetics* (Vol. 4, Issue 8, pp. 626–637). Nature Publishing Group. https://doi.org/10.1038/nrg1125

Kurasawa, T., Yachi, M., Suto, M., Kamagata, Y., Takao, S., & Tomita, F. (1992). Induction of Cellulase by Gentiobiose and Its Sulfur-Containing Analog in Penicillium purpurogenum. *Applied and Environmental Microbiology*, *58*(1), 106–110. https://doi.org/10.1128/AEM.58.1.106-110.1992

Kutay, U., Wild, T., Horvath, P., Wyler, E., Widmann, B., Badertscher, L., Zemp, I., Kozak, K., Csucs, G., & Lund, E. (2010). A protein inventory of human ribosome biogenesis reveals an essential function of exportin 5 in 60S subunit export. *PLoS Biology*, *8*(10), 1000522. https://doi.org/10.1371/journal.pbio.1000522

la Touche, C. J. (1948). A Chætomium-like Thermophile Fungus. *Nature 1948 161:4087*, *161*(4087), 320–320. https://doi.org/10.1038/161320a0

Lai, E. C. (2002). Micro RNAs are complementary to 3′ UTR sequence motifs that mediate negative post-transcriptional regulation. *Nature Genetics*, *30*(4), 363–364. https://doi.org/10.1038/ng865

Lamb, T. M., Vickery, J., & Bell-Pedersen, D. (2013). Regulation of gene expression in Neurospora crassa with a copper responsive promoter. *G3 (Bethesda, Md.)*, *3*(12), 2273–2280. https://doi.org/10.1534/g3.113.008821

Lau, B., Cheng, J., Flemming, D., la Venuta, G., Berninghausen, O., Beckmann, R., & Hurt, E. (2021). Structure of the Maturing 90S Pre-ribosome in Association with the RNA Exosome. *Molecular Cell*, *81*(2), 293-303.e4. https://doi.org/10.1016/J.MOLCEL.2020.11.009

Lebreton, A., Tomecki, R., Dziembowski, A., & Séraphin, B. (2008). Endonucleolytic RNA cleavage by a eukaryotic exosome. *Nature*, *456*(7224), 993–996. https://doi.org/10.1038/nature07480

Leidig, C., Thoms, M., Holdermann, I., Bradatsch, B., Berninghausen, O., Bange, G., Sinning, I., Hurt, E., & Beckmann, R. (2014). 60S ribosome biogenesis requires rotation of the 5S ribonucleoprotein particle. *Nature Communications*, *5*(1), 3491. https://doi.org/10.1038/ncomms4491

Leppek, K., & Barna, M. (2019). An rRNA variant to deal with stress. *Nature Microbiology 2019 4:3*, *4*(3), 382–383. https://doi.org/10.1038/s41564-019-0396-7

Li, A. N., & Li, D. C. (2009). Cloning, expression and characterization of the serine protease gene from Chaetomium thermophilum. *Journal of Applied Microbiology*, *106*(2), 369–380. https://doi.org/10.1111/J.1365-2672.2008.04042.X

Li, X., Han, C., Li, W., Chen, G., & Wang, L. (2020). Insights into the cellulose degradation mechanism of the thermophilic fungus Chaetomium thermophilum based on integrated functional omics. *Biotechnology for Biofuels*, *13*(1), 1–18. https://doi.org/10.1186/S13068-020-01783-Z/FIGURES/6

Lilia Torres-Machorro, A., HernándezHern, R., & María Cevallos, A. (2009). *Ribosomal RNA genes in eukaryotic microorganisms: witnesses of phylogeny?* https://doi.org/10.1111/j.1574-6976.2009.00196.x

Lindahl, L., Archer, R. H., & Zengel, J. M. (1992). A new rRNA processing mutant of Saccharomyces cerevisiae. *Nucleic Acids Research*, *20*(2), 295–301. https://doi.org/10.1093/nar/20.2.295

Liu, Q., Greimann, J. C., & Lima, C. D. (2006). Reconstitution, Activities, and Structure of the Eukaryotic RNA Exosome. *Cell*, *127*(6), 1223–1237. https://doi.org/10.1016/j.cell.2006.10.037

Liu, R., Chen, L., Jiang, Y., Zhou, Z., & Zou, G. (2015). Efficient genome editing in filamentous fungus Trichoderma reesei using the CRISPR/Cas9 system. *Cell Discovery*, *1*. https://doi.org/10.1038/celldisc.2015.7

Ma, C., Wu, S., Li, N., Chen, Y., Yan, K., Li, Z., Zheng, L., Lei, J., Woolford, J. L., & Gao, N. (2017). Structural snapshot of cytoplasmic pre-60S ribosomal particles bound by Nmd3, Lsg1, Tif6 and Reh1. *Nature Structural & Molecular Biology*, *24*(3), 214–220. https://doi.org/10.1038/NSMB.3364

Mandels, M., Parrish, F. W., & Reese, E. T. (1962). Sophorose as an inducer of cellulase in Trichoderma viride. *Journal of Bacteriology*, *83*, 400–408. https://doi.org/10.1128/JB.83.2.400-408.1962

Marmier-Gourrier, N., Cléry, A., Schlotter, F., Senty-Ségault, V., & Branlant, C. (2011). A second base pair interaction between U3 small nucleolar RNA and the 5′-ETS region is required for early cleavage of the yeast pre-ribosomal RNA. *Nucleic Acids Research*, *39*(22), 9731–9745. https://doi.org/10.1093/NAR/GKR675

Martinez, D., Berka, R. M., Henrissat, B., Saloheimo, M., Arvas, M., Baker, S. E., Chapman, J., Chertkov, O., Coutinho, P. M., Cullen, D., Danchin, E. G. J., Grigoriev, I. v., Harris, P., Jackson, M., Kubicek, C. P., Han, C. S., Ho, I., Larrondo, L. F., de Leon, A. L., … Brettin, T. S. (2008). Genome sequencing and analysis of the biomass-degrading fungus Trichoderma reesei (syn. Hypocrea jecorina). *Nature Biotechnology*, *26*(5), 553–560. https://doi.org/10.1038/nbt1403

Matsuo, Y., Granneman, S., Thoms, M., Manikas, R. G., Tollervey, D., & Hurt, E. (2014). Coupled GTPase and remodelling ATPase activities form a checkpoint for ribosome export. *Nature*, *505*(7481), 112–116. https://doi.org/10.1038/nature12731

Melnikov, S., Ben-Shem, A., Garreau De Loubresse, N., Jenner, L., Yusupova, G., & Yusupov, M. (2012). One core, two shells: Bacterial and eukaryotic ribosomes. In *Nature Structural and Molecular Biology* (Vol. 19, Issue 6). https://doi.org/10.1038/nsmb.2313

Mercer, M., Jang, S., Ni, C., & Buszczak, M. (2021). The Dynamic Regulation of mRNA Translation and Ribosome Biogenesis During Germ Cell Development and Reproductive Aging. *Frontiers in Cell and Developmental Biology*, *9*, 3023. https://doi.org/10.3389/FCELL.2021.710186/BIBTEX

Meyer, V., Wanka, F., van Gent, J., Arentshorst, M., van den Hondel, C. A. M. J. J., & Ram, A. F. J. (2011). Fungal Gene Expression on Demand: an Inducible, Tunable, and Metabolism-Independent Expression System for Aspergillus niger. *Applied and Environmental Microbiology*, *77*(9), 2975–2983. https://doi.org/10.1128/AEM.02740-10

Mojzita, D., Rantasalo, A., & Jäntti, J. (2019). Gene expression engineering in fungi. In *Current Opinion in Biotechnology* (Vol. 59). https://doi.org/10.1016/j.copbio.2019.04.007

Neiman, A. M. (2005). Ascospore Formation in the Yeast Saccharomyces cerevisiae . *Microbiology and Molecular Biology Reviews*, *69*(4), 565–584. https://doi.org/10.1128/mmbr.69.4.565-584.2005

Nora, L. C., Westmann, C. A., Guazzaroni, M. E., Siddaiah, C., Gupta, V. K., & Silva-Rocha, R. (2019). Recent advances in plasmid-based tools for establishing novel microbial chassis. In *Biotechnology*

Advances (Vol. 37, Issue 8, p. 107433). Elsevier Inc. https://doi.org/10.1016/j.biotechadv.2019.107433

Oeffinger, M., Dlakić, M., & Tollervey, D. (2004). A pre-ribosome-associated HEAT-repeat protein is required for export of both ribosomal subunits. *Genes & Development*, *18*(2), 196–209. https://doi.org/10.1101/GAD.285604

Oeffinger, M., Zenklusen, D., Ferguson, A., Wei, K. E., el Hage, A., Tollervey, D., Chait, B. T., Singer, R. H., & Rout, M. P. (2009). Rrp17p Is a Eukaryotic Exonuclease Required for 5′ End Processing of Pre-60S Ribosomal RNA. *Molecular Cell*, *36*(5). https://doi.org/10.1016/j.molcel.2009.11.011

Osheim, Y. N., French, S. L., Keck, K. M., Champion, E. A., Spasov, K., Dragon, F., Baserga, S. J., & Beyer, A. L. (2004). Pre-18S ribosomal RNA is structurally compacted into the SSU processome prior to being cleaved from nascent transcripts in Saccharomyces cerevisiae. *Molecular Cell*, *16*(6), 943–954. https://doi.org/10.1016/j.molcel.2004.11.031

Passmore, H. C., Kobori, J. A., Zimmerer, E. J., Spinella, D. G., Hood, L., Malone, R. E., Chattoraj, D. K., Faulds, D. H., Stahl, M. M., Stahl, F. W., Mol, J., Meyerowitz, E., Passmore, H., Shastri, N., Siu, G., Smnith, L., Bachmair, A., Finley, D., & Varshavsky, A. (1986). In Vivo Half-Life of a Protein Is a Function of Its Amino-Terminal Residue. *Science*, *234*(4773), 179–186. https://doi.org/10.1126/SCIENCE.3018930

Pel, H. J., de Winde, J. H., Archer, D. B., Dyer, P. S., Hofmann, G., Schaap, P. J., Turner, G., de Vries, R. P., Albang, R., Albermann, K., Andersen, M. R., Bendtsen, J. D., Benen, J. A. E., van den Berg, M., Breestraat, S., Caddick, M. X., Contreras, R., Cornell, M., Coutinho, P. M., … Stam, H. (2007). Genome sequencing and analysis of the versatile cell factory Aspergillus niger CBS 513.88. *Nature Biotechnology*, *25*(2), 221–231. https://doi.org/10.1038/nbt1282

Penzo, M., Carnicelli, D., Montanaro, L., & Brigotti, M. (2016). A reconstituted cell-free assay for the evaluation of the intrinsic activity of purified human ribosomes. *Nature Protocols*, *11*(7), 1309–1325. https://doi.org/10.1038/nprot.2016.072

Pérez-Fernández, J., Martín-Marcos, P., & Dosil, M. (2011). Elucidation of the assembly events required for the recruitment of Utp20, Imp4 and Bms1 onto nascent pre-ribosomes. *Nucleic Acids Research*, *39*(18), 8105–8121. https://doi.org/10.1093/NAR/GKR508

Pertschy, B., Saveanu, C., Zisser, G., Lebreton, A., Tengg, M., Jacquier, A., Liebminger, E., Nobis, B., Kappel, L., van der Klei, I., Högenauer, G., Fromont-Racine, M., & Bergler, H. (2007). Cytoplasmic Recycling of 60S Preribosomal Factors Depends on the AAA Protein Drg1. *Molecular and Cellular Biology*, *27*(19), 6581–6592. https://doi.org/10.1128/MCB.00668-07/SUPPL_FILE/FIGURES1.ZIP

Pfaffl, M. W. (2001). A new mathematical model for relative quantification in real-time RT-PCR. *Nucleic Acids Research*, *29*(9), E45. https://doi.org/10.1093/NAR/29.9.E45

Prielhofer, R., Cartwright, S. P., Graf, A. B., Valli, M., Bill, R. M., Mattanovich, D., & Gasser, B. (2015). Pichia pastoris regulates its gene-specific response to different carbon sources at the transcriptional, rather than the translational, level. *BMC Genomics*, *16*(1), 1–17. https://doi.org/10.1186/S12864-015-1393-8/TABLES/6

Quehenberger, J., Reichenbach, T., Baumann, N., Rettenbacher, L., Divne, C., & Spadiut, O. (2019). Kinetics and predicted structure of a novel xylose reductase from Chaetomium thermophilum. *International Journal of Molecular Sciences*, *20*(1). https://doi.org/10.3390/ijms20010185

Rahman, Z., Shida, Y., Furukawa, T., Suzuki, Y., Okada, H., Ogasawara, W., & Morikawa, Y. (2009). Evaluation and characterization of Trichoderma reesei cellulase and xylanase promoters. *Applied Genetics and Molecular Biotechnology*, 899–908. https://doi.org/10.1007/s00253-008-1841-3

Rantasalo, A., Landowski, C. P., Kuivanen, J., Korppoo, A., Reuter, L., Koivistoinen, O., Valkonen, M., Penttilä, M., Jäntti, J., & Mojzita, D. (2018). A universal gene expression system for fungi. *Nucleic Acids Research*. https://doi.org/10.1093/nar/gky558

Rantasalo, A., Vitikainen, M., Paasikallio, T., Jäntti, J., Landowski, C. P., & Mojzita, D. (2019). Novel genetic tools that enable highly pure protein production in Trichoderma reesei. *Scientific Reports*, *9*(1), 1–12. https://doi.org/10.1038/s41598-019-41573-8

Reilly, M. C., Kim, J., Lynn, J., Simmons, B. A., Gladden, J. M., Magnuson, J. K., & Baker, S. E. (2018). Forward genetics screen coupled with whole-genome resequencing identifies novel gene targets for improving heterologous enzyme production in Aspergillus niger. *Applied Microbiology and Biotechnology*, *102*(4), 1797–1807. https://doi.org/10.1007/s00253-017-8717-3

Reyes, M. G., Hernández, R. I. B., Rodríguez, G. A. V., Olivares, C. C., Moreno, S. A. M., Santillán, L. F. J., & Constantino, C. A. L. (2017). FORMATION, MORPHOLOGY AND BIOTECHNOLOGICAL APPLICATIONS OF FILAMENTOUS FUNGAL PELLETS: A REVIEW. *Revista Mexicana de Ingeniería Química*, *16*(3), 703–720. http://rmiq.org/ojs/index.php/rmiq/article/view/63

Romes, E. M., Sobhany, M., & Stanley, R. E. (2016). The Crystal Structure of the Ubiquitin-like Domain of Ribosome Assembly Factor Ytm1 and Characterization of Its Interaction with the AAA-ATPase Midasin. *The Journal of Biological Chemistry*, *291*(2), 882–893. https://doi.org/10.1074/JBC.M115.693259

Rossell, D., Attolini, C. S. O., Kroiss, M., & Stöcker, A. (2014). Quantifying alternative splicing from paired-end-sequencing data. *The Annals of Applied Statistics*, *8*(1), 309–330. https://doi.org/10.1214/13-AOAS687

Roychowdhury, A., Joret, C., Bourgeois, G., Heurgue-Hamard, V., Lafontaine, D. L. J., & Graille, M. (2019). The DEAH-box RNA helicase Dhr1 contains a remarkable carboxyl terminal domain

essential for small ribosomal subunit biogenesis. *Nucleic Acids Research*, *47*(14), 7548–7563. https://doi.org/10.1093/nar/gkz529

Sajith S, Priji, P., Sreedevi, S., & Benjamin, S. (2016). *An overview on fungal cellulases with an industrial perspective.* Journal of Nutrition and Food Sciences. https://www.cabdirect.org/globalhealth/abstract/20163161629

Sardana, R., Liu, X., Granneman, S., Zhu, J., Gill, M., Papoulas, O., Marcotte, E. M., Tollervey, D., Correll, C. C., & Johnson, A. W. (2015). The DEAH-box Helicase Dhr1 Dissociates U3 from the Pre-rRNA to Promote Formation of the Central Pseudoknot. *PLOS Biology*, *13*(2), e1002083. https://doi.org/10.1371/JOURNAL.PBIO.1002083

Schmitt, M. E., & Clayton, D. A. (1993). Nuclear RNase MRP is required for correct processing of pre-5.8S rRNA in Saccharomyces cerevisiae. *Molecular and Cellular Biology*, *13*(12), 7935–7941. https://doi.org/10.1128/mcb.13.12.7935-7941.1993

Shaner, N. C., Steinbach, P. A., & Tsien, R. Y. (2005). A guide to choosing fluorescent proteins. *Nature Methods*, *2*(12), 905–909. https://doi.org/10.1038/nmeth819

Shchepachev, V., & Tollervey, D. (2016). Motoring toward pre-60S-ribosome export. In *Nature Structural and Molecular Biology* (Vol. 23, Issue 1, pp. 3–4). Nature Publishing Group. https://doi.org/10.1038/nsmb.3154

Shen, X. X., Steenwyk, J. L., LaBella, A. L., Opulente, D. A., Zhou, X., Kominek, J., Li, Y., Groenewald, M., Hittinger, C. T., & Rokas, A. (2020). Genome-scale phylogeny and contrasting modes of genome evolution in the fungal phylum Ascomycota. *Science Advances*, *6*(45). https://doi.org/10.1126/SCIADV.ABD0079

Shi, Z., Fujii, K., Kovary, K. M., Genuth, N. R., Röst, H. L., Teruel, M. N., & Barna, M. (2017). Heterogeneous ribosomes preferentially translate distinct subpools of mRNAs genome-wide. *Molecular Cell*, *67*(1), 71. https://doi.org/10.1016/J.MOLCEL.2017.05.021

Singh, A., Schermann, G., Reislöhner, S., Kellner, N., Hurt, E., & Brunner, M. (2021). Global Transcriptome Characterization and Assembly of the Thermophilic Ascomycete Chaetomium thermophilum. *Genes*, *12*(10), 1549. https://doi.org/10.3390/genes12101549

Soltanieh, S., Osheim, Y. N., Spasov, K., Trahan, C., Beyer, A. L., & Dragon, F. (2015). DEAD-Box RNA Helicase Dbp4 Is Required for Small-Subunit Processome Formation and Function. *Molecular and Cellular Biology*, *35*(5), 816–830. https://doi.org/10.1128/MCB.01348-14

Stoklosa, R. J., & Hodge, D. B. (2012). Extraction, recovery, and characterization of hardwood and grass hemicelluloses for integration into biorefining processes. *Industrial and Engineering Chemistry Research*, *51*(34). https://doi.org/10.1021/ie301260w

Strauss, J., Horvath, H. K., Abdallah, B. M., Kindermann, J., Mach, R. L., & Kubicek, C. P. (1999). The function of CreA, the carbon catabolite repressor of Aspergillus nidulans, is regulated at the transcriptional and post-transcriptional level. *Molecular Microbiology*, *32*(1), 169–178. https://doi.org/10.1046/j.1365-2958.1999.01341.x

Stricker, A. R., Grosstessner-Hain, K., Würleitner, E., & Mach, R. L. (2006). Xyr1 (Xylanase Regulator 1) regulates both the hydrolytic enzyme system and D-xylose metabolism in Hypocrea jecorina. *Eukaryotic Cell*, *5*(12), 2128–2137. https://doi.org/10.1128/EC.00211-06/SUPPL_FILE/FIG_S1.ZIP

Stricker, A. R., Mach, R. L., & de Graaff, L. H. (2008). Regulation of transcription of cellulases- and hemicellulases-encoding genes in Aspergillus niger and Hypocrea jecorina (Trichoderma reesei). *Applied Microbiology and Biotechnology*, *78*(2), 211–220. https://doi.org/10.1007/S00253-007-1322-0/FIGURES/4

Strunk, B. S., Loucks, C. R., Su, M., Vashisth, H., Cheng, S., Schilling, J., Brooks, C. L., Karbstein, K., & Skiniotis, G. (2011). Ribosome assembly factors prevent premature translation initiation by 40S assembly intermediates. *Science*, *333*(6048), 1449–1453. https://doi.org/10.1126/science.1208245

Strunk, B. S., Novak, M. N., Young, C. L., & Karbstein, K. (2012). A Translation-Like Cycle Is a Quality Control Checkpoint for Maturing 40S Ribosome Subunits. *Cell*, *150*(1), 111–121. https://doi.org/10.1016/J.CELL.2012.04.044

Stucki, M., & Jackson, S. P. (2004). MDC1/NFBD1: A key regulator of the DNA damage response in higher eukaryotes. In *DNA Repair* (Vol. 3, Issues 8–9, pp. 953–957). Elsevier. https://doi.org/10.1016/j.dnarep.2004.03.007

Suzuki-Fujimoto, T., Fukuma, M., Yano, K.-I., Sakurai, H., Vonika, A., Johnston, S. A., & Fukasawa, T. (1996). Analysis of the galactose signal transduction pathway in Saccharomyces cerevisiae: interaction between Gal3p and Gal80p. *Molecular and Cellular Biology*, *16*(5), 2504–2508. https://doi.org/10.1128/MCB.16.5.2504

Takashima, S., Iikura, H., Nakamura, A., Masaki, H., & Uozumi, T. (1996). Analysis of Crel binding sites in the Trichoderma reesei cbhl upstream region. In *FEMS Microbiology Letters* (Vol. 145). https://doi.org/10.1111/j.1574-6968.1996.tb08601.x

Tanaka, M., Ichinose, S., Shintani, T., & Gomi, K. (2018). Nuclear export-dependent degradation of the carbon catabolite repressor CreA is regulated by a region located near the C-terminus in Aspergillus oryzae. *Molecular Microbiology*, *110*(2), 176–190. https://doi.org/10.1111/MMI.14072

Thermes, C. (2014). Ten years of next-generation sequencing technology. In *Trends in genetics : TIG* (Vol. 30, Issue 9, pp. 418–426). Elsevier Current Trends. https://doi.org/10.1016/j.tig.2014.07.001

Thoms, M., Ahmed, Y. L., Maddi, K., Hurt, E., & Sinning, I. (2016). Concerted removal of the Erb1-Ytm1 complex in ribosome biogenesis relies on an elaborate interface. *Nucleic Acids Research*, *44*(2), 926–939. https://doi.org/10.1093/nar/gkv1365

Thoms, M., Thomson, E., Baßler, J., Gnädig, M., Griesel, S., & Hurt, E. (2015). The Exosome Is Recruited to RNA Substrates through Specific Adaptor Proteins. *Cell*, *162*(5), 1029–1038. https://doi.org/10.1016/j.cell.2015.07.060

Thomson, E., & Tollervey, D. (2010). The Final Step in 5.8S rRNA Processing Is Cytoplasmic in Saccharomyces cerevisiae . *Molecular and Cellular Biology*, *30*(4), 976–984. https://doi.org/10.1128/MCB.01359-09/ASSET/436C61FE-7BC7-44EE-B456-BD6E4D1B5BC3/ASSETS/GRAPHIC/ZMB9991084720008.JPEG

Torchet, C., Jacq, C., & Hermann-Le Denmat, S. (1998). Two mutant forms of the S1/TPR-containing protein Rrp5p affect the 18S rRNA synthesis in Saccharomyces cerevisiae. *RNA*, *4*(12), 1636–1652. https://doi.org/10.1017/S1355838298981511

Tsuchiya, K., Tada, S., Gomi, K., Kitamoto, K., Kumagai, C., & Tamura, G. (1992). Deletion Analysis of the Taka-amylase A Gene Promoter Using a Homologous Transformation System in Aspergillus oryzae. *Bioscience, Biotechnology, and Biochemistry*, *56*(11), 1849–1853. https://doi.org/10.1271/BBB.56.1849

Turowski, T. W., & Tollervey, D. (2015). Cotranscriptional events in eukaryotic ribosome synthesis. *Wiley Interdisciplinary Reviews: RNA*, *6*(1), 129–139. https://doi.org/10.1002/WRNA.1263

Ulbrich, C., Diepholz, M., Baßler, J., Kressler, D., Pertschy, B., Galani, K., Böttcher, B., & Hurt, E. (2009). Mechanochemical Removal of Ribosome Biogenesis Factors from Nascent 60S Ribosomal Subunits. *Cell*, *138*(5), 911–922. https://doi.org/10.1016/j.cell.2009.06.045

van Peij, N. N. M. E., Visser, J., & de Graaff, L. H. (1998). Isolation and analysis of xlnR, encoding a transcriptional activator co-ordinating xylanolytic expression in Aspergillus niger. *Molecular Microbiology*, *27*(1), 131–142. https://doi.org/10.1046/j.1365-2958.1998.00666.x

Varshavsky, A. (2011). The N-end rule pathway and regulation by proteolysis. *Protein Science : A Publication of the Protein Society*, *20*(8), 1298. https://doi.org/10.1002/PRO.666

Vogel, C., & Marcotte, E. M. (2012). Insights into the regulation of protein abundance from proteomic and transcriptomic analyses. *Nature Reviews Genetics 2012 13:4*, *13*(4), 227–232. https://doi.org/10.1038/nrg3185

Vogt, K., Bhabhra, R., Rhodes, J. C., & Askew, D. S. (2005). Doxycycline-regulated gene expression in the opportunistic fungal pathogen Aspergillus fumigatus. *BMC Microbiology*, *5*(1), 1. https://doi.org/10.1186/1471-2180-5-1

Waring, R. B., May, G. S., & Morris, N. R. (1989). Characterization of an inducible expression system in Aspergillus nidulans using alcA and tubulin-coding genes. *Gene*, *79*(1), 119–130. https://doi.org/10.1016/0378-1119(89)90097-8

Warner, J. R. (1999). The economics of ribosome biosynthesis in yeast. In *Trends in Biochemical Sciences* (Vol. 24, Issue 11, pp. 437–440). Trends Biochem Sci. https://doi.org/10.1016/S0968-0004(99)01460-7

Weatheritt, R. J., Sterne-Weiler, T., & Blencowe, B. J. (2016). The ribosome-engaged landscape of alternative splicing. *Nature Structural & Molecular Biology 2016 23:12*, *23*(12), 1117–1123. https://doi.org/10.1038/nsmb.3317

Weis, F., Giudice, E., Churcher, M., Jin, L., Hilcenko, C., Wong, C. C., Traynor, D., Kay, R. R., & Warren, A. J. (2015). Mechanism of eIF6 release from the nascent 60S ribosomal subunit. *Nature Structural and Molecular Biology*, *22*(11), 914–919. https://doi.org/10.1038/nsmb.3112

Wells, G. R., Weichmann, F., Colvin, D., Sloan, K. E., Kudla, G., Tollervey, D., Watkins, N. J., & Schneider, C. (2016). The PIN domain endonuclease Utp24 cleaves pre-ribosomal RNA at two coupled sites in yeast and humans. *Nucleic Acids Research*, *44*(11), 5399–5409. https://doi.org/10.1093/nar/gkw213

West, M., Hedges, J. B., Chen, A., & Johnson, A. W. (2005). Defining the Order in Which Nmd3p and Rpl10p Load onto Nascent 60S Ribosomal Subunits. *Molecular and Cellular Biology*, *25*(9), 3802–3813. https://doi.org/10.1128/MCB.25.9.3802-3813.2005/ASSET/FDF5CDD8-2C73-4C02-8ED9-C57AF9F41F93/ASSETS/GRAPHIC/ZMB0090549720009.JPEG

Wethmar, K., Barbosa-Silva, A., Andrade-Navarro, M. A., & Leutz, A. (2014). uORFdb--a comprehensive literature database on eukaryotic uORF biology. *Nucleic Acids Research*, *42*(Database issue), D60-7. https://doi.org/10.1093/nar/gkt952

Wightman, B., Ha, I., & Ruvkun, G. (1993). Posttranscriptional regulation of the heterochronic gene lin-14 by lin-4 mediates temporal pattern formation in C. elegans. *Cell*, *75*(5), 855–862. https://doi.org/10.1016/0092-8674(93)90530-4

Winson IY, M. K., Swift, S., Hill, P. J., Sims, C. M., Griesmayr, G., Bycroft, B. W., Williams, P., & SAB Stewart, G. (1998). Engineering the luxCDABE genes from Photorhabdus luminescens to provide a bioluminescent reporter for constitutive and promoter probe plasmids and mini-Tn5 constructs. *FEMS Microbiology Letters*, *163*(2), 193–202. https://doi.org/10.1111/J.1574-6968.1998.TB13045.X

Wong, K. K. Y., & Saddler, J. N. (1992). Trichoderma xylanases, their properties and application. *Critical Reviews in Biotechnology*, *12*(5–6), 413–435. https://doi.org/10.3109/07388559209114234

Woolford, J. L., & Baserga, S. J. (2013). Ribosome biogenesis in the yeast Saccharomyces cerevisiae. *Genetics*, *195*(3), 643–681. https://doi.org/10.1534/genetics.113.153197

Wu, S., Tutuncuoglu, B., Yan, K., Brown, H., Zhang, Y., Tan, D., Gamalinda, M., Yuan, Y., Li, Z., Jakovljevic, J., Ma, C., Lei, J., Dong, M. Q., Woolford, J. L., & Gao, N. (2016). Diverse roles of assembly factors revealed by structures of late nuclear pre-60S ribosomes. *Nature 2016 534:7605*, *534*(7605), 133–137. https://doi.org/10.1038/nature17942

Yamashita, A., Shichino, Y., & Yamamoto, M. (2016). The long non-coding RNA world in yeasts. In *Biochimica et Biophysica Acta - Gene Regulatory Mechanisms* (Vol. 1859, Issue 1, pp. 147–154). Elsevier. https://doi.org/10.1016/j.bbagrm.2015.08.003

Yusupova, G., & Yusupov, M. (2014). High-Resolution Structure of the Eukaryotic 80S Ribosome. *Annual Review of Biochemistry*, *83*(1), 467–486. https://doi.org/10.1146/annurev-biochem-060713-035445

Zhang, J., Harnpicharnchai, P., Jakovljevic, J., Tang, L., Guo, Y., Oeffinger, M., Rout, M. P., Hiley, S. L., Hughes, T., & Woolford, J. L. (2007). Assembly factors Rpf2 and Rrs1 recruit 5S rRNA and ribosomal proteins rpL5 and rpL11 into nascent ribosomes. *Genes & Development*, *21*(20), 2580–2592. https://doi.org/10.1101/GAD.1569307

Zhang, L., Lin, J., & Ye, K. (2013). Structural and functional analysis of the U3 snoRNA binding protein Rrp9. *RNA (New York, N.Y.)*, *19*(5), 701–711. https://doi.org/10.1261/rna.037580.112

Zhu, J., Liu, X., Anjos, M., Correll, C. C., & Johnson, A. W. (2016). Utp14 Recruits and Activates the RNA Helicase Dhr1 To Undock U3 snoRNA from the Preribosome. *Molecular and Cellular Biology*, *36*(6), 965–978. https://doi.org/10.1128/mcb.00773-15

Zorbas, C., Nicolas, E., Wacheul, L., Huvelle, E., Heurgué-Hamard, V., & Lafontaine, D. L. J. (2015). The human 18S rRNA base methyltransferases DIMT1L and WBSCR22-TRMT112 but not rRNA modification are required for ribosome biogenesis. *Molecular Biology of the Cell*, *26*(11), 2080–2095. https://doi.org/10.1091/MBC.E15-02-0073/ASSET/IMAGES/LARGE/MBC-26-2080-G008.JPEG